Evaluating the potential role of natural products from *Cleome gynandra* in urease inhibition and nitrogen utilization for enhancing soil health-A rhizosphere manipulation strategy

Submitted by

Rajashree Dutta

Doctor of Philosophy (Science)

Department of Life Science and Biotechnology

Faculty of Science

Jadavpur University

Kolkata, India

2025

INDIAN STATISTICAL INSTITUTE

Suparna Mandal Biswas, PhD
Associate professor
Biological Science Division
Agricultural & Ecological Research Unit

203 Barrackpore Trunk Road
Kolkata 700 108, INDIA
(033)-25753225 (O), (91)-9830171362 (M)
Email: suparna@isical.ac.in

This is to certify that the thesis entitled "Evaluating the potential role of natural products from *Cleome gynandra* in urease inhibition and nitrogen utilization for enhancing soil health-A rhizosphere manipulation strategy" Submitted by Ms. Rajashree Dutta who got her name registered on 27th August, 2019 (INDEX No.: 95/19/Life Sc./26] for the award of Ph. D. (Science) Degree of Jadavpur University, is absolutely based upon her own work under the supervision of Dr. Suparna Mandal Biswas and that neither this thesis nor any part of it has been submitted for either any degree / diploma or any other academic award anywhere before.

Suparna Mandal Biswas
30.04.2025

(Signature of the Supervisor date with official seal)

Dr. Suparna Mandal Biswas
Head, Agric & Ecol. Res. Unit
Indian Statistical Institute
203, B.T. Road, Kolkata - 700108

From:

Dr. Suparna Mandal Biswas

HEAD & Associate Professor, Agric. and Ecol. Res. Unit

Indian Statistical Institute, 203, B.T. Road, Kolkata

Email: suparna@isical.ac.in

Acknowledgements

The author expresses her deep sense of gratitude and heartiest thanks to Dr. Suparna Mandal Biswas, Head and Associate Professor, Agricultural and Ecological Research Unit, Biological Sciences Division, Indian Statistical Institute, Kolkata, India, , for her valuable guidance, cooperation, continuous encouragement and affection throughout, leading to the completion of this work.

The author also is extremely grateful to the Professor-in- Charge and Head of the Agricultural and Ecological Research Unit, ISI Kolkata for their constant support and encouragement.

The author expresses her heartfelt thanks to Prof. Panchanan Pramanik, Scientific advisor, AERU, ISI for his valuable suggestions and support.

The author is thankful to Director, ISI, Kolkata for providing the lab facilities and to Dean of Studies, ISI, Kolkata for providing the fellowship during the whole tenure of this research.

The author is grateful to the Dean of Studies, Faculty of Science, and Head, Department of Life Science and Biotechnology, Jadavpur University for their cooperation.

The author is obliged to have Dr. Nirjhar Dasgupta, Dr. Debabrata Das, Dr. Supriya Majumder, Dr. Rahul Bose, Dr. Anjan Hazra, Dr. Ekta Bhattacharya, Miss. Madhurima Dutta, Miss. Sreemoyee Mitra and Miss. Suvasri Dutta as her colleagues who helped her at every step of this doctoral journey.

The author is thankful to her family members for their profound support, love and help that has been the source of inspiration and zeal behind the completion of this research work.

Preface

Rhizosphere manipulation using natural urease inhibitors is gaining significant attention in agriculture for its potential to enhance the efficiency of nitrogen fertilizers. By slowing the hydrolysis of urea, these inhibitors reduce ammonia volatilization and increase nutrient availability to crop plants, all while maintaining environmental sustainability. In this context, the present thesis explores the potential of plant-based natural urease inhibitors, providing the first comprehensive study on the urease-inhibiting properties of *Cleome gynandra*, an underutilized yet highly nutritious herb from the Cleomaceae family, a sister group to Brassicaceae, known for its rich micronutrient content and medicinal properties.

Chapter 1 presents a comprehensive overview of the nitrogen cycle, emphasizing the influence of the rhizosphere and the key processes contributing to nitrogen loss in soils. The indiscriminate use of fertilizers, coupled with poor distribution and management practices, has emerged as a global concern. The rapid increase in fertilizer consumption, particularly urea, driven by population growth, has led to nutrient-depleted soils, reduced food production, and adverse effects on human health. Elevated urease activity further exacerbates nitrogen loss through ammonia volatilization, hindering plant growth and degrading soil fertility, thereby posing serious challenges to sustainable agricultural practices. Therefore, the last part of this chapter focuses on enzyme kinetics and the mechanism by which enzymes interact with specific substrates.

Chapter 2 comprises an extensive literature review of strategies aimed at enhancing the efficiency of urea fertilizers, with a primary focus on mitigating excessive urease activity, a key factor responsible for up to 70% nitrogen loss from urea. Thereby, suppressing the urease activity slows down urea hydrolysis, which in turn gives the plant more time to absorb the urea, resulting in a reduction of nitrogen loss. This chapter delves into a range of urease inhibitors, both

synthetic and natural, with particular emphasis on the potential of plant-derived extracts. The insights gained from this literature review guided the identification of a novel, safe, and cost-effective natural urease inhibitor with promising advantages for both human health and environmental sustainability. Priority was given to native plant species rich in bioactive compounds and health-promoting properties, especially those that grow naturally without cultivation and exhibit broad genetic diversity across different ecological zones, making them ideal candidates for sustainable urease inhibition.

Chapter 3 outlines a concise overview of the research objectives, beginning with a detailed examination of the problem statement presented in tabular form. The research approach was initiated with the selection of a locally available plant based on specific criteria, leading to the identification and validation of *Cleome gynandra* as a promising natural urease inhibitor. The research involved collecting plant material, followed by sequential extraction and kinetic analysis to evaluate the urease-inhibitory potential of each fraction. This was followed by the identification of the bioactive components by HR-LCMS analysis based on retention time and molecular weight. Finally, molecular docking studies were conducted to assess the binding affinity and interactions of the identified compounds with the urease enzyme, along with molecular dynamics simulations to evaluate their stability and behaviour over time within a biological system.

Chapter 4 details the process of investigating, collecting, and purifying the selected *Cleome gynandra* plant sample. The plant was accurately identified based on key morphological characteristics, including its leaves, stems, flowers, and root structure. Following identification, the raw plant material underwent extraction, chromatographic separation, and purification. Initial experiments involved the use of concentrated extracts, referred to as crude extracts, prepared from different plant parts. These crude extracts were subsequently fractionated

using solvents of varying polarity to isolate and identify the bioactive constituents.

Chapter 5 focuses on the urease inhibition study and evaluates the IC_{50} value of the crude extract from each plant part (leaf, stem, root, and whole plant) at different urea concentrations. The overall IC_{50} comparison revealed significant differences between the leaf and stem extracts when compared to the standard inhibitor, thiourea, while the root and whole plant showed minimal variation in their inhibitory activity. A box plot analysis further highlighted the root as a promising candidate, prompting a fraction-wise evaluation of root extracts based on solvent polarity to explore their individual inhibitory potentials. This investigation was complemented by a double reciprocal plot to analyze enzyme kinetics and determine the mode of inhibition.

Chapter 6 mainly focuses on the identification of bioactive compounds present in the water, methanol, and acetone fractions of the root through HR-LCMS analysis. The detection of distinct, sharp peaks at multiple retention times reflects a wide spectrum of bioactive constituents, many of which are recognized for their therapeutic relevance in the treatment of various diseases.

Chapter 7 delves into the molecular interactions between selected ligands and the urease enzyme, with a focus on elucidating their binding mechanisms using computational molecular docking approaches. The compounds present in the root water fractions were selected as ligands owing to its maximum inhibitory potential.

Chapter 8 provides insights into the dynamic behaviour of atoms within a protein molecule over time, assessing the ligand–protein interactions under conditions simulating the human physiological environment through molecular dynamics (MD) simulations. Time-series analyses yielded RMSD (Root Mean Square Deviation), RMSF (Root Mean Square Fluctuation), and RG (Radius of Gyration)

values, offering a detailed understanding of biomolecular changes throughout the simulation period. This analysis was further supported by in vivo ADMET (Absorption, Distribution, Metabolism, Excretion, and Toxicity) profiling to assess the drug-likeness and pharmacokinetic properties of the selected ligands.

In conclusion, *Cleome gynandra* emerges as a promising novel source of bioactive compounds with natural urease-inhibiting properties. This study offers a new perspective on exploring the plant's phytochemical potential to mitigate urea hydrolysis. This would be safer, cost-effective, and environmentally sustainable strategy to address the global issue of nitrogen loss, which significantly impacts fertilizer efficiency. These findings provide a solid basis for future experimental studies and the development of potent urease inhibitors.

List of Tables

List of Figures

List of Abbreviations

AOB: Ammonia-oxidizing bacteria

AOA: Ammonia-oxidizing archaea

AMO: Ammonia monooxygenase

NOB: Nitrate oxidizing bacteria

HAO: Hydroxylamine oxidoreductase

NUE: Nitrogen Use Efficiency

GS: Glutamine synthetase

GOAT: Glutamine oxoglutarate aminotransferase

GDH: Glutamate dehydrogenase

UAN: Urea ammonium nitrate

NPK: Nitrogen, Phosphorous, Potassium

JBU: Jack bean urease

PPD: Phosphorodiamidates

NBPT: N-(butyl) thiophosphoric acid triamide

NBPTO: Oxo- N-(butyl) thiophosphoric acid triamide

NPPT: N-(n-propyl) thiophosphoric triamide

SAR: Structure-activity relationship

MG: Methyl gallate

PGG: 1,2,3,4,6-penta-O-galloyl-β-D-glucopyranose

AHA: Acetohydroxamic acid

GLs: Glucosinolates

ITCs: Isothiocyanates

HPLC-PDA: High-performance liquid chromatography-photodiode array

MD: Molecular dynamics

TLC: Thin layer chromatography

THAM: Tris (hydroxymethyl) aminomethane

EDTA: Ethylenediaminetetraacetic acid

HR-LCMS: High-resolution liquid chromatography-mass spectrometry

HPLC: High performance liquid chromatography

GCP: Glucocapparin

FP: Fluticasone Propionate

RA: Ritterizine A

LHS: Lauryl Hydrogen Sulphate

OA: Obtusilactone A

LPL: Lipoprotein lipase

PDB: Protein Data Bank

NMR: Nuclear magnetic resonance

RCSB-PDB: Research Collaboratory for Structural Bioinformatics Protein Data Bank

SDF: Structured Data Format

UCSF-Chimera: University of California, San Francisco, Chimera

RMSD: Root Mean Square Deviation

RMSF: Root Mean Square Fluctuation

RG: Radius of Gyration

PSF: Protein Structure File

PK: Pharmacokinetic

ADMET: Absorption, Distribution, Metabolism, Excretion, and Toxicity

SMILES: Simplified Molecular Input Line Entry System

TPSA: Topological polar surface area

ROS: Reactive oxygen species

CONTENTS

Chapter 1

1. Introduction

Soil supports various life forms on earth by providing an adequate environment for the growth of plants, animals, and humans. Healthy soil nurtures strong plants, which in turn increases food production. Therefore, prioritizing soil health is crucial for a high-quality and abundant food supply.

1.1 Rhizosphere

The health of plants is deeply influenced by the microorganisms that reside in the rhizosphere. The rhizosphere is the zone surrounding the plant's root. These microorganisms are indispensable for plant nutrition, development, and disease interactions **(Ling et al., 2022).** A vast number of microbial inhabitants that reside in the rhizosphere perform various functions that impact the development of plants. The rhizosphere is divided into three zones: ectorhizosphere, rhizoplane, and endorhizosphere **(McNear Jr et al., 2013).**

a. Ectorhizosphere: this is the outmost part of the root which is associated with the loose soil.
b. Rhizoplane: this involves the intermediate region of the root that comprises the cells.
c. Endorhizosphere: It is the part which is sandwiched between the root cortex and endodermis which has a rich source of microbiota having a wide range of mineral ions that are present in the apoplastic region in between two cells.

The rhizosphere region does not have a fixed size or shape; it encompasses a variety of biological, chemical, and physical properties surrounding the root in all directions and positions (**Philippot et al., 2013**).

1.1.1 Rhizomicrobiome

The microorganisms that live in the interface of soil and roots significantly influence the different processes that take place in the rhizosphere. Plants have an unusual adaptability at the time of nutrient scarcity. It often changes the root morphology by engaging specific microorganisms and modifying the chemical properties of the rhizosphere **(Tian et al., 2020; Jamil et al., 2022).** Nitrogen and phosphorous are considered to be the most regulating nutrients in the growth of plants. The atmosphere consists of approximately 78% nitrogen gas (N_2), but this form is only accessible for utilization by nitrogen-fixing organisms (**Jickells et al., 2013**). Therefore, the inorganic form of nitrogen (nitrate; NO3- and ammonium; NH4+) needs to be added to the soil for plant uptake. Soil has low nitrogen availability due to loss by leaching of nitrate through rainwater, volatilization of ammonia, and denitrification by soil bacteria (**Cameron et al., 2013; Rotz et al., 2004**).

Various soil microorganisms are responsible for secreting enzymes that play a crucial role in soil nutrient cycling and other functions. One of these enzymes, urease, is commonly found in soils. Urea is hydrolyzed by urease-producing microorganisms to ammonia and carbonic acid **(Cabrera et al., 1991).** Several bacteria species that are aerobic (i.e., *Proteus* sp, *Pseudomonas* sp, *Clostridium* sp, *Fusobacterium* sp, *Ureaplasma* sp, *Sarcina* sp, *Lactobacillus* sp, *Streptococcus* sp, and *Enterobacter* sp) are some of the urease producing bacterial species that undergoes hydrolysis of urea present in the soil under aerobic environment **(Mekonnen et al., 2021).** Urea fertilizer is one of the most extensively used nitrogen-containing fertilizers used in agriculture **(Bremner et al., 1995).**

1.2 Nitrogen cycle

Nitrogen is circulated in nature in various forms. Nitrogen, an important component of amino acids and nucleic acids is an essential element on Earth

(Ohyama et al., 2010). The atmosphere comprises 78% nitrogen gas by volume, but this abundant reservoir of nitrogen is unusable by most organisms in the ecosystem. So, nitrogen is converted into multiple chemical forms as it circulates in the atmosphere through the soil and passes through different organisms, which ultimately returns to the soil **(Bremner et al., 1965).** Numerous processes are involved, which are nitrogen fixing, nitrification, denitrification, decaying, and decomposition **(Fowler et al., 2013).**

Nitrogen gas comprises both organic and inorganic forms. The form that is present in living organisms is organic nitrogen, which is distributed in the food chain through food consumption **(Hutchinson et al., 1912).**

Nitrates and nitrites, the inorganic form of nitrogen, are available in huge quantities in the atmosphere. These two forms of nitrogen are the most accessible, and it is produced by microbial activities that are involved in the conversion of inert nitrogen gas **(Vitousek et al., 2002).**

A balanced, sustainable ecosystem requires a transformation of nitrogen in various forms. The different forms of nitrogen extend to several biomes in the environment. Among the various biomes, the nitrogen cycle in the marine ecosystem has the most complicated biogeochemical cycles **(Herbert et al., 1999).**

1.2.1 Nitrification

Microorganisms present in the soil are involved in the conversion of ammonia to nitrate **(Wallace et al., 1969).** Firstly, nitrites are formed with the help of *Nitrosomas* sp bacterial species by the oxidation of ammonia. The nitrite produced is then oxidized into nitrates by the bacterial species *Nitrobacter*. As ammonia gas is toxic to plants, this conversion is very much essential **(Ward et al., 2011).**

Nitrification involves the following reactions:

$$2NH_3 + 3O_2 \rightarrow 2NO_2^- + 2H_2O + 2H^+$$

$$2NO_2^- + O_2 \rightarrow 2NO_3^-$$

- **Ammonia oxidation**

Ammonia oxidation is the first stage of nitrification, where ammonium (NH4+) or ammonia (NH_3) is converted to nitrites (NO_2^-). This initial process is known as nitritation. Ammonia-oxidizing bacteria (AOB) and ammonia-oxidizing archaea (AOA) are responsible for carrying out this crucial step **(Lehtovirta-Morley et al., 2018).**

- **Ammonia-oxidizing bacteria (AOB)**

This bacterial community belongs to Betaproteobacteria (a class of gram-negative bacteria) and Gammaproteobacteria (the bacterial class that belongs to the phylum Pseudomonadota) **(Fierer et al., 2009).** AOB are typical gram-negative bacteria. They reside in different environments, such as soil, wastewater treatment plants, and aquatic systems. They possess a unique ability to utilize ammonia as their energy source through a peculiar enzyme that is present in their system called ammonia monooxygenases (AMOs), which catalyzes the conversion of ammonia to an intermediate crucial product called hydroxylamine (NH_2OH) **(Shen et al., 2008).** This enzyme is influenced by various environmental factors such as pH, temperatures, availability of oxygen, moisture content of soil, and availability of substrate. It has copper metal ions and a non-heme iron group **(Stein et al., 1998).**

$$\textbf{Ammonia} + AH_2 + O_2 \rightleftharpoons NH_2OH + A + H_2O$$

AOB plays a central role in the soil nitrification process by contributing to its role in transforming ammonia from organic matter decomposition or applied fertilizers to nitrite, which in turn behaves as a substrate for bacteria undergoing nitrate oxidation (NOB) **(Van Kessel et al., 2015).**

- **Ammonia-oxidizing archaea (AOA)**

Besides the contribution of ammonia-oxidizing bacteria (AOB), the detection of ammonia-oxidizing archaea (AOA) in 2005 has greatly marked the capability of archaea in performing ammonia oxidation. *Nitrosopumilus maritimus* and *Nitrososphaera viennensis*, the cultivation of these two isolates showed the dominance of AOA in soil and aquatic environments. A biomarker of AOA involving ammonia oxidation is the presence of biological membrane lipids, namely Crenarchaeol **(Zhang et al., 2012).**

- **Nitrite oxidation**

The next step involves the conversion of nitrite to nitrate, carried out by bacterial species such as *Nitrospirota* sp., *Pseudomonadota* sp., and *Chloroflexota* sp., which are predominantly found in soil and aquatic environments **(Lees et al., 1957).**

Nitrification is a stepwise enzymatic process of oxidation of nitrogen involving the transfer of electrons to oxygen atom from nitrogen atom and performed by various bacterial species as follows:

$$2NH_4^{+}+3O_2 \longrightarrow 2NO_2^{-}+4H^{+}+2H_2O$$

(Performed by bacterial species such as *Nitrosomonas*, *Comammox*)

$$2NH_4^{+}+3O_2 \longrightarrow 2NO_2^{-}+4H^{+}+2H_2O$$

(Performed by bacterial species such as *Nitrosomonas*, *Comammox*)

$$2NO_2^{-}+O_2 \longrightarrow 2NO_3^{-}$$

(Performed by bacterial species such as *Nitrobacter* sp, *Nitrospira* sp)

OR

$$NH_3+O_2 \longrightarrow NO_2^{-}+3H^{+} \qquad NO_2^{-}+H_2O \longrightarrow NO_3^{-}+2H^{+}$$

Ammonia monooxygenase (AMO) catalyzes the initial oxidation step (converting ammonia to hydroxylamine) in *Nitrosomonas europaea* **(Remde et al., 1990).**

$$NH_3+O_2+2H^{+} \longrightarrow NH_2OH+H_2O$$

Hydroxylamine is converted to nitric oxide in the second step by hydroxylamine oxidoreductase (HAO) enzyme **(Boon et al., 1962).**

$NH_2OH \rightarrow NO + 3H^+ + 3e^-$ **$NH_2OH \rightarrow NO + 3H^+ + 3e^-$**

The last step is performed in separate organisms where nitrite is converted to nitrate **(Maia et al., 2014)**

Nitrite + acceptor= nitrate + reduced acceptor

1.2.2 Assimilation

The growth and development of plants are significantly influenced by nitrogen assimilation. As primary producers, plants absorb nitrogen compounds from the soil through their root hairs, which are available in various forms, such as ammonia, nitrite ions, nitrate ions, or ammonium ions. Plants have different transporters, including ammonia transporters and nitrate transporters, which facilitate the absorption of ammonium ions and nitrate, respectively. Nitrogen is then transported from the roots to the shoots through the xylem in the form of nitrate, dissolved ammonia, or amino acids **(Xu et al., 2012).**

For every nitrate reduced to ammonia, one OH- ion is produced. To maintain pH balance, plants release this ion into the surrounding medium or neutralize it with organic acids. As a result, nitrate uptake raises the pH of the medium around the plant roots **(Miflin et al., 1976).**

The amount of nitrogen that a plant utilizes from the environment is referred to as Nitrogen Use Efficiency (NUE). Enhancing NUE in modern agriculture is crucial for improving fertilizer uptake, making farming more sustainable and cost-effective by boosting crop yield and reducing pollution. Improving fertilizer efficiency, nitrogen uptake, and crop management practices can contribute to higher NUE **(Dobermann et al., 2005).**

1.2.3 Ammonification

When organisms such as bacteria and fungi decompose organic matter in the soil, they derive energy by breaking down dead plant or animal material. These decomposers transform complex nitrogen-containing compounds into simpler

forms, such as ammonia, which is essential for a sustainable ecosystem **(Strock et al., 2008).**

The enzymes involved in this process include **(Ladd et al., 1982):**

- Glutamine synthetase (GS) is a key enzyme in nitrogen metabolism.
- Glutamine oxoglutarate aminotransferase (GOAT) or glutamate synthase helps in the assimilation of nitrogen.
- Glutamate dehydrogenase (GDH) plays a role in ammonia metabolism.

1.2.4 Denitrification

In denitrification, nitrate is transformed into gaseous nitrogen, which is then released into the atmosphere. This is the final stage in the nitrogen cycle that takes place under anaerobic conditions. Various denitrifying bacteria, such as *Clostridium* sp. and *Pseudomonas* sp., carry out this process by converting nitrate into nitrous oxide and dinitrogen oxide, ultimately releasing nitrogen gas **(Knowles et al., 1982).**

The biological reduction of nitrate to nitrogen gas by denitrifying bacterial species involves a series of enzymatic processes carried out by facultative anaerobic bacteria, such as *Pseudomonas* sp. and *Clostridium* sp. These bacteria perform this activity in the absence of oxygen or the presence of a very low concentration of oxygen. The various enzyme sequences involved in this process are **(Firestone et al., 1982):**

- Nitrate reductases
- Nitrite reductases
- Nitric oxide reductases
- Nitrous oxide reductases

A series of reactions are involved, including nitrate (NO_3^-), nitrite (NO_2^-), nitric oxide (NO), and nitrous oxide (N_2O), ultimately leading to the production of free nitrogen gas, which is released into the environment **(Firestone et al., 1982).**

The complete stepwise redox reaction is as follows:

- $NO_3^- + 2H^+ \rightarrow NO_2^- + H_2O$
- $NO_2^- + 2H^+ \rightarrow NO + H_2O$
- $2NO + 2H^+ \rightarrow N_2O + H_2O$
- $N_2O + 2H^+ \rightarrow N_2 + H_2O$

The rate of denitrification is influenced by pH, temperature, moisture, and soil conditions. The amount of carbon and nitrogen in the soil significantly affects the completion of the denitrification process. The genes associated with denitrification in microorganisms are *nir* (nitrite reductase), *nos* (nitrous oxide reductase), and *nrf* (nitrate reductase; the presence of this gene allows the direct reduction of nitrate to ammonium gas) **(Zumft et al., 1997).**

1.3 Nitrogen loss

Deposition of nitrogen in soil occurs through different pathways, including the application of manure and fertilizers, as well as nitrogen fixation by leguminous plants. However, this nitrogen is lost from the soil through several mechanisms, such as volatilization, leaching, denitrification, crop removal, soil erosion, and runoff **(Cameron et al., 2013).**

Fertilizer	**Percentage of nitrogen (%)**
Urea	46
Urea ammonium nitrate (UAN)	28-32
Ammonium sulphate	21
Ammonium nitrate	34-35
Calcium ammonium nitrate	24-28

Table 1.1: Common nitrogen fertilizers with their nitrogen content percentage (**Isleib et al., 2017**)

1.3.1 Volatilization

Nitrogen fertilizers, commonly used in agriculture, are prone to nitrogen loss or volatilization. The rate of volatilization depends on how quickly urea or other

ammonium-based fertilizers are hydrolyzed. The chemical reactions involved in volatilization are as follows **(Rodriguez et al., 2005):**

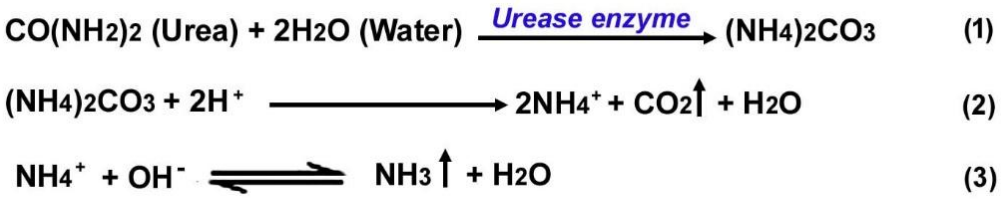

Soil moisture content during fertilizer application can create a great impact on nitrogen loss since the presence of water in the soil accelerates the rate of urea hydrolysis.

Similar to moisture content, pH and temperature are key factors that contribute to ammonia volatilization. With the application of urea fertilizer, soil pH is increased, which results in increased availability of dissolved ammonia in the soil to be converted to ammonia gas lost to the atmosphere. High temperature on the other hand unable to hold ammonia and thereby increases volatilization. Lower temperatures also do not ensure a decrease in volatilization as during low temperatures, the soil remains moist for a longer period. However, these conditions hold dissolved ammonia for an extended period, thereby slowing down the loss of ammonia (**Freney et al., 1981**).

During the application of urea fertilizers, the urease enzyme produced by microorganisms plays a vital part in urea hydrolysis. Additionally, the presence of crop residues or thatch can significantly increase the rate of volatilization, as these areas have a higher abundance of microorganisms **(Hargrove et al., 1981).**

Understanding the factors that influence nitrogen volatilization from soils, along with implementing proper management strategies before fertilizer application, can enhance nitrogen uptake efficiency and reduce the undesirable loss of ammonia gas into the environment **(Table 1.2).**

High volatilization condition	Lower volatilization condition
High soil moisture and high dew content	Lower moisture content or dry soil
Higher soil pH greater than 7	Lower soil pH less than 6
Rise in soil temperatures above 70°F	Lower soil temperatures
Residual crops or thatching	Barren land
Cation exchange soil capacity is low	Cation exchange soil capacity is high
Soil with low buffering capacity	Soil with high buffering capacity

Table 1.2: Important Factors that influence the risk of nitrogen volatilization on fertilizer application in soils (**Jones et al., 2007**).

1.3.2 Leaching

The movement of water through the soil carries away nitrogen. This passing down of nitrogen into groundwater, oceans, streams, and other water bodies is termed nitrogen leaching. Leaching occurs when there is an excess of water, such as during the monsoon season, floods, or excessive irrigation. The two main forms of nitrogen, nitrate (NO3-) and ammonium (NH4+), are readily absorbed by plants. Nitrates are the primary leaching component as they move easily through the soil, while ammonium remains attached to the soil particles. In recent years, nitrate contamination has greatly affected human health and the environment. Soil water retention capacity affects leaching, with clay soils retaining more water than sandy soils. It is essential to measure the amount of nitrate already present in the soil before applying nitrogen fertilizers. Other environmental factors that affect leaching include the amount of rainfall and the water supply in the respective field of study **(Padilla et al., 2018).**

- **Health hazards due to nitrate leaching**

  When nitrates reach groundwater or aquatic ecosystems, they can significantly impact oxygen levels. Elevated nitrate levels are particularly concerning for newborns and pregnant animals, as they can lead to anoxia and blue baby

syndrome (methemoglobinemia). This is a deadly disease that causes the skin color to turn bluish, resulting in increased heart rate, decrease in blood pressure, stomach ache, and vomiting. Additionally, nitrate leaching raises the risk of various cancers and infectious diseases **(Forster et al., 1982).**

- **Eutrophication**

Eutrophication is a condition caused by the accumulation of excessive nutrients in water bodies, leading to an increase in the population of aquatic organisms. This, in turn, significantly reduces the oxygen-carrying capacity of the water, resulting in the death of marine life **(Smith et al., 2009).**

Implementing effective management practices involves sampling soil to measure nitrate concentrations and understanding the drainage system of the area. While nitrate is essential for food production, excessive application should be avoided. Water content and residual nitrate levels in the soil should be monitored, and the water supply should be managed in a controlled manner. Balanced fertilizer use involves applying essential plant nutrients in the correct amounts and proportions at the right time and by using the most suitable methods. Soil water movement can be managed in two ways: by monitoring water uptake by plants and by assessing the water left in the soil. Proper management of water addition involves keeping track of the timing of water application and checking the remaining soil moisture. Besides such practices, intensive research of particular cropland in different ecological zones is essential **(Gilbert et al., 2005).**

1.3.3 Nitrogen loss by denitrification

Biological nitrogen loss occurs when nitrates and nitrites are reduced into different volatile gases, commonly nitrous oxide, dinitrogen oxide, or nitrogen gas. This process is primarily carried out by a range of microorganisms that use nitrate as an electron acceptor instead of oxygen. The formation of nitrous oxide

gas leads to environmental pollution by reacting with the ozone layer in the atmosphere. Denitrification is influenced by several key factors, including:

- Soil saturated with water and lack of air in its pore spaces
- Dense soil conditions where the soil particles become compact
- Ambient warm temperature of soil and aeration
- Easily breakable organic matter

These factors create an anoxic environment suitable for denitrification, resulting in nitrogen unavailability for healthy crop growth (**Ward et al., 2009**).

1.3.4. Crop Removal

When crops are withdrawn from fields, it results in nitrogen losses. It greatly impacts soil quality, water, and the sustainability of agriculture. This has a long-term impact on the overall nutrient content of the soil. Leaving the crop residues on the field generally enhances soil nutrient levels, leading to increased crop productivity **(Blanco-Canqui et al., 2009).**

1.3.5. Soil Erosion and Runoff

Soil erosion is the removal of soil particles, which can occur naturally due to weather calamities or crop harvesting. It is often exacerbated by poor agricultural practices or human activities. Erosion greatly reduces the land's water-holding capacity, which can lead to the loss of natural microbiota from the area, ultimately degrading soil quality. This negatively impacts natural resources and can result in land abandonment. Uncontrolled rainfall and wind are the main reasons behind soil erosion and runoff. When the soil's water retention capacity is exceeded, surface soil is carried away. Soil erosion is followed by the detachment of soil particles by water flow, rainfall, and water splash, which continues with the transportation of the detached soil particles through the running water. To control soil erosion, various practices should be implemented based on the specific situation, including cultural protocol and structural framework, which involve

changing the landform and studying the topographical features of a particular area **(Zuazo et al., 2009).**

Forms of soil erosion:

- **Erosion caused by rainwater**: Rainwater-induced erosion occurs when raindrops strike the soil surface, dislodging and washing away fine particles from the topsoil.
- **Erosion caused by wind**: Wind can move loose soil from one location to another. While it is a natural process, it can become severe during strong winds or storms.
- **Erosion due to rill formation**: Heavy rainfall can cause small rills or channels around the hillside, making farming difficult.
- **Concentrated flow erosion or gully erosion**: This occurs when water forms shallow channels during heavy rainfall.

Soil erosion can be managed by implementing proper ground cover in farming areas. Areas prone to erosion from heavy rainfall or wind should adopt soil conservation practices. Additionally, different tillage methods should also be taken into consideration **(Telkar et al., 2015).**

1.4 Fertilizers

Fertilizers play a vital role in crop growth and development by providing essential nutrients such as nitrogen, potassium, and phosphorus. These nutrients boost overall productivity by enriching soil quality, raising crop yields, and supporting global food production. In addition to the primary nutrients, plants also require smaller amounts of secondary nutrients, including sulfur (S), magnesium (Mg), calcium (Ca), zinc (Zn), iron (Fe), boron (B), manganese (Mn), copper (Cu), molybdenum (Mo), chlorine (Cl), nickel (Ni), and iodine (I) **(Alley et al., 2009).** Apart from providing essential nutrients, fertilizers also enhance the soil's water-holding capacity and improve aeration. With the growing global population, the

demand for food continues to rise, making it challenging to enhance food production and achieve high-quality crop yields without fertilizers that supply essential nutrients.

The three main macronutrients (NPK) are:

- Nitrogen (N): Essential for energy metabolism, synthesis of protein, and growth of leaves and stems.
- Phosphorus (P): Required for cell division and development of growing tip of roots and leaf.it is the main component of ATP that is essential for energy transformation.
- Potassium (K): It promotes cell growth, flowering, and fruit production, and plays a role in water uptake, pest control, and disease management **(Delgado et al., 2016).**

The most widely used fertilizer is nitrogen fertilizer. Nitrogen is a vital component of amino acid, nucleic acid, and a major component of chlorophyll where photosynthesis takes place which converts carbon dioxide to sugar and oxygen. Based on the sources there are two types of nitrogen fertilizers **(Frink et al., 1999):**

- **Organic and natural sources:** Nitrogen from these sources is naturally released through the fermentation and decomposition of materials such as manure, compost, animal waste, and fish emulsion. This type of fertilizer contributes to more sustainable crop production.
- **Synthetic or chemical:** Here nitrogen is transformed into different nitrogen-based forms like nitrates or ammonium and in this type of fertilizer the percentage of nitrogen varies, typically in the range 26-32%.

From the microbiological aspect, the involvement of two enzymatic reactions greatly affects the efficacy of nitrogen-based fertilizers **(Fixen et al., 2002):**

- **Urease enzyme:** This soil enzyme is accountable for the hydrolysis of the applied urea. The source of the urease enzyme is the microbial community present in the soil that possesses this enzyme and catalyzes the hydrolysis of urea to ammonium ($NH4^+$) and bicarbonate ion (HCO_3^-).
- **Ammonia oxidizing bacteria:** This class of bacteria performs nitrification by oxidizing ammonia to nitrite. This ammonia-oxidizing bacteria or nitrifying bacteria belong to the species of genera *Nitrosomonas*, *Nitrosococcus*, etc. Nitrite-oxidizing bacteria such as *Nitrobacter* oxidize nitrite to nitrate.

1.4.1. Fertilizer classification

Fertilizers can be classified in various ways based on the type of nutrients they supply **(Bafoev et al., 2022):**

- **Single nutrient fertilizers:** These fertilizers provide single primary nutrients such as nitrogen, potassium, or phosphorous. They are also called straight fertilizers.
- **Multi-nutrient** fertilizers: These fertilizers are complex fertilizers that deliver a combination of nutrients, such as nitrogen and phosphorus.

Straight single-nutrient fertilizers include two key straight nitrogen-based fertilizers ammonia (NH_3), and ammonium (NH_4^+), and their solutions such as ammonium nitrate, urea, calcium ammonium nitrate, and calcium nitrate. Superphosphates are among the straight phosphate-based fertilizers. Two types of superphosphates are: single superphosphate comprising 14-18% P_2O_5 and triple superphosphate consisting of 44–48% of P_2O_5. Double superphosphate is made up of a combination of single superphosphate with triple superphosphate. Most superphosphates are highly soluble in water **(Young et al., 1980).**

Multi-nutrient fertilizers contain more than one nutrient component which includes (**Ni et al 2012**):

- Binary fertilizers which include NP, NK, and PK. The major two component binary fertilizers are nitrogen and phosphorous. Monoammonium phosphate ($NH_4H_2PO_4$) or MAP which has 11% nitrogen with 48% phosphorous pentoxide, diammonium phosphate $(NH_4)_2HPO_4$ or DAP which has 18% nitrogen and 46% phosphorous pentoxide are the major NP fertilizers.
- **NPK fertilizers** are three-component fertilizers containing nitrogen, phosphorus, and potassium, created by blending individual nutrient fertilizers. The NPK ratio is represented by three numbers, indicating the percentage of each nutrient present in the mixture.
- Other nutrients include micronutrients, which are absorbed in very small amounts. These are primarily needed for enzyme function, playing key roles in plant metabolism and enzyme-driven reactions. Boron, zinc, molybdenum, manganese, and iron are characteristic micronutrients that are supplied as water-soluble salts **(Shuman et al., 2017).**

1.4.2 Global consumption of agricultural fertilizers

The global consumption of fertilizer has increased severalfold over the decades. Due to the potential rise in human population fertilizer consumption is thought to increase rapidly with an increase in food production. Random use of fertilizers and lack of proper distribution and management of fertilizers worldwide has been a serious concern. This results in nutrient-deficient agricultural lands that limit the production of crops and insufficient food distribution affecting human health.

The consumption of chemical-based fertilizer in the year 1965 was about 46.3 million metric tons which almost jumped to 187.92 million tons in the year 2022. Fertilizers widely used in today's agriculture are typically composed of one or more of the three indispensable nutrients- nitrogen, potassium, and phosphorous

for the growth and improvement of plants. In the year 2022, data revealed that out of the three essential nutrient elements, nitrogen accounts for 58% of total globally consumed agricultural fertilizers followed by 23% and 18% of phosphate and potassium fertilizers respectively. Nitrogen has a noteworthy effect on global mineral use, followed by potassium and phosphate. Fertilizer consumption is the per unit usable plant nutrient in arable land. It quantifies the amount of plant nutrients **(Randive et al., 2021).**

Country	**Total N use in million tons per annum (MTPA)**	**N use in feeding and pasteurization (MTPA)**
China	18.70	3.00
India	11.90	NA
U.S.	9.10	4.70
France	2.50	1.30
Germany	2.00	1.20
Brazil	1.70	0.70
Canada	1.60	0.90
Turkey	1.50	0.30
UK	1.30	0.90
Mexico	1.30	0.30
Spain	1.20	0.50
Argentina	0.40	0.10

Table 1.3: Topmost consumers of nitrogen-based fertilizers (**Steinfeld et al., 2006**).

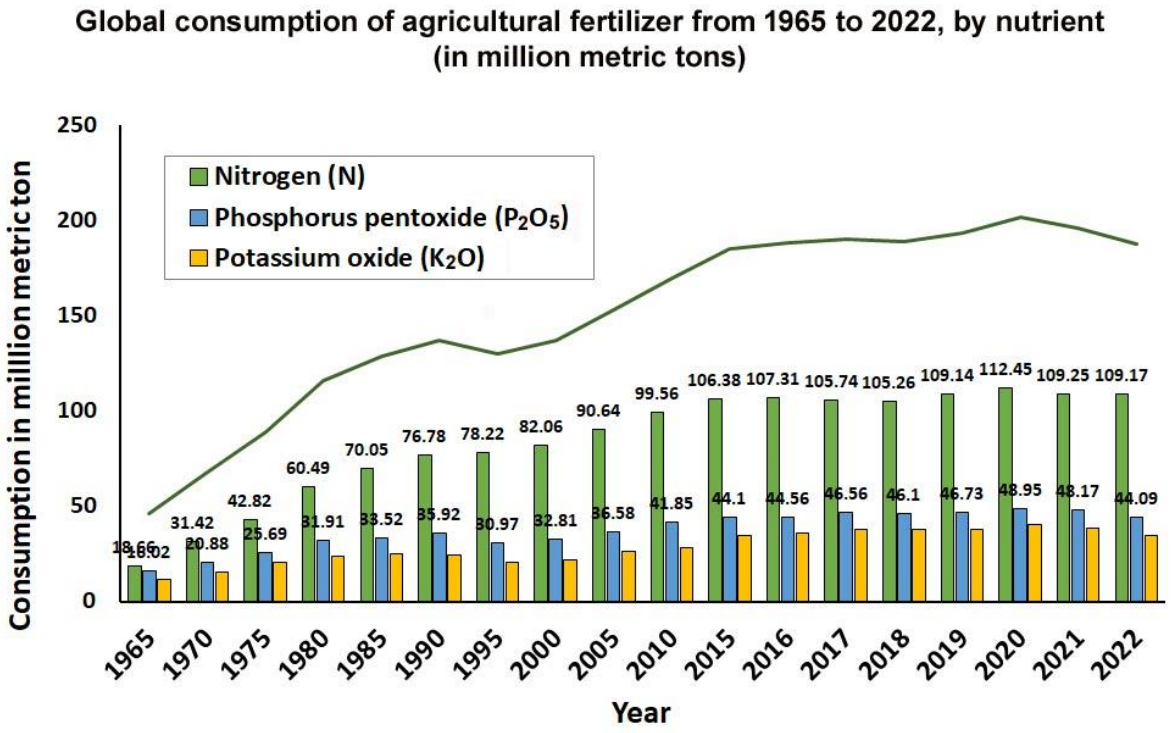

Figure 1.1: Global consumption of agricultural fertilizers from 1965-2022

Urea is the most widely used nitrogen-based fertilizer in today's market having the highest nitrogen content of almost 46%. This organic compound forms white crystals and has a neutral pH, making it adaptable to various soil types. It is a natural excretory waste product formed from the metabolism of proteins in humans, as well as in other mammals, amphibians, and aquatic animals. Urea has gained wide importance in agricultural sectors where it is used together as a fertilizer and animal food stabilizer **(Gasser et al., 1964).**

The use of urea fertilizers has increased tremendously over the last few decades in both advanced and emerging countries. It plays a key role in enhancing the growth of green leafy vegetables and supports optimal crop yields. Urea offers several benefits compared to other nitrogen-based fertilizers. These advantages include **(Gagnon et al., 2012):**

- Greater Nitrogen content
- Low production cost, naturally sourced

- Non-ignitable and involves no storage risk
- Versatile usage across a wide range of crops and soil types
- Impartial pH and safe towards all crops and soil

After application in soil, urea fertilizer is converted into ammonium carbonate through the action of the hydrolytic enzyme urease. While the ammonium ion remains stable in the soil, the unstable ammonium carbonate quickly breaks down into ammonia, carbon dioxide, and water **(Vitolo et al., 2022).**

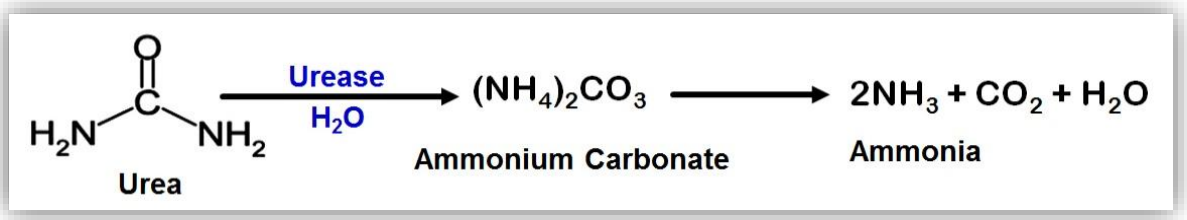

Figure 1.2: Reaction of urease on application of urea fertilizer

Urease primarily originates from soil microorganisms, though it can also come from plant and animal sources. In the soil, the enzyme exists in an accumulated form, bound to organic matter and soil particles, often forming complexes with humus. Accumulated urease in the soil exhibits higher activity than the urease newly produced by specific microorganisms. This stored enzyme rapidly hydrolyzes urea, raising the surrounding pH and generating ammonia, which is then released into the atmosphere **(Klose et al., 2000).** This free ammonia affects the germinating seedlings and hampers the growth of young plant, and it may also volatilize into the air. High concentrations of ammonia and elevated pH levels hinder the oxidation of nitrites to nitrates, leading to nitrite buildup. The increasing nitrite concentration can be severely toxic as it enters the nearby water bodies causing eutrophication and ammonia volatilization leading to air pollution. Up to 70% of nitrogen is lost through volatilization in the atmosphere, the average loss being 20-30% due to excessive urease activity after application of urea fertilizer. Nitrous oxide, a byproduct of denitrification, represents another form of nitrogen lost through volatilization. This gas not only contributes to the

depletion of the stratospheric ozone layer but also acts as a potent greenhouse gas, significantly impacting the atmosphere **(Ahmed et al., 2017).**

1.5.1 Urease

Urease, also known as urea aminohydrolase (E.C.3.5.1.5), was the first enzyme to be crystallized, a milestone achieved by Sumner in 1926. His discovery demonstrated that proteins could function as enzymes, paving the way for the broader understanding that most enzymes are proteins. Urease has since been isolated from various sources, including bacteria, fungi, algae, and higher plants. It is also recognized as the first metalloenzyme identified to contain nickel and possesses a high molecular weight. In 1995, P. A. Karplus successfully determined its crystal structure. Urease enzymes from various sources share similar amino acid sequences and typically consist of one to three polypeptide chains. Jack bean urease has a molecular weight between 480 and 545 kDa, with each molecule containing 845 amino acids, including 90 cysteine residues **(Caruso et al., 2024).**

The ureases of plant and fungal origin are homo-oligomeric proteins composed of identical 90 kDa subunits. In contrast, bacterial ureases consist of more than one subunit comprising (UreA and UreB), or three (UreA, UreB, and UreC) subunits having distinct molecular mass that forms different complexes.

Bacterial ureases consist of three subunits comprising of large catalytic alpha (α) 60-75kDa subunit, a smaller beta (β) 8-21kDa (β) subunit, and a smaller gamma (γ) 6-14kDa subunit, forming (αβγ) 3 trimers.

A unique urease is found in Helicobacter sp where it is made up of two different subunits, α (molecular weight between 26–31 kDa) and β (molecular weight between 61–66 kDa) **(Mobley et al., 2001).** Plants in addition to fungal ureases are assembled in two fashion trimmers and hexamers and consist of similar subunits of 90kDa each. A common example is jack bean urease which consists of two subunits that are structural and assemble to form protein complexes and

one subunit that is involved in catalysis, the α subunit being the active one (**Lippard et al 1995**). Ureases from a variety of sources (bacteria, plants, and fungi) display high homology in amino acid sequence although they are made of dissimilar subunits. The active site nearby to the nickel metal ions is highly preserved and performs mechanisms similar to that of the catalytic site **(Mazzei et al., 2017).**

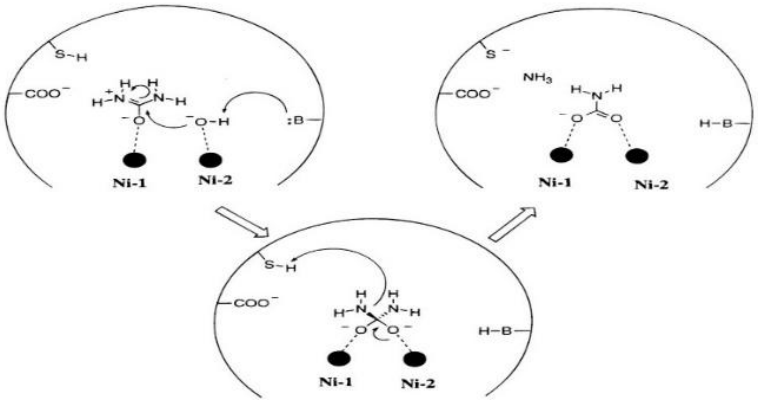

Figure1.3: Mechanism of urease reaction (*K.aerogenes*) as proposed by P. Andrew and Karplus in the year 1997.

Several mechanistic models have been proposed to explain the reaction catalyzed by urease, with contributions from numerous researchers (**Dixon et al., 1980; Zerner et al., 1991; Jabri et al., 1995; Karplus et al., 1997; Meyer et al., 1998; Ciurli et al., 1999**). A widely accepted feature across these models is the central role played by the enzyme's two nickel ions. One nickel ion binds and activates the urea substrate, while the other coordinates with and activates a nucleophilic water molecule.

Karplus et al. (1997) presented a detailed mechanism based on the crystal structure of *Klebsiella aerogenes* urease. In their model, the carbonyl oxygen of urea coordinates with the first nickel ion, whereas the second nickel ion binds the hydrolytic water molecule. This configuration supports hydrogen bonding between the four urea protons and the protein: three protons interact with backbone oxygen atoms, while the fourth forms a hydrogen bond with the cysteine residue Cys-319. The carbonyl carbon of urea is attacked by the

hydroxide of the second nickel atom to form the intermediate tetrahedral hydrated urea.

Ciurli et al. (1999) proposed an alternative mechanism in which urea, upon entering the active site, displaces three water molecules and fits snugly into the site due to its complementary shape and size.

Ureases derived from different sources exhibit a wide range of specific activities, which are highly influenced by factors such as pH, temperature, buffer composition, and ionic strength. Most microbial ureases, as well as plant-based ones like jack bean urease, typically show optimal activity around pH 7. However, certain microorganisms, such as *Spirulina maxima*, have a higher optimal pH of around 8.7, while a few rare acidophilic ureases function best at very low pH levels, around pH 2. The activity of urease, like that of many other enzymes, can be described using the Michaelis-Menten equation of enzyme kinetics.

Urease sources:	Molecular weight (kDa)	Specific activity (µmol urea/min mg protein)	K_m (Mm)	Optimum pH	Optimum temp. (°C)	Reference sources
Jack bean urease	480.0	35.0 (phosphate buffer, pH 7.0)	9.1			Goldstein et al., 1983; Martins et al., 1987; Huang and Chen 1991; Qin et al., 1994; Leszko et al., 1995; Elcin and Sacak, 1996; Krajewska et al., 1988.
		128.0 (phosphate buffer, pH 7.40)	3.1			
		23.6 (phosphate, pH 7.0)	2.0			
		75 (phosphate pH, 7.0)	2.47		60	
		46.35 (buffer free, pH 7.0)	7.5	7.2		
		56.4 (tris buffer, pH 7.20)	4.4			
		32.3 (phosphate buffer, pH 6.5)	2.82	7.0		
		18.90 (phosphate buffer, pH 7.0)	3.41			
Ureases (acidic):						
Lactobacillus fermentum	300.0		1.2	4.0	60-70	Matsumoto, 1993
Arthrobactur mobilis	240.0		3.6	4.41	35	Matsumoto, 1993
Other ureases (microbial origin):						
Aspergillus niger	250.0	1341	3.0	8.0		Smith et al., 1993
Arthrobacter oxydans	242.0	219	12.5	7.6		Mobley and Hausinger, 1989
Brevibacterium ammoniagenes	200.0	3570	18-72	7.0		Mobley and Hausinger, 1989
Klebsiella aerogenes	224.0	2200	2.8	7.75		Mobley and Hausinger, 1989
Proteus mirabilis	212.0	2057	13	7.5		Mobley and Hausinger, 1989
Providencia stuartii	230.0	5520	9.3			Mobley and Hausinger, 1989
Staphylococcus saprophyticus	250.0	150	7.36	6.8		Mobley and Hausinger, 1989
Ureaplasma urealyticum	380.0	180,000	2.5	7.2-7.5		Mobley and Hausinger, 1989
Aspergillus nidulans	240.0	670	1.33	8.5		Mobley and Hausinger, 1989
Spirulina maxima	232.0	9.27	0.12	8.7		Mobley and Hausinger, 1989

Table 1.4: The particular nature of ureases that are soluble from several origins.

1.6 Enzyme properties

Enzymes are biocatalysts that undergo catalysis in living systems. It reacts with substrates that act as reactants that are quite specific in nature. Enzymes act on specific substrates and produce specific products during the chemical reaction. They are protein in nature, but their activity is sometimes highly dependent on a non-protein counterpart called cofactor. During such situations when the enzyme catalysis is highly dependent on a cofactor, the inactive component is termed an apoenzyme. The cofactor can be typically a metal ion or an organic molecule, termed a coenzyme. The active enzyme component including the cofactor is called the holoenzyme. Enzymes are highly specific and catalyze a single reaction or group of reactions. The efficiency of the enzyme is dependent on pH and temperature. Some enzymes remain inactive in the absence of a reactant or a substrate. The efficiency of an enzyme to catalyze a reaction is called its activity. The amount of enzyme required for the conversion of one millimole of substrate into the product is defined as one international unit (IU) of enzyme activity. Sometimes activity is expressed by some pre-defined units. For example, when the rate of an enzyme-catalyzed reaction is very high then one enzyme unit can be defined as the amount of enzyme that will produce one mole of product from the substrate in one minute or one millimole of product in one second whereas on the rate of reaction is very slow then one enzyme unit is defined as one micromole product formed per minute or one nanomole product in one minute. Therefore, in enzyme activity, the unit in which it should be expressed must be mentioned clearly (**Cooper et al., 2000**).

According to **McDonald et al. (2023)**, enzymes can be broadly categorized into two main types:

- **Constitutive enzymes**: These enzymes are consistently present in the system, regardless of whether their specific substrate is available. The majority of enzymes belong to this category.

- **Inducible enzymes**: These enzymes are typically absent under normal conditions but are synthesized in response to the presence of their specific substrate. Their production is therefore regulated by substrate availability. Some of these enzymes exist in both active and inactive forms, with the inactive precursors referred to as *zymogens*.

1.6.1 Factors influencing reaction velocity of enzymes

A hyperbolic substrate saturation curve is obtained when reaction velocity is plotted against substrate concentration. This hyperbolic nature of the curve indicates that at a low concentration of substrate, the reaction velocity is directly proportional to the substrate concentration, it follows the first-order reaction kinetics initially concerning substrate concentration. Further increases in substrate concentration do not increase the reaction velocity and at high substrate concentration reaction follows zero-order kinetics with respect to substrate concentration. Additionally, enzyme concentration also affects reaction velocity, especially when the reaction is monitored at a fixed substrate concentration (**Cooper et al., 2000**).

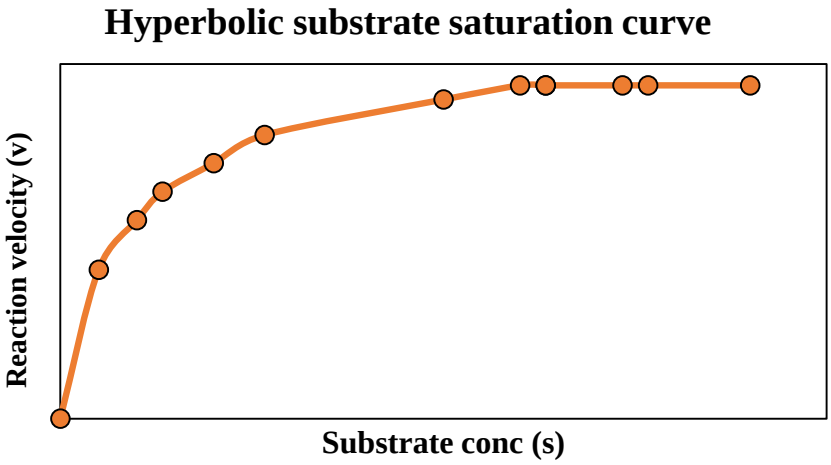

Figure 1.4: Hyperbolic substrate saturation curve

When reaction velocity (v) is plotted against enzyme concentration (E), initially a linear increase in velocity is observed with enzyme concentration. However, this linear relationship eventually breaks down at higher enzyme concentrations.

At low enzyme concentrations, the substrate is present in excess, enabling the reaction to occur at its maximum rate; therefore, the reaction velocity is directly proportional to the enzyme concentration. As enzyme concentration increases, the available substrate may no longer be sufficient to maintain maximum reaction velocity. This leads to a deviation from linearity, as the enzyme becomes unsaturated due to limited substrate availability.

The substrate concentration required for the reaction to proceed at maximum velocity is known as the substrate saturation level. At higher enzyme concentrations, a proportionally larger amount of substrate is needed to saturate the enzymes. If this level is not reached, the reaction cannot proceed at its maximum rate. Therefore, during in-vitro enzyme activity assays, enzyme concentrations are typically kept low to ensure the reaction follows first-order kinetics with respect to enzyme concentration **(Bugg et al., 2012).**

When product formation (P) is plotted against reaction time, it initially shows a linear relationship, indicating that product formation is directly proportional to time. This occurs because the substrate concentration is high at the start, allowing the reaction to proceed at maximum velocity. However, as the reaction progresses, the substrate is gradually converted into product, leading to a decrease in substrate concentration. Once the substrate concentration drops below the saturation level, the reaction no longer proceeds at maximum velocity, and the linear relationship breaks down. Therefore, in in vitro activity assays, the reaction should be monitored only during the phase when product formation remains proportional to time.

Reaction velocity is also influenced by the pH of the reaction medium. When reaction velocity is plotted against time typically forms a bell-shaped curve. This curve indicates that at a particular pH, the reaction proceeds with maximum velocity and this pH is known as the optimum pH of the enzyme. When the pH is below or above the optimum pH the reaction does not proceed with maximum

velocity. For most of the enzymes, the optimum pH lies between 6 to 7.5 **(Bianucci et al., 1990).**

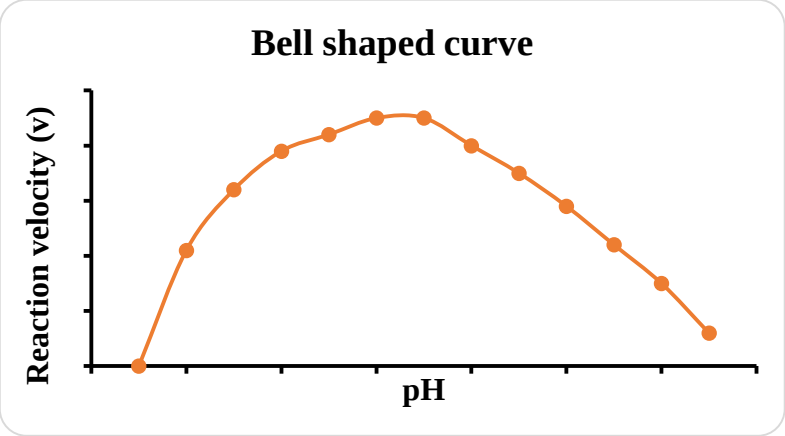

Figure 1.5: Bell- shape enzyme kinetics curve

Enzymes are protein molecules composed of amino acids linked together by peptide bonds. Depending on the pH, these amino acids can undergo ionization, resulting in specific ionic forms within the protein structure. Though the carboxylic group and amino group are involved in peptide bond formation, only one amino group and one carboxyl group remain free which capable of ionization. Additionally, the side chains of amino acids can also ionize, leading to different ionic forms of the enzyme at various pH levels. The ionic form present at the enzyme's optimal pH is typically its most active state **(Bianucci et al., 1990).**

Temperature also plays a significant role in affecting the rate of a reaction. When reaction velocity is plotted against temperature, a bell-shaped curve is obtained which indicates that every enzyme has an optimum temperature where it shows maximum activity. As the temperature rises, the reaction rate typically increases; however, excessive heat can lead to denaturation of the enzyme by destructing its secondary and tertiary structures, which are essential for its activity. Consequently, enzyme activity decreases at elevated temperatures due to the loss of structural integrity. While the optimal temperature for most enzymes is approximately 30°C, some enzymes retain their activity even at higher temperatures. Therefore, for in vitro activity measurements, it is important to

maintain the reaction at the enzyme's optimal pH and temperature **(Belgasem et al., 2015).**

1.6.3 Enzyme kinetics

Michaelis first proposed that enzymes interact with substrates to form an enzyme-substrate complex, which subsequently breaks down to yield the enzyme and the product. He also proposed that this process follows the law of mass action. He also noticed that one molecule of substrate usually combines with one molecule of enzyme and at the early stage of the reaction, the amount of product formed is minimal, allowing the reverse reaction to be disregarded **(Cornish-Bowden et al., 2013).**

$$E + S \underset{k_{-1}}{\overset{k_1}{\rightleftharpoons}} ES \xrightarrow{k_2} P + E$$

If K_1, K_{-1}, K_2 are the rate constant, at steady state the rate of formation of [ES] complex should be equal to rate of breakdown of enzyme substrate complex.

So, $K_1[E][S]-K_{-1}[ES]= K_2 [ES]$

Or, $K_1[E][S] =(K_{-1}+K_2) [ES]$

Therefore $[E][S]/[ES]=K_{-1}+K_2/K_1=K_m$

Or, $[E]/[ES]=K_m/S$ where $K_m$is the Michaeli's constant.

During any stage of reaction, some enzyme remains as free enzyme and some as [ES] complex

$E_{total}= [E]+[ES]$

Or, $[E]= E_{total}-[ES]=[E_t]-[ES]$

Therefore, $E_t-[ES]/[ES]=K_m/[S]$

Or, $[E_t]/[ES]=K_m/[S]+1=K_m+[S]/[S]$

Velocity(v) of the reaction is proportional to [ES] complex and the enzyme reaction will proceed with maximum velocity when the total enzyme binds with the substrate. So maximum velocity of enzyme is proportional to E_t.

Therefore, $V_{max}/v=K_m+[S]/[S]$

Or, $v=V_{max}[S]/K_m+[S]$

This equation is known as Michaelis Menten equation. When reaction velocity is half of maximum velocity then, $v=V_{max}/2$

Therefore, $v=V_{max}/2=V_{max}[S]/K_m+[S]$

Or, $K_m=[S]$

So, K_m is defined as the substrate concentration at which the reaction velocity is half of its maximum velocity, K_m has the unit that of substrate concentration and usually expressed in molar units. K_m is a constant for a particular enzyme and particular substrate. If E and S are altered, K_m also changes (**Cornish-Bowden et al 2013**).

$$\mathbf{K_m=K_{-1}+K_2/K_1}$$

$K_m$can also be defined in terms of rate constants and this constant changes with the change of enzyme or substrate and as a result K_m changes. When an enzyme acts on more than one substrate it will have different K_m for different substrate. The substrate for which K_m is the lowest is the best substrate for the enzyme. K_m is not the dissociation constant for the [ES] complex. It indicates affinity of enzyme for the substrate. Lower the K_m higher the affinity. To determine K_m and V_{max} of enzyme catalyzed reaction, it is first necessary to determine the reaction velocity of enzyme reaction at different substrate concentration. K_m can be determined by different graphical methods. By definition, K_m is the substrate concentration when reaction velocity is half of maximum velocity. From the hyperbolic substrate saturation curve, it is very difficult to calculate K_m. plot of inverse of reaction velocity and inverse of substrate concentration gives a straight line (**Chrisman et al 2023**).

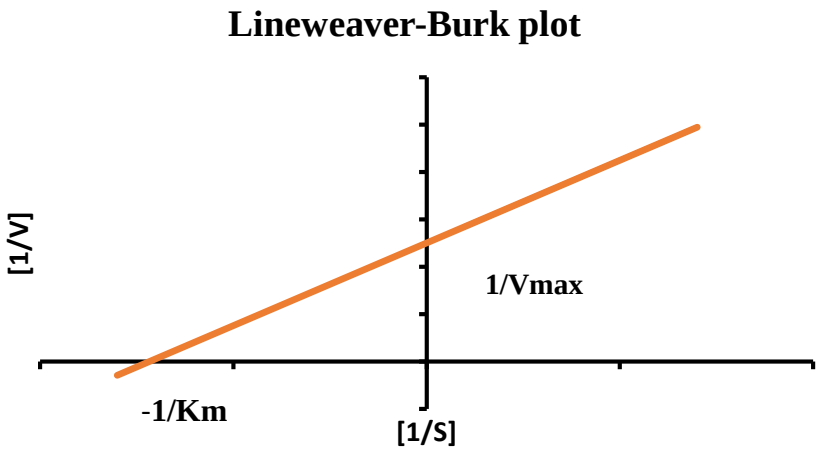

Figure 1.6: Lineweaver-burk plot of enzyme kinetics

The Lineweaver-Burk plot, also known as the double reciprocal plot, displays an intercept of 1/Vmax on the 1/velocity (1/V) axis and $1/K_m$ on the 1/substrate concentration (1/[S]) axis. It is commonly used to determine the values of K_m and Vmax **(Lineweaver et al., 1934).**

The enzyme urease catalyzes the hydrolysis of urea according to the Michaelis-Menten model of enzyme kinetics. In this process, urease quickly binds to urea, forming an enzyme-substrate [ES] complex that subsequently breaks down to release the free enzyme along with ammonia and carbon dioxide as products. The reaction rate increases with rising substrate concentration until it reaches a saturation point, where all urease active sites are fully occupied by urea **(Chen et al., 2010).**

The kinetic parameters of urease, K_m and Vmax, are significantly affected by both pH and temperature. The K_m values typically range from 1 to 4 mM, depending on the pH conditions. At room temperature, urease exhibits a bell-shaped Vmax profile with optimal activity observed between pH 7 and 8. However, K_m values reported in the literature can vary significantly based on the methodologies used to assess enzyme activity (**Ninfa et al., 2009**). Vmax also varies depending on the enzyme source and experimental conditions. For instance, urease isolated

from the microaerophilic human gastric bacterium *Helicobacter pylori* showed a Vmax of 1100 µmol/min/mg protein at 22°C in 31 mM Tris-HCl buffer at pH 8.0 (Dunn et al., 1990). In contrast, urease extracted from *Bacillus sphaericus* MTCC 5100, used for urea biosensor development, demonstrated a K_m of 2.0 ± 0.5 mM and a V_{max} of 1.82 µM/min **(Singh et al., 2017).**

Chapter 2

2.1 Urease inhibition

The rapid growth of the global population presents a major challenge in meeting the increasing demand for food production and safety. Urea fertilizer, currently the most widely used nitrogen fertilizer due to its high nitrogen content (46%), plays a crucial role in agriculture. However, up to 70% of its nitrogen content can be lost to the atmosphere through urease-catalyzed hydrolysis on the soil surface **(Wei et al., 2024).** To combat this issue, significant research has focused on urease inhibition as a means of slowing down the hydrolysis of urea. By delaying this process, plants are given more time to absorb nitrogen, thereby reducing ammonia volatilization and improving nitrogen bioavailability. Consequently, urease inhibitors play a vital role and offer a wide range of practical applications **(Da Fonseca et al., 2023):**

I. **Therapeutic Role*:*** Urease inhibitors play a key role in managing various health conditions such as peptic ulcers, kidney stone formation, hepatic encephalopathy, and pyelonephritis particularly those associated with urease-producing *Helicobacter pylori.*
II. **Prevention of Nitrogen Loss:** The use of urea fertilizer can negatively impact the environment through processes like urea hydrolysis, nitrification, and denitrification, which release greenhouse gases (NH_3, CO_2, N_2O, NO) and contribute to nitrate leaching. These effects not only harm the environment but also reduce nitrogen availability for crops, leading to decreased food production. By slowing urea breakdown, urease inhibitors minimize nitrogen loss, enhance fertilizer efficiency, and contribute to a more sustainable and eco-friendly agricultural system.
III. A systematic approach to identifying and regulating enzyme-inhibiting compounds.

According to Upadhyay et al. (2012), urease inhibitors can be broadly classified into two main categories:

a. **Substrate analogs** – These compounds, such as hydroxyurea and thiourea, share structural similarities with urea and bind to the enzyme's active site in the same manner as the natural substrate.
b. **Mechanism-based inhibitors** – Compounds like phosphorodiamidates and imidazoles that interfere directly with the enzyme's catalytic mechanism.

Based on chemical structures, urease inhibitors are classified into four major groups:

1. **Thiolate anions** – These directly target the enzyme's active metallocenter.
2. **Hydroxamic acid and its derivatives** – These compete with urea for binding to the active site of urease.
3. **Substituted phosphorodiamidates** – Considered the most effective inhibitors, they strongly block enzymatic activity.
4. **Moderate inhibitors** – This group includes metal-chelating agents and ligands, such as fluoride ions and certain peptides, which bind to the nickel ions essential for urease function.

2.1.1 Inhibition by Heavy Metals

Heavy metals accumulate in soil over time and can substantially hinder the activity of urease enzymes. Urease is particularly sensitive to trace levels of heavy metals due to the presence of the cysteine residue (Cys 319) at its active site. These metals interact with the cysteine-rich region, forming mercaptide complexes that alter the enzyme's structure and reduce its activity. Heavy metals react with this cysteine-rich domain, forming mercaptide complexes that that alter the enzyme's structure and reduce its activity. The sulfhydryl group at the catalytic center is especially prone to binding with silver ions, resulting in the

formation of metal sulfides **(Zaborska et al., 2004).** Metals that generate insoluble sulfides tend to exhibit the strongest inhibitory effects. The relative inhibitory strength of various heavy metal ions has been outlined by **Huang et al., (2023)** as follows:

$$\mathbf{Ag^{+1}=Hg^{2+} > Cu^{2+} > Zn^{2+} > Cd^{2+} > Ni^{2+} > Pb^{2+} > Co^{2+} > Fe^{3+} > As^{3+}}$$

Metal ions are reported to show time-dependent inhibition, suggesting a slow-binding competitive inhibition mechanism. Initially, their effect on the enzyme is minimal, but as the interaction progresses, slight conformational changes in the enzyme facilitate stronger binding of the metal ions. The formation of mercaptides and the bridging of sulfate ions are closely linked to the solubility of the corresponding metal sulfides. Among the ions studied, Hg^{2+} and Cu^{2+} exhibit the strongest inhibitory effects due to the extremely low solubility of their sulfides. In contrast, Zn^{2+}, Cd^{2+}, Ni^{2+}, Co^{2+}, and Pb^{2+} act as moderate inhibitors due to their comparatively higher sulfide solubilities. As^{3+} appears to be the weakest inhibitor, likely due to its relatively low sulfide solubility compared to the others **(Doelman et al., 1986).**

Heavy metal compounds	**Cation of metallic compound**	**Percent inhibition in slit clayey loam (%)**	**Percent inhibition in clayey loam (%)**
Silver nitrate	Ag^{+}	65	60
Silver sulfate	Ag^{+}	63	61
Cuprous chloride	Cu^{+}	16	14
Lead nitrate	Pb^{+}	3	2
Mercuric chloride	Hg^{2+}	42	38
Mercuric sulfate	Hg^{2+}	40	16
Cupric chloride	Cu^{2+}	16	13
Cupric sulfate	Cu^{2+}	14	15
Lead chloride	Pb^{2+}	4	4
Cobaltous chloride	Co^{2+}	4	6
Nickelous chloride	Ni^{2+}	1	2

Gold chloride	Au^{3+}	18	20
Chromium chloride	Cr^{3+}	3	2
Zinc chloride	Zn^{2+}	0	0
Manganous chloride	Mn^{2+}	0	0
Ferric chloride	Fe^{3+}	0	0

Table 2.1: Urease inhibition percentage of heavy metals on two types of soil (**Bremner et al., 1971**).

2.1.2 Hydroxamic acid inhibition

Hydroxamic acid derivatives have been extensively studied as a significant class of urease-specific inhibitors, primarily functioning through non-competitive inhibition. This class of inhibitors was discovered by **Kobashi et al., 1962** and has been evaluated against various sources of urease including plant-based enzymes like jack bean urease and microbial enzymes from species such as *Escherichia coli*, *Proteus mirabilis*, *Proteus vulgaris*, and *Staphylococcus aureus*. Acetohydroxamic acid (AHA) has been the most widely studied inhibitor in this category. Due to its structural similarity to urea, AHA is a stable, weakly acidic, and highly polar synthetic compound that effectively inhibits urease activity. It demonstrates rapid and complete inhibition of the metalloenzyme, with a Ki value of 5 µM at 25°C **(Fishbein et al., 1965).**

Hydroxamic acid chelates the nickel ions located in the active site of urease. It has been reported as an uncompetitive inhibitor of watermelon urease, with a Ki value of 2.5 mM **(Prakash et al., 2004).** In contrast, urease from *Klebsiella aerogenes* is inhibited competitively by AHA. The compound binds in a pseudo-tetrahedral coordination in a way similar to urea binding and act as a monodentate ligand. Additionally, AHA has been explored as a therapeutic agent for *Helicobacter pylori* infections in the gastrointestinal tract using a lipobead-mediated drug delivery system **(Smith et al., 1993).**

The effect of eleven mono hydroxamic acids was examined on ammonia volatilization from urea fertilizers. Among them, caprylohydroxamic acid and

AHA showed the highest inhibitory effects, reducing ammonia loss by 25% and 6%, respectively, after eight days of incubation. In contrast, compounds such as N-phenyl-chloropropionohydroxamic acid, dimethylaminopropionohydroxamic acid, and bromoacetohydroxamic acid exhibited only 3%, 5%, and 8% inhibition after one day of incubation, with no observable effect beyond the first day **(Kiss et al., 2002).**

Inhibition of soybean urease by seven omega-(naphthoxy) alkanohydroxamic acids has been reported to be more effective at lower concentrations compared to acetohydroxamic acid, benzohydroxamic acid, and phenoxy-acetohydroxamic acid. These compounds were applied as additives to urea fertilizers at concentrations ranging from 0.1% to 5%. An additional benefit of these inhibitors is their ability to suppress the development of soil-borne pathogens without negatively impacting crop growth **(Kobashi et al., 1978).**

2.1.3 Fluoride inhibition

Fluoride inhibition was first observed in bovine rumen urease (Kumar et al., 2010). It was later identified to inhibit both jack bean urease (JBU) and watermelon urease by different binding modes. It acted as a competitive inhibitor in the case of JBU and a non-competitive inhibitor in the case of watermelon urease. Urease from *Klebsiella aerogenes* has also been reported to undergo inhibition by fluoride in a pseudo-uncompetitive mode. Fluoride binding weakens in the presence of the substrate, and its dissociation rate decreases as substrate concentration increases. As a result, fluoride functions as a slow-binding inhibitor both in the presence and absence of urea. Its binding is also pH-dependent, with fluoride replacing the water molecule typically bound at the enzyme's active site **(Todd et al., 2000).** Kinetic studies on *Sporosarcina pasteurii* urease have shown that fluoride targets the conserved metal ion catalytic site. Initially, one fluoride ion binds competitively to a nickel (II) ion, while other binds uncompetitively by bridging with a hydroxide ion. This dual binding interferes with the nucleophilic

attack on urea, effectively inhibiting the enzyme's activity **(Todd et al., 2000; Benini et al., 2014).**

2.1.4 Thiols inhibition

Urease inhibition by thiol compounds has been well documented, with most thiols acting as competitive inhibitors. Among them, cysteamine, which contains a positively charged beta-amino group, has shown effective inhibitory activity. In contrast, thiol compounds with an anionic carboxyl group, such as cysteine and 3-mercaptopropionate, are relatively poor inhibitors. A major limitation of thiol-based inhibitors is their lack of specificity **(Krajewska et al., 2007).**

2.1.5 Phosphorodiamidate (PPD) Inhibition

Phosphorodiamidates (PPDs) represent another class of synthetic urease inhibitors known for their strong inhibitory effects. The inhibition begins with compounds like phosphoramidate and diamidophosphate, which are modified into more effective forms such as phenyl phosphoramidates and N-acyl phosphoric triamides. The phenyl phosphorodiamidate is known to obstruct the urease enzyme activity in urease-synthesizing bacteria present in the soil.

Simple phosphoramidates irreversibly inhibit jack bean urease, exhibiting a Ki value of 1.9 mM and a dissociation rate of 8.4×10^{-4}/sec **(Amtul et al., 2002).** Amido products of phosphoric and triphosphoric acids and N-acyl products of phosphoric triamides inhibit soil urease-producing bacteria such as *Proteus vulgaris*, *Mycobacterium smegmatis*, *Ureaplasma urealyticum*, and *Proteus mirabilis*. Phenyl phosphoramidates, though relatively slow inhibitors, demonstrate stronger inhibition against plant urease compared to other types. They exhibit tight binding to the nickel-chelated active site of the enzyme.

PPDs are considered a promising group of synthetic inhibitors due to their unique molecular structure, which offers notable properties such as high specificity, durability, potent inhibitory activity, and low toxicity. These characteristics have

also opened the door to potential medical applications **(Byrnes et al., 1983).** Various PPD derivatives have been studied by **McCarty et al., (1990),** focusing on kinetic constraints in the pursuit of optimal inhibition.

Compounds	**Concentration for plant urease inhibition (nM)**	**Concentration for microbial urease inhibition(nM)**
phenylphosphorodiamidate	10-80	5-40
4-chlorophenylphosphorodiamidate	100-800	100-800
phosphoric triamide	5-40	5-40
benzamide (B P A)	100-800	100-800
N -(diaminophosphinyl)benzeneacetamide	100-800	200-1600
4-chloro-*N*-(diaminophosphinyl) benzamide	100-800	200-1600
N-(4-nitrophenyl) phosphoric triamide	100-800	100-800
N- (diaminophosphinyl)-3-pyridinecarboxamide	200-1600	200-1600
N-(diaminophosphinyl)-isopentenoylamide (IPA)	-	-

Table 2.2: Phosphorodiamidates derivatives studied for urease (plant and microbial) inhibition (**McCarty et al., 1990**).

This data reinforces earlier findings that these complexes act as slow-binding inhibitors, showing significantly higher affinity for plant ureases than for microbial ones.

The most known phosphoramidate that is used as a urease inhibitor in the field of agriculture worldwide is N-(butyl) thiophosphoric acid triamide (NBPT). NBPT

inhibits urease by forming a tridentate bond with the enzyme, including a carbamate bridge with an oxygen atom that links two metal ions. This interaction blocks the three active sites of the enzyme, and preventing urea from accessing the nickel-containing catalytic centre **(Cantarella et al., 2018).**

NBPT does not directly inhibit the urease but it is converted into its respective oxo-analogue called oxo-NBPT or N-(n-butyl) phosphoric triamide or NBPTO. Although the exact mechanism of this transformation remains unclear, NBPTO is highly effective at suppressing soil urease activity. This conversion process occurs rapidly under aerobic conditions within minutes a few hours of application depending on the soil type and environmental factors. Under anaerobic conditions, however, the transformation may take several days.

Since the mid-1990s, NBPT has been marketed in the United States under the trade name Agrotain and is now globally distributed under various commercial labels as a urea additive. Limus, which is a formulation of NBPT and NPPT (N-(n-propyl) thiophosphoric triamide has been tested successfully and has been marketed for the last few years **(Peters et al., 2022).**

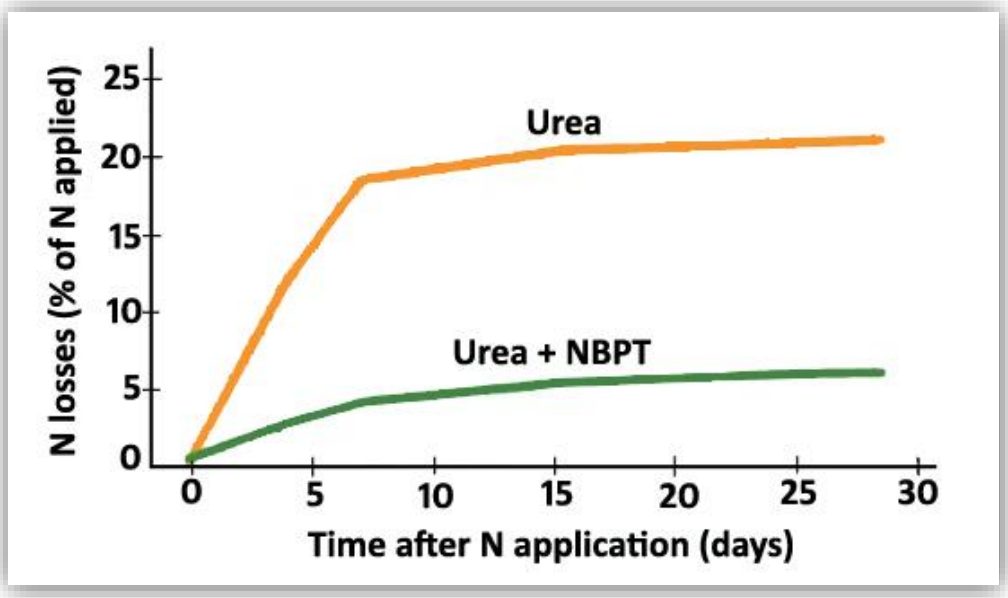

Figure 2.1: Percentage of nitrogen loss after NBPT application with urea fertilizers.

Findings by **Wang et al., (2020)** reveal that that NBPT-treated urea can reduce ammonia volatilization by up to 50%, depending on soil and climatic conditions. It generally is adsorbed by the plants which alters the metabolic pathways and thus hinders nitrogen assimilation by suppressing urease and glutamine synthetase activity.

The use of NBPT has been reported to have some adverse side effects, such as lip tip scorch, transient yellowing of leaves after application, and urea toxicity. Once applied to soil, NBPT undergoes microbial degradation, with the rate influenced by factors like soil pH, microbial activity, and temperature. The oxidized product of NBPT, NBPTO, is more prone to degradation. Although disruptions to the plant's internal nitrogen metabolism caused by NBPT are typically short-term, they can still affect plant health. In acidic soil conditions, NBPT degrades faster compared to alkaline conditions which affects the life span of the inhibitor thereby unable to prevent nitrogen loss for a longer period. Temperature also plays a crucial role in its stability: in warm climates, NBPT can break down within 2 to 4 days, while in cooler environments, the degradation process may extend to 10 to 15 days. The overall effectiveness of such inhibitors largely depends on their persistence in the soil. Despite their widespread use, the long-term impacts of these compounds remain insufficiently understood. As a result, naturally derived compounds—particularly those from plant sources—that offer similar benefits may present a more sustainable alternative for agricultural use **(Trenkel et al., 2021).**

2.1.6 Hydroxyurea inhibition

Hydroxyurea is recognized as a potent inhibitor of jack bean urease, exhibiting approximately 50% inhibition at a concentration of around 5×10^{-5} M **(Gale et al., 1965).** When the inhibitor is added prior to the substrate and followed by incubation, the degree of inhibition increases over time. In contrast, simultaneous addition of the substrate and inhibitor results in a significantly lower level of

inhibition. Recent studies have highlighted the enhanced inhibitory potential of N-substituted hydroxyurea derivatives. Among sixteen hydroxyurea derivatives evaluated, those substituted with *m*-methyl and *m*-methoxy-phenyl groups demonstrated the strongest urease-inhibiting activity. They are more efficient in inhibiting jack bean urease compared to hydroxyurea which is a weak competitive inhibitor**.**

2.1.7 Inhibition by α-Hydroxyketones and α-Diketones

Thirteen α-hydroxyketones have been evaluated for their ability to inhibit urease, particularly plant-derived urease. Among them, compounds such as 2,2'-thenoin, furion, 2-hydroxy-1-phenylethanone, and acetol demonstrated notable inhibitory activity, with IC_{50} values of 0.18 mM, 0.36 mM, 0.47 mM, and 2.9 mM, respectively **(Tanaka et al., 2004).** The effectiveness of these inhibitors is influenced by their structural characteristics and the absence of sulfhydryl groups. It is suggested that these compounds may interact with cysteine residues in the enzyme's active site; however, the exact mechanism of inhibition remains to be elucidated.

2.1.8 Triketone oxime inhibition

Triketone oximes act as nickel ion chelators and inhibit urease activity by competitively binding to the enzyme's active site, thereby preventing urea from accessing it. This results in partial or complete inhibition of urea hydrolysis. The inhibition constant (K_i) for triketone oximes ranges from 2.7 to 143 µM, depending on their specific structural configuration. For optimal inhibitory activity, the molecule should have a carbonyl group at position one, an alkyl group at position two, and a $–COOCH_3$ group at position four of the ring structure. The efficacy of their inhibition is not only dependent on their structure but also on steric factors especially for beta-triketones and triketoneoximes **(Tarun et al., 2004).**

2.1.9 Phosphate inhibition

Phosphate competitively inhibits jack bean urease at pH 7.0 which was reported in the year 1949. Inhibition studies conducted over a pH range of 5.80 to 8.07 involved varying concentrations of urea and buffer solutions to assess the effect of phosphate on JBU activity **(Harmon et al., 1949).** Results indicated that phosphate buffer did not inhibit urease at pH 7.48; however, the inhibitory effect increased as the pH decreased. An inhibition study on *Klebsiella aerogenes* urease demonstrated competitive inhibition within the pH range of 5.0 to 7.0. At pH levels above 7.0, the inhibition deviated from purely competitive behavior, and below pH 5.0, the urease enzyme became unstable **(Todd et al., 1989).**

2.1.10 Inhibition by Sulfur Compounds

Urease is classified as a sulfhydryl enzyme, meaning it contains reactive sulfhydryl (-SH) groups in its active site. As a result, compounds capable of oxidizing these groups can act as urease inhibitors. Ambrose et al. (1950) were among the first to report the inhibitory effects of sulfur-containing compounds on urease activity. The compounds tested included sodium sulfate, sodium benzene sulfonate, and sodium benzenesulfonate. Of these, sulfinates were found to be the most potent inhibitors, followed by sulfites, with sulfates and sulfonates showing comparatively weaker inhibitory effects **(Gould et al., 1978).**

2.1.11 Biscoumarins: A New Class of Urease Inhibitors

Biscoumarins are of natural origin and also can be synthesized by various methods. They possess different kinds of biological activities that include anticoagulant, molluscicide, antianthelmintic, hypnotic, and insecticidal **(Schonberg et al., 1954). Khan et al., (2014)** synthesized a series of biscoumarin derivatives and evaluated their urease inhibitory activity. These compounds exhibited a wide range of inhibition constants (K_i), from 15.06 to 91.35 µM. Among them, methylene-bis-4-hydroxycoumarin demonstrated the highest inhibitory potential, with an IC_{50} value of 15.01 µM. The degree of urease

inhibition was influenced by structural factors such as molecular size and electron-donating or withdrawing effects of the substituents **(Khan et al., 2014).**

Most commercially available synthetic urease inhibitors are often, unstable, and non-ecofriendly in nature. To enhance human health and boost food production, there is a growing need to explore plant-derived natural compounds as potential candidates for developing treatments for diseases associated with elevated urease activity, as well as for creating improved nitrogen fertilizer formulations. A significant challenge lies in developing urease inhibitors that are stable, non-toxic to both plants and animals, effective at low concentrations, compatible with urea-based fertilizers, and cost-efficient. Plant-derived urease inhibitors, along with their associated chemical classes, hold considerable promise for both agricultural and medicinal applications.

2.2 Potential phytochemicals in enzyme inhibition

2.2.1 Terpenoids

Terpenoids in plants are commonly found in the form of glycosides, esters, or or in protein-bound forms. These organic compounds occur abundantly in nature and exhibit a wide range of structural diversity. They are known to perform a variety of physiological functions in both humans and animals **(Brown et al., 2003; Takshak et al., 2014).**

- **Monoterpenoids**

  Vernonione, a novel derivative of 7-deoxycarvotacetone and a monoterpene isolated from the methanolic fraction of *Vernonia cinerascens* root extract, exhibited anti-JBU (jack bean urease) activity in a concentration-dependent manner, with an IC_{50} value of 227.6 μmol **(Ahmad et al., 2012).**

- **Diterpenoids**

  A diterpenoid ester isolated from the herb *Euphorbia decipiens*, featuring an amyrsinol-like skeleton, namely **3,7,15-Tri-O-acetyl-5-O-nicotinoyl-13,14-**

dihydroxymyrsinol, demonstrated moderate inhibition of the enzyme JBU, with an IC_{50} value of 81.9 mM. This activity was evaluated in comparison to the standard inhibitor, thiourea **(Ahmad et al., 2003).** Additionally, the same compound has been reported to inhibit microbial urease from *Bacillus pasteurii*, with a Ki value of 117.4 mM. Molecular docking studies further revealed that this compound acts as an uncompetitive inhibitor of urease **(Lodhi et al., 2006).**

- **Triterpenoids**

  The methanolic extract of *Plumeria rubra* yielded two triterpenoid compounds, Rubrajaleelol with an IC_{50} value of 24.2mM and Rubrajaleelic aciddemonstrating an IC_{50} of 58.9 mM, both of which demonstrated inhibitory activity against human urease **(Akhtar et al., 2013).** Isolation of Sorbicin A and Sorbicin B from the chloroform-soluble fraction of the methanolic extract of *Sorbus cashmiriana* revealed inhibition of jack bean urease (JBU), with IC_{50} values of 85.2 mM and 17.8 mM, respectively. Among these two triterpenoids, sorbicin B showed more potency in urease inhibition compared to sorbicin A and standard inhibitor thiourea having an IC50 value of 21.6 mM **(Kazmi et al., 2011).** Isolation of five bioactive compounds from the aerial parts of *Zygophyllum fabago* which sulfated saponins of ursane type. All these five compounds revealed inhibitory activity against urease from *B. pasteurii*. Of these, Zygofaboside A showed the highest activity, achieving nearly 87% inhibition at a concentration of 500 µM, compared to 98% inhibition by thiourea. Structure-activity relationship (SAR) analysis suggested that the presence of sulfate groups is crucial for urease inhibition, as they assist in anchoring the molecules to the enzyme's active site **(Khan et al., 2014).**

2.2.2 Phenolic Compounds

Plants produce phenolic compounds through specialized metabolic pathways. These compounds are characterized by aromatic benzene rings bearing one or

more hydroxyl groups and exhibit a wide range of biological activities, including antioxidant, antimicrobial, anti-inflammatory, antiviral, and enzyme inhibitory effects. They are derived from multiple plant pathways such as pentose phosphate, shikimate, and phenyl-propanoid pathways. Common examples of phenolic compounds include simple phenols, flavonoids, coumarins, xanthones, quercetin, stilbenes, and lignans **(Li et al., 2014; Carocho et al., 2013; Das et al., 1984).**

- **Phenols**

  A notable compound, 2-Hydroxy-3-methoxy-5-(2-propenyl)-phenol, found in the medicinal plant *Vernonia cinerascens*, has demonstrated anti-plant urease activity with an IC_{50} of 64.8 mM **(Ahmad et al., 2011).** Syringaldehyde, isolated from the stem bark of *Stereospermum acuminatissimum* K. Schum, showed adequate JBU inhibition with an IC_{50} value of 432.2mM **(Ramsay et al 2012).**

  Two phloroglucinol-type phenolic compounds, Indigoferin B with an IC_{50} value of 23.3 mM and Indigoferin C demonstrating an IC_{50} of 58.9 mM, were isolated from the cell walls of *Indigofera gerardiana*. Both compounds displayed potent inhibitory activity against JBU in comparison to the standard inhibitor thiourea showing IC_{50} values of 21Mm. Enzyme kinetic studies revealed that both acts as competitive inhibitors, with structure-activity relationship (SAR) analysis indicating that their aliphatic side chains play a crucial role in urease inhibition **(Tariq et al., 2011).**

  Isolation of Dalbergiophenol from the chloroform and ethyl acetate fractions of *Ranunculus repens*, exhibited inhibitory activity against JBU with an IC_{50} value of 35.01mM and and *Bacillus pasteurii* urease with an IC_{50} value of 25.63 mM. It functions as a competitive urease inhibitor, with its hydroxyl group playing a key role by interacting with the nickel ion at the enzyme's active site **(Khan et al., 2006).**

- **Phenolic Acids**

Numerous phenolic acids derived from various plant sources have been reported to inhibit urease enzymes from different origins.

Two purified compounds, Methyl gallate (MG) and 1,2,3,4,6-penta-O-galloyl-β-D-glucopyranose (PGG), isolated from the roots of *Paeonia lactiflora*, exhibited inhibitory activity against *Helicobacter pylori* urease. Among them, PGG showed stronger activity with an IC_{50} value of 72 mM, while MG exhibited moderate inhibition displaying an IC_{50} value of 242.6 mM, in comparison to the standard inhibitor acetohydroxamic acid (AHA) **(Ngan et al., 2012).**

Anacardic acid, isolated from *Anacardium occidentale*, inhibited both the growth of *H. pylori* and its urease enzyme, with an IC_{50} value of 20.5 mM. Molecular modelling studies confirmed that anacardic acid acts as a competitive inhibitor **(Kubo et al., 1999).**

Atranorin and ellagic acid, obtained from the stem bark of *Stereospermum acuminatissimum* K. Schum, displayed notable anti-JBU activity. The IC_{50} value of atranorin was found to be 18.2mM which appears to be higher than standard inhibitor thiourea having IC_{50} value of 21.7 mM while ellagic acid demonstrated effective inhibition with an IC_{50} value of 90 mM. Both compounds were identified as competitive inhibitors **(Ramsay et al., 2012).**

A prominent antioxidant compound, bergenin, extracted from the acetone bark extract of *Mallotus philippensis*, also showed anti-urease activity against *Bacillus pasteurii* urease. Molecular docking studies revealed that bergenin binds competitively at the enzyme's active site by interacting with the central nickel ion and surrounding amino acid residues **(Arfan et al., 2012).**

- **Phenylpropanoid Acids**

  Two phenylpropanoid acids, caffeic acid and isoferulic acid, isolated from *Vernonia cinerascens*, exhibited inhibitory activity against jack bean urease **(Ahmad et al., 2011).** Similarly, caffeic acid tetracosyl ester, a phenylpropanoic acid derivative obtained from the cell wall of the shrub *Hypericum oblongifolium*, demonstrated significant urease inhibition with an IC_{50} of 20.96 mM. This was slightly more effective than the standard inhibitor thiourea, which exhibited an IC_{50} of 21.03 mM **(Arfan et al., 2010).**

2.2.3 Stilbenes

Resveratrol, a well-known stilbene with strong antioxidant properties, was isolated from *Vitis vinifera* and demonstrated significant anti-urease activity against three different *Helicobacter pylori* strains. At a concentration of 1.75 mM, resveratrol inhibited nearly 90% of urease activity. Kinetic studies revealed that it functions as a non-competitive and reversible inhibitor of urease **(Paulo et al., 2011).**

An Oligostilbenoids, shoreaphenol, isolated from the stem bark of *Hopea exalata*, showed inhibitory activity against jack bean urease (JBU) with an IC_{50} value of 126.8 mM. Another naturally occurring compound, 2,3,4,4'-Tetrahydroxy-dihydrostilbene, commonly found in higher plants, displayed notable *H. pylori* urease inhibition with an IC_{50} of 30 mM in a time-regulated manner. Kinetic analysis indicated that this compound acts as a competitive inhibitor, and its urease-inhibitory effect was attributed to the presence of hydroxyl groups responsible for binding to the enzyme's active site **(Ge et al., 2006).**

2.2.4 Flavonoids

Flavonoids are a diverse class of natural compounds known for their complex structural variety, making them valuable in both medical and agricultural research. For example, gastritis and urinary tract infections are treated with flavonoids isolated from green tea and cranberries **(Loes et al., 2014).** Similarly,

flavonoids like daphnretusic acid, transilitin, dihydroluteolin, gossypol, gossypolone, and apogossypol, isolated from plants including *Daphne retusa*, *Pistacia atlantica*, and cotton, have demonstrated significant inhibitory activity against jack bean urease at micromolar concentrations.

Epigallocatechin gallate, gallocatechin gallate, gallocatechin, and epigallocatechin, which are catechin flavonoids abundant in green tea, have demonstrated inhibitory effects on *H. pylori* urease. Research suggests that these compounds function as competitive inhibitors of the enzyme **(Mansoor et al., 2014; Uddin et al., 2016; Chen et al., 2015).**

Quercetin, a flavone derived from the *Psidium guajava* plant, is a strong antioxidant and has demonstrated inhibitory activity against both jack bean urease and *Helicobacter pylori* urease **(Shabana et al., 2010).** Another two flavones, myricetin and luteolin, isolated from *Lonicera japonica,* were also found to inhibit *H. pylori* urease **(Xiao et al., 2012).** Datisdirin from *Datisca cannabina* Linn, ethyl acetate fraction 3'-Methylquercetin from *V. cinerascens* showed anti-JBU activity **(Ahmad et al., 2008).**

A quercetin derivative identified as quercetin-4'-O-β-D-glucopyranoside, isolated from *Allium cepa*, showed inhibitory activity against jack bean urease (JBU) with an IC_{50} value of 190 μM. Furthermore, two quercetin glycosides, avicularin and guaijaverin, extracted from *Psidium guajava*, also demonstrated notable anti-urease effects **(Shabana et al., 2010).**

Several flavonols including quercetin, myricitrin, rutin, and luteolin 7-O-glucoside, extracted from *Lonicera japonica* Thunb, were shown to inhibit *H. pylori* urease **(Xiao et al., 2012).** The flavone glucuronide baicalin, obtained from the roots of *Scutellaria baicalensis*, acted as a non-competitive inhibitor of JBU by targeting thiol-containing groups within the enzyme's active site **(Tan et al., 2013).** Scutellarin, another flavone glucuronide from *Erigeron breviscapus*, a traditional Chinese medicinal plant, was reported to interact with the enzyme's

sulfhydryl group in a concentration-dependent manner, as evidenced by molecular docking studies **(Wu et al., 2013).**

Rubranonoside, isolated from *Plumeria rubra*, exhibited anti-human urease activity with an IC_{50} of 212.3 μM **(Akhtar et al., 2013).** Some glycosyl flavonoids like vitexin, orientin, isoswertiajaponin and isoswertisin, derived from the butanol fraction of *Celtis africana*, were found to inhibit JBU. Their inhibitory activity is mainly due to the presence of sugar moieties that interfere with the enzyme's binding domain **(Perveen et al., 2011).**

2.2.5 Xanthones

Xanthones are bioactive organic compounds naturally occurring in certain higher plants, fungi, and lichens, and are known for their diverse medicinal properties. Two xanthones isolated from the shrub *Hypericum oblongifolium* namely 1,2,8-trihydroxyxanthone with an IC_{50} of 37.6 μm and 2,4,7-trihydroxyxanthone having IC_{50} of 138.4 μm exhibited strong inhibitory activity against JBU **(Arfan et al., 2010).** Hypericorin C, hypericorin D, and 1,2-dihydroxy-8-methoxyxanthone, three newly discovered xanthones from the root of the same plant showed considerable JBU inhibitory activity compared to the standard inhibitor, thiourea **(Ali et al., 2014).**

2.2.6 Coumarins

Coumarins are naturally occurring aromatic compounds recognized for their wide range of therapeutic benefits. One such compound, 7-hydroxy-4-methylcoumarin, found in the stems of *Lawsonia alba* Lam., has been reported to inhibit jack bean urease (JBU) with an IC_{50} value of 62.1 μM **(Uddin et al., 2013).** Six coumarin glycosides isolated from the roots of Daphne oleoides herb showed concentration-dependent inhibitory effects on both JBU and *Bacillus pasteurii* urease. The sugar moiety of these glycosides was found to play a crucial role in the inhibition mechanism **(Ayaz et al., 2006).**

2.2.7 Alkaloids

Alkaloids, naturally occurring nitrogen-containing organic compounds derived from various plants, play a significant role in inhibiting jack bean urease (JBU). Notable examples include 3'-hydroxyepiglucoisatisin and epiglucoisatisin, isolated from *Isatis tinctoria*, which have demonstrated inhibitory activity against both JBU and *Bacillus pasteurii* urease **(Ahmad et al., 2008).** Alkaloids extracted from *Corydalis govaniana* herbal plant such as govaniadine, caseadine, caseamine, and protopine also showed excellent JBU inhibitory activities, comparable to those of the standard inhibitor acetohydroxamic acid (AHA) **(Shrestha et al., 2013).**

2.2.8 Glucosinolates

Glucosinolates (GLs) are thioglucosidic secondary metabolites primarily found in angiosperms, particularly within the order *Brassicales*, and in families such as *Capparidaceae*, *Moringaceae*, and *Resedaceae*. Upon degradation, GLs yield biologically active compounds known as isothiocyanates (ITCs). Among the most widely studied GL-containing plants are members of the *Brassicaceae* family, including commonly consumed vegetables like cabbage, broccoli, cauliflower, Brussels sprouts, radish, and turnip. These compounds are most concentrated in the youngest plant tissues, although roots, stems, leaves, and seeds also contain significant amounts.

Studies have reported higher ammonium (NH_4^+-N) accumulation in soils treated with glucosinolate-rich plant tissues from *Brassicales* compared to those amended with lower GL concentrations **(Brown et al., 2009).** Plant juices from cabbage and Brussels sprouts have been shown to inhibit jack bean urease (JBU) activity **(Olech et al., 2014).**

Broccoli, in particular, demonstrates notable anti-urease properties. Compounds such as iberin and sulforaphane, isolated from broccoli, inhibited both JBU and *H. pylori* urease. The inhibition of two ureases by iberin displayed IC_{50} values of

178.8 mM and 190.5 mM respectively whereas sulforaphane inhibited two ureases with IC_{50} values of 216.8 mM and 225.7 mM, respectively. Their sulfur-containing moiety is mainly responsible for the inhibitory activity **(Fahey et al., 2013).**

2.3 Research Gap in Advancing Urease Inhibition Strategies

Plant secondary metabolites, known for their diverse chemical structures and biological functions, hold significant potential as natural urease inhibitors. This extensive knowledge base can be harnessed to guide the development of novel, safe, and cost-effective inhibitors. Such inhibitors could enhance both human and animal health through therapeutic applications, improve food quality and productivity, and contribute to the reduction of greenhouse gas emissions. However, several key challenges remain in this area. These include the identification and isolation of active compounds from promising plant extracts, the establishment of structure-activity relationships using in silico molecular docking studies, understanding the mechanisms of action of isolated natural compounds, and scaling up the production of these bioactive when they are scarce in nature.

Native plants that grow rapidly, are widely available, and possess notable nutritional and health-enhancing qualities represent valuable candidates for scientific investigation. These plants should contain a wide array of bioactive compounds and demonstrate the ability to adapt to diverse soil types and climatic conditions. Moreover, the presence of therapeutic properties such as antioxidant, antimicrobial, anthelmintic, and anti-inflammatory effects further increases their appeal. Genetic diversity across various geographic regions also adds to their potential utility. Notably, species rich in flavonoids and glucosinolates particularly those from the Brassicaceae family have emerged as strong contenders in the field of urease inhibition research.

Research has confirmed the presence of glucosinolates in various plant tissues, where they play a vital role in nitrogen accumulation and act as natural nitrification inhibitors. This, in turn, enhances the efficiency of urea-based fertilizers and supports increased food production. In addition to their urease inhibitory properties, plants from the Brassicaceae family have also been associated with anticancer, antimicrobial, and neuroprotective activities (Shankar et al., 2019). Glucosinolates (GLs) and their hydrolysis products, particularly isothiocyanates, have demonstrated activity against clinical isolates of *Helicobacter pylori* **(Na et al., 2023).** Notably, broccoli seeds and forage rape roots are rich sources of the aliphatic glucosinolate glucoraphanin, a precursor of R-sulforaphane known for its urease inhibition potential. Furthermore, selenium-containing glucosinolates (Se-GLs) have been reported in the tissues of cauliflower, broccoli, and rape **(Sharma et al., 2024).**

Building upon existing research, our focus shifted to the Cleomaceae family, a lesser-studied but phylogenetically related group to the Brassicaceae. This family shares several key characteristics, notably the presence of bioactive secondary metabolites like flavonoids and glucosinolates across different plant tissues. Among its members, *Cleome gynandra* stood out as a naturally thriving species found growing in household waste areas, requiring no external cultivation. Due to its phytochemical resemblance and similar biological activities to those observed in Brassicaceae species, *Cleome gynandra* was selected for further investigation. This plant is widely distributed throughout tropical and subtropical regions, favoring humid environments, and is commonly consumed as a leafy vegetable across South, East, and West Africa, as well as in South Asia **(Mishra et al., 2011).**

2.4 Previous Studies on *Cleome gynandra*

Cleome gynandra belongs to the family Cleomaceae (formerly classified under Capparaceae), within the subfamily Cleomoideae. Its genus shares a close

evolutionary relationship with the Cruciferae (Brassicaceae) family. African cabbage, wild spider flower, African spider flower, and cat's whiskers are a few preferred common names for this plant.This weed is widely distributed across tropical and subtropical regions around the world. Owing to its rich nutritional and medicinal properties, it is cultivated as a valuable crop in many rural communities. *C. gynandra* is an erect, branched, annual herbaceous plant that typically grows to a height of 250–600 mm **(Mishra et al., 2011).**

The stems of the plant are sticky due to the presence of glandular hairs and become woody as they mature. In India, it is known by the common names "karaila" or "kurkur." The plant produces bisexual flowers that elongate as the fruit develops, with the flower petals initially appearing white and gradually fading to pink or purple over time **(Shilla et al., 2019).**

The primary flavonoids identified in *C. gynandra* are quercetin, a flavonol glycoside, along with isorhamnetin and kaempferol. Among the glucosinolates found in *C. gynandra*, 3-hydroxypropyl glucosinolate is the most prevalent in most plants. Additionally, various methyl glucosinolates, such as glucocapparin (an aliphatic methyl glucosinolate) and glucocleomin (2-hydroxy-2-methylbutyl glucosinolate), have also been reported within the *Cleome* genus **(Mano et al., 2024).**

Cleome gynandra plants cultivated under controlled environmental conditions in greenhouse chambers have been found to produce higher levels of total glucosinolates, including those containing an indole moiety. Hydroxylated derivatives 4-hydroxy-3-indolylmethyl glucosinolate and 3-indolylmethyl glucosinolate were identified in spider plants growing in environmentally regulated conditions **(Omondi et al., 2017).**

2.4.1 Taxonomy and nomenclature

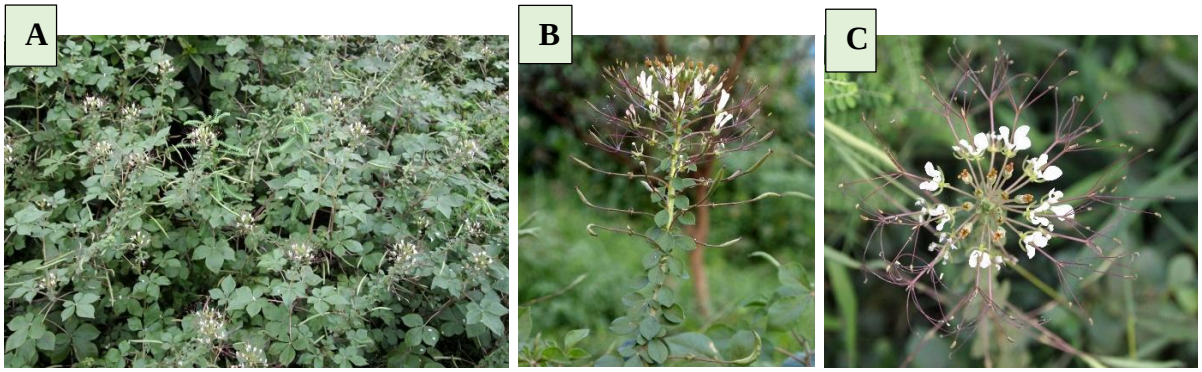

Figure 2.2: *Cleome gynandra* plant, (A) natural habitat where the plant grows, (B and C) the flower containing twig of the plant

Domain: Eukaryota

Kingdom: Plantae

Phylum: Spermatophyta

Subphylum: Angiospermae

Class: Dicotyledonae

Order: Capparidales

Family: Capparaceae

Genus: Cleome

Species: *Cleome gynandra*

2.4.2 Medicinal Importance

The use of tender leaves, shoots, and flowers of *Cleome gynandra* across various African and Asian countries has highlighted not only its nutritional value but also its medicinal significance. Though widely consumed as a vegetable, *C. gynandra* is renowned for its broad range of therapeutic properties. Every part of the plant (leaf, stem, root, flowers) has been of great importance in treating several

diseases. Various pain-related ailments like headache, stomach pain, chest pain, rheumatoid arthritis etc. are treated by the leaflet and flowers of spider plant **(Van den Heever et al., 2006).** A decoction made by boiling the leaves and roots is used to treat fevers, coughs, colds, and other respiratory issues. The seeds of the plant are ground into fine powder for the treatment of hemorrhages. Due to the high iron content in leaves treatment of anemic conditions has also been reported **(Omondi et al., 2017).**

2.4.3 Nutritional Properties

The young leaves, stems, shoots, and flowers of *Cleome gynandra* are rich in essential dietary nutrients, including vitamin E, vitamin C, provitamin A (carotenoids), and various minerals **(Glew et al., 2009).** Both micronutrients and macronutrients are present in the leaf of *C. gynandra*. Key macronutrients identified include potassium, magnesium, phosphorus, calcium, and sulfur, while micronutrients such as zinc, iron, and manganese are also present. In comparison to the commercially obtainable Swiss chard (*Beta vulgaris*) and cabbage (*Brassica oleracea*) the spider plant has higher levels of phosphorous, potassium, calcium, iron, and zinc concentrations **(Moyo et al 2018).**

In rural areas of the United Republic of Tanzania, up to 50% of dietary vitamin A intake is sourced from the leafy vegetable *Cleome gynandra* (spider plant). Using a high-performance liquid chromatography-photodiode array (HPLC-PDA) the existence of carotenoids, vitamin C and vitamin A has been confirmed in leaf, petioles, and young stems of *C. gynandra.* Alpha-carotene, beta-carotene, lutein, violaxanthin, and beta-cryptoxanthin are the main carotenoids found in spider plants. Since the human body cannot synthesize vitamins, they must be obtained through vitamin-rich foods, particularly those with antioxidant properties. Three vitamin E forms are present in the leaves of spider plant which includes alpha-tocopherol, beta-tocopherol, and gamma-tocopherol. Vitamin C which are water-soluble antioxidant has also been quantified in the leaves of this

plant which are present in greater concentration in contrast to Swiss chard as well as cabbage **(Gowele et al., 2019, Gee et al., 2011).**

2.4.4 Phytochemistry and pharmacological properties

Cleome species are rich in bioactive compounds that have great therapeutic interest and thereby this species has gained importance globally.

In the spider plant (*Cleome gynandra*), varying concentrations of phenolic acids such as hydroxycinnamic and hydroxybenzoic acids have been identified in the leaves. Additionally, other classes of compounds, including terpenes, flavonoids, and glucosinolates, are also present in notable amounts. Among these, phenolic acids are particularly recognized for their strong antioxidant, antimicrobial, and anti-inflammatory properties. Ferulic acid, a key phenolic compound, is known for a broad spectrum of biological activities, including anti-inflammatory, anti-allergic, antimicrobial, antiviral, anticarcinogenic, antioxidant, and vasodilatory effects **(Jiang et al., 2016; Singh et al., 2018).**

2.4.5 Antimicrobial Activity

Different solvent extracts of *Cleome gynandra* have demonstrated notable antimicrobial properties through standardized antimicrobial assays. The hexane and methanol fractions, in particular, exhibited antibacterial activity, as evidenced by zone of inhibition tests conducted on a range of gram-positive and gram-negative bacteria **(Heinrich et al., 2020).**

Among the tested bacterial strains, *Bacillus subtilis* and *Streptococcus faecalis* were the most susceptible, while *Escherichia coli* and *Pseudomonas aeruginosa* showed the highest resistance. The various plant parts and their different solvent fractions exhibited a wide range of antibacterial activities. *C. gynandra* also exhibited anti-fungal antifungal activity against seven fungal strains, including species from the genera *Candida*, *Trichophyton*, and *Aspergillus*. These effects

were confirmed using both zone of inhibition assays and microdilution tests **(Ajaiyeoba et al., 2020).**

2.4.6 Anthelmintic Activity

The treatment of parasitic infections in humans and livestock has long been a major concern, and the use of plant-based remedies is widely recognized. Extracts from the stem and leaves of *Cleome gynandra* have demonstrated significant anthelmintic activity against various parasitic worms, including three liver flukes and a tapeworm species—*Fasciola gigantica*, *Pheritima pasthuma*, and *Taenia solium*. The effectiveness of the methanol extract was assessed based on the time taken to induce paralysis and death in the parasites. Among the tested samples, the leaf extract exhibited stronger anthelmintic effects than the stem extract at equivalent concentrations. The results were compared against piperazine, a standard anthelmintic drug used as the positive control **(Ajaiyeoba et al., 2001).**

2.4.7 Anti-inflammatory activity

Almost all human disease is associated with pain and inflammation and exploring plant-based remedies for their treatment has become a significant area of research. The spider plant has shown promising anti-inflammatory effects in arthritic rat models, where it effectively restored plasma levels of lysosomal enzymes, carbohydrate-bound proteins, and TNF-alpha to normal. Furthermore, stem extracts of the plant reduced paw edema in rats by 47%, compared to 52% inhibition observed with the positive control **(Narendhirakannan et al., 2007).**

2.4.8 Immunomodulation and vasodilatory activity

Cleome gynandra, also known as spider plant, exhibits notable immunomodulatory effects that can enhance immune function, especially in

individuals with weakened immunity. By supporting the immune response, it may aid in combating infections and reducing the likelihood of diseases such as cancer. Traditionally recognized as a natural stimulant, the plant is considered a health booster for the improvement of the immune system. The ethanolic extract of the aerial part of the plant has been shown to stimulate immunity in a dose-dependent manner. Furthermore, the plant demonstrates vasodilatory properties, which may contribute to lowering the risk of cardiovascular diseases. These properties suggest that *C. gynandra* holds promise as a functional food supplement, offering protective and wide-ranging health benefits **(Kori et al., 2009; Runnie et al., 2004).**

2.4.9 Anticancer and antioxidant activity

Different solvent extract of *Cleome gynandra* have demonstrated significant antioxidant activity, as indicated by the DPPH assay. Methanolic leaf extract (50%) exhibited better radical scavenging activities compared to the water extract. Flavonoid fractions of spider plants have shown antioxidant activity by scavenging superoxide radicals on macrophages and lymphocytes. The methanol extract also exhibited anticancer activity by significantly reducing ($p<0.01$) the tumor size, and tumor mass and Ehrlich's Ascites Carcinoma (EAC) mice's life span expanded. In addition to its antioxidant potential, the methanol extract showed notable anticancer properties. It significantly reduced tumor size and mass ($p < 0.01$) in Ehrlich's Ascites Carcinoma (EAC) mice, while also prolonging their lifespan. Furthermore, the extract positively influenced hematological profiles such as hemoglobin level, erythrocyte count, and leukocyte count by relapsing to the usual level **(Bala et al., 2010; Heinrich et al., 2020).**

Chapter 3

3.1 Objectives of the study

The major objectives of the study are listed as follows:

1. Study and investigate new plant sources that can effectively and specifically undergo urease inhibition.
2. Collection of plant samples and preparation of extract based on solvent polarity starting from non-polar to polar solvents.
3. Study of each fraction's ability to inhibit urease inhibition and to determine the mechanism of enzyme inhibition using Lineweaver-Burk kinetic analysis.
4. HR-LCMS analysis for the identification of bioactive compounds in each fraction responsible for targeted urease inhibition.
5. Molecular docking studies to ascertain the binding affinity and interaction mode of the identified compounds with the urease active site.
6. Perform individual molecular dynamics (MD) simulations to evaluate the stability of the protein-ligand complexes depending on time scale.

Table 3.1: Methodological framework illustrating the aims of the study.

	Approach to the problem	Aim of the study
1.	Focus the study on investigating readily available local plant sources that significantly inhibit urease enzyme activity.	Study and investigate new plant sources that can effectively and specifically undergo urease inhibition.
2.	Collection of the targeted plant sample and sequential extraction of different fractions from different parts of the plant by following elution sequence.	Collection of plant samples and preparation of extract based on solvent polarity starting from non-polar to polar solvents.

3.	Kinetic analysis of the plant to study the affinity of each fraction toward the targeted enzyme and recognize the type or mode of enzyme inhibition to augment the efficiency of urea fertilizer uptake.	Study of each fraction's ability to inhibit urease inhibition and to determine the mechanism of enzyme inhibition using Lineweaver-Burk kinetic analysis.
4.	Identification of the bioactive compounds present in the sample extracts based on molecular formula and retention time.	HR-LCMS analysis for the identification of bioactive compounds in each fraction responsible for targeted urease inhibition.
5.	Examine the molecular interactions and binding affinities of bioactive compounds at the specific active site of the urease enzyme.	Molecular docking studies to ascertain the binding affinity and interaction mode of the identified compounds with the urease active site.
6.	Analyze the behavior and stability of the molecular system over time by simulating a dynamic virtual environment.	Perform individual molecular dynamics (MD) simulations to evaluate the stability of the protein-ligand complexes depending on time scale.

Chapter 4

INVESTIGATION, COLLECTION AND PURIFICATION OF THE SELECTED PLANT SAMPLE

4.1 Introduction

Natural urease inhibitors play a crucial role in mitigating negative effects in both medical and agricultural applications. An ideal plant source for such inhibitors should be fast-growing, widely distributed, ecologically dominant, and possess therapeutic potential due to its phytochemical constituents. Among the various plant groups, angiosperms represent the most dominant and diverse form of plant life globally.

Cleomaceae appears as a valuable plant model for its pioneering medicinal properties in the herbaceous plant family. About 3700 species of the Brassicaceae family are distributed in cooler climatic conditions whereas 270 species of its sister families are frequently scattered in warmer humid climatic regions.

Previously, Cleomaceae was classified under the Capparaceae family. However, advances in DNA analysis have led to its reclassification as a distinct family closely related to Brassicaceae. The three families Capparaceae, Brassicaceae, and Cleomaceae have been placed in a single order called Brassicales or Capparales **(Raza et al., 2020; Franzke et al., 2011).**

Families under the order Brassicales

- Akaniaceae
- Brassicaceae
- Capparidaceae
- Caricaceae
- Cleomaceae
- Gyrostemonaceae
- Limnanthaceae

- Moringaceae
- Pentadiplandraceae
- Resedaceae
- Salvadoraceae
- Tovariaceae
- Tropaeolaceae

Other families under the order Brassicales (very scarcely distributed)

- Bataceae
- Emblingiaceae
- Koeberliniaceae
- Setchellanthaceae

Following an extensive review of the literature and a thorough investigation into urease inhibition, our findings highlighted the significance of plant secondary metabolites, particularly flavonoids and glucosinolates, as well as the role of species within the Brassicaceae family in inhibiting urease activity. Guided by these insights, we selected *Cleome gynandra* as a suitable candidate for our study. This plant is commonly found around Kolkata, West Bengal, and grows abundantly in the region without requiring much care. Its seeds are widely dispersed by wind, water, gravity, and various human activities, reflecting its strong adaptability and high reproductive potential in its native habitat.

Cleome gynandra possesses long taproots with root hairs and a limited number of secondary roots. Its stems are sticky in texture and densely covered with glandular hairs. The plant exhibits a variety of pigmentations, ranging from pink to purple, often showing a blend of both hues. The leaves generally comprise five leaflets, with petioles measuring 25–50 mm in length and also bearing glandular hairs. Leaflets are obovate to elliptic in shape, with colors ranging from green to

deep green, and dimensions varying between 3–10 cm in length and 2–5 cm in width **(Mishra et al., 2011).**

4.2 Collection of Plant Sample

Cleome gynandra was collected during the monsoon season from areas surrounding Kolkata (22.5726°N, 88.3639°E). The plant was accurately identified based on characteristic features such as leaf structure, flower morphology, sticky stems, and root system. After collection, the samples were thoroughly cleaned to remove any dirt or mud.

An appropriate storage environment was essential to prevent pest infestation. The plant samples were sorted into different categories (roots, stems, leaves, and whole plants), and each was placed in separate, clearly labeled containers. These containers were stored in a cool, low-light setting. To ensure proper preservation, the storage area or containers were kept completely dry, with no residual moisture, and positioned in well-ventilated outdoor spaces away from direct sunlight.

Depending on the prevailing climatic conditions, complete air-drying of each plant part typically required between 7 to 14 days. The absence of moisture indicated that the samples were properly dried and ready for the next steps. Thorough drying is critical to ensure the quality and integrity of the plant material for subsequent use.

4.3 Raw Material Processing

The quality of plant samples is influenced by a range of factors, including the conditions under which the plant was grown, its geographic location, the stage of growth at the time of harvesting, weather conditions, the drying method employed, and the temperature during storage.

The initial handling of raw plant material is a critical step in preserving its bioactive constituents. This stage must be managed carefully to minimize the degradation or loss of valuable phytochemicals. Drying is particularly important, as it halts metabolic activity within the plant tissue and stabilizes its chemical composition. Proper drying also helps prevent microbial growth and contamination, while simultaneously reducing the volume and weight of the material, facilitating easier storage and transport.

After drying, each plant part was ground separately into a fine powder using a sample milling machine. Approximately 100 grams of each powdered sample was then weighed and stored in individual airtight zip-lock bags for further use.

4.4 Extraction

This initial stage plays a vital role in separating valuable bioactive compounds from the unprocessed raw plant material. Various extraction techniques are available, each based on different principles, including solvent extraction, distillation, pressing, and sublimation. Among these, solvent extraction is the most widely used method.

The selection of an appropriate solvent depends on several factors, such as the type of plant material, the specific part of the plant being utilized, and the availability of suitable solvents. Polar solvents commonly used include water and methanol, while non-polar solvents like hexane and ethyl acetate are also employed, depending on the nature of the target compounds.

The process of natural product extraction typically involves the following steps:

a) Perforation of solvent into the solid grid
b) Plant solute diffuse within the solvent
c) Diffusion of solute out of the solid grid
d) Extracted solute collection

Solvent selection is a critical aspect of the extraction process, as it directly influences the efficiency and quality of the extracted compounds. Key factors to consider include the solvent's specificity, solubility, reactivity, recovery potential, cost, and safety. An important consideration is the polarity of both the solute and the solvent, which aligns with the principle of "like dissolves like." Solvents with polarity values similar to that of the target solute generally exhibit higher extraction efficiency.

The particle size of the plant material also plays a significant role. It should be standardized to allow effective solvent penetration and optimal solute diffusion. However, excessively fine particles may result in over-absorption of solute, potentially complicating the purification process.

Maintaining an ambient temperature during extraction is essential. While moderate heat can enhance solubility and diffusion, excessively high temperatures may cause solvent evaporation, leading to the extraction of unwanted impurities or degradation of heat-sensitive compounds. Extraction efficiency typically increases with time, up to an optimal range, beyond which prolonged duration may not yield proportional benefits.

The solvent-to-solute ratio also affects extraction yield—the higher the ratio, the greater the yield, although excessive solvent volumes can extend the time required for subsequent concentration steps.

Extraction solvents are selected based on their polarity, ranging from non-polar to polar. It is often beneficial to use a combination of both polar and non-polar solvents for comprehensive extraction.

A typical polarity gradient of solvents, from non-polar to polar, is hexane, petroleum ether, diethyl ether, ethyl acetate, chloroform, dichloromethane, acetone, butanol, ethanol, methanol, and water.

4.4.1 Commonly used extraction methods for natural products

I. **Maceration:** Maceration is a straightforward extraction technique suitable for crude plant materials that are not finely powdered, such as stem bark or roots. In this method, the plant material is placed in a container, and solvent is poured over it until fully submerged. The container is then sealed tightly and left undisturbed for 3 to 4 days, with occasional stirring or shaking to enhance extraction. After the soaking period, the mixture is filtered, and the solvent is separated from the extract through evaporation, typically using a furnace or water bath. Although this method is time-consuming, it is particularly suitable for extracting heat-sensitive compounds **(Ingle et al., 2017).**

II. **Infusion:** In this method, the raw plant material is first ground into a fine powder and then placed in a container, into which the solvent is added. The solvent saturates the powdered material and is allowed to remain in contact for a relatively short duration. For effective extraction, the bioactive compounds must be readily soluble in the chosen solvent. The solvent-to-solute ratio typically ranges from 4:1 to 16:1, depending on the characteristics of the solute **(Pandey et al., 2014; Ingle et al., 2017).**

III. **Digestion:** Digestion is an extraction method that involves the application of gentle heat throughout the process. In this technique, the solvent is first poured into a clean, dry vessel, followed by the addition of finely powdered raw plant material. The container is then placed in a water or thermal bath maintained at a temperature of 45–50°C. This controlled heating reduces the viscosity of the solvent, thereby enhancing the extraction efficiency and facilitating the release of secondary plant metabolites **(Majekodunmi et al., 2015; Pandey et al., 2014; Ingle et al., 2017).**

IV. **Decoction:** This method is typically employed when the extract contains a significant amount of impurities. However, it is not suitable for volatile or

heat-sensitive plant materials. The process involves continuous heating in the presence of a specific volume of water. The dried, powdered plant material is placed in a clean, moisture-free container, and water is added with thorough stirring to ensure proper mixing. Heat is then applied for approximately 15 minutes to speed up the extraction process. The solvent-to-drug ratio is generally maintained at either 4:1 or 16:1, depending on the nature of the material **(Pandey et al., 2014; Azwanida et al., 2015**).

V. **Percolation:** This is an efficient extraction technique in which saturated solvent is gradually replaced with freshly prepared solvent. The apparatus used for this process is known as a percolator. The finely powdered sample is soaked in solvent and kept in a clean container followed by the addition of more solvents which is kept for 3 to 4 hours. The mixture is then transferred to a percolator and left undisturbed for 24 hours to allow complete saturation of the plant material. During this period, the lower outlet of the percolator remains closed. Extraction occurs through gravitational flow when the bottom outlet is opened, allowing the solvent to drain downward. The resulting extract is then filtered and decanted **(Ingle et al., 2017; Azwanida et al., 2015).**

VI. **Soxhlet Extraction:** Soxhlet extraction is a method that requires a continuous supply of heat for effective operation. The apparatus, known as a Soxhlet extractor, is typically made of glass and is available in various sizes. It consists of a round-bottom boiling flask, an extraction chamber, a siphon tube, and a condenser located at the top. The finely powdered, dried plant material is placed in a thimble—a porous container made of filter paper or clean cloth—which is then securely sealed and positioned within the extraction chamber. Solvent is added to the boiling flask at the bottom, which is then heated continuously. As the solvent evaporates, it rises to the condenser where it cools and drips back down into the extraction chamber, soaking the plant material. When the solvent level in the chamber reaches

the top of the siphon tube, it is siphoned back into the boiling flask, carrying with it the extracted compounds. This cycle repeats automatically until the extraction is complete **(Majekodunmi et al., 2015; Pandey et al., 2014).**

VII. **Microwave-Assisted Extraction:** This advanced extraction technique operates through mechanisms like dipolar rotation and ionic conduction, which involve the movement of charged ions present in both the solvent and plant material. The process utilizes electromagnetic waves ranging between 300 MHz and 300 GHz to interact with materials that absorb these waves, thereby generating heat. This heat facilitates the interaction between the solvent and the plant matrix. When a polar solvent is used, the resulting ion migration and dipole rotation enhance solvent penetration, significantly improving extraction efficiency. Non-polar solvents are generally unsuitable for this method, as they do not effectively absorb microwave energy to generate the required heat. Microwave-assisted extraction is particularly effective for isolating flavonoids **(Azwanida et al., 2015; Majekodunmi et al., 2015).**

VIII. **Ultrasound-Assisted Extraction:** This method uses sound energy at frequencies above 20 kHz to enhance the surface area of plant material, allowing better solvent penetration. It significantly reduces extraction time and does not require the application of heat. Ultrasound-assisted extraction is especially suitable for small sample sizes and requires less solvent compared to conventional methods. However, a major drawback is that the high energy input can degrade secondary metabolites and lead to the formation of free radicals **(Pandey et al., 2014).**

4.4.2 Commonly Used Chromatographic Methods for Separation of Bioactive Compounds

I. Paper Chromatography:

This technique operates on the principle of partition chromatography, where compounds are separated based on their differing affinities for the stationary and mobile phases. In this method, a small amount of the sample is applied

onto filter paper, which serves as the stationary phase. The paper is then placed in a solvent that functions as the mobile phase. As the solvent moves upward through the paper via capillary action, the components of the sample travel at different rates depending on their individual properties. The cellulose fibers in the paper retain water molecules, supporting the stationary phase. Paper chromatography is cost-effective and highly sensitive, making it suitable for analyzing small sample quantities. However, its limitations include the fragility of the paper and the relatively long duration required for separation **(Sasidharan et al., 2011; Ingle et al., 2017).**

II. Thin Layer Chromatography (TLC):

In this technique, a small portion of the sample from the mixture is spotted in a thin adsorbent glass or plate that is coated with silica gel or alumina. The prepared plate is then placed upright in a closed chamber containing a suitable solvent, which serves as the mobile phase. The solvent moves upward towards the plate through capillary action and the components of the sample travel at varying rates depending on its association with the mobile and stationary phase. After the separation process is completed, it is visible as spots that climb to different positions on the glass or plate depending on its solubility which is envisioned using ultra-violet light or staining. Identification of the separated compounds is done by calculating their retardation factor (Rf), which is the ratio of the distance traveled by the compound to that traveled by the solvent front. The Rf values are then compared to those of known standards. Individual spots can be scraped off with a spatula and re-extracted using appropriate solvents. TLC is a quick, cost-effective method that provides clear and distinct spots for easy identification of compounds **(Sasidharan et al., 2011; Ingle et al., 2017; Banu et al., 2015).**

III. Column Chromatography:

In this method, a solution mixture is passed through a column filled with a stationary phase. The column, typically a long glass tube equipped with a

tap at the bottom, contains a filter made of glass wool to hold the stationary material in place. Common stationary phases include silica gel, cellulose, or sephadex, while the mobile phase is usually a liquid solvent. The column is carefully packed with the stationary phase to avoid the formation of air bubbles, ensuring even flow. The sample extract is then introduced from the top of the column, with its movement influenced by the polarity of the compounds. Different solvent fractions are collected sequentially as they elute from the column, and these fractions are subsequently analyzed and characterized **(Ingle et al., 2017).**

IV. Gas Chromatography:

This technique utilizes two immiscible phases. The mobile phase is a gas, typically an inert gas like helium, while the stationary phase consists of a liquid coated onto an inert solid support. Compounds that are more soluble in the gaseous phase remain in it, whereas those with greater affinity for the liquid phase migrate accordingly. This differential partitioning enables effective separation of components. A key advantage of gas chromatography is its ability to separate substances contaminated with volatile pesticides, making it particularly useful for quality control assays **(Ingle et al., 2017; Banu et al., 2015).**

V. High-Performance Liquid Chromatography (HPLC):

HPLC is a pressure-assisted flow of the mobile phase through a packed column containing the stationary phase. The mobile phase is typically a liquid solvent, while the stationary phase consists of tightly packed solid particles. The sample is introduced into the system near the base, where it mixes with the mobile phase as it flows from the solvent reservoir. Once the tap is opened, the pressure pump propels the solvent to blend with the injected sample. This mixture then travels through the column and reaches

the diode-array detector, which helps in identifying and separating the different compounds present **(Ingle et al., 2017; Banu et al., 2015).**

4.5 Extraction and Purification of Plant Extract

In the current study, Soxhlet extraction was employed due to its efficiency as a continuous and automated method, allowing the use of a large amount of plant material while minimizing solvent consumption. This process enhances extraction efficiency and reduces the loss of plant constituents, as it does not require filtration. Different parts of the plants were extracted individually. The resulting brownish extract, containing a range of polar and non-polar compounds, was collected and concentrated using a rotary vacuum evaporator.

A rotary vacuum evaporator gradually and efficiently eliminates the solvents from the sample through evaporation. By applying a vacuum, the boiling point of the solvent is lowered, allowing it to evaporate at reduced temperatures. Simultaneously, the flask containing the solution rotates, increasing the surface area for evaporation, which facilitates solvent removal while preserving the solute.

The main components of a rotary evaporator include:

- **Motor unit**: Rotates the flask containing the solution.
- **Vapor duct**: An airtight channel that allows vapor to escape from the sample while also serving as the rotation axis.
- **Vacuum system**: Reduces the pressure inside the apparatus to enable low-temperature evaporation.
- **Water bath**: Heats the sample to promote evaporation.
- **Condenser**: Contains a coiled tube where a coolant (like dry ice or acetone) circulates to condense the vapor.
- **Receiving flask**: Collects the condensed solvent that drips down from the condenser.

- **Lift mechanism**: A manual or motorized device to raise or lower the evaporating flask from the water bath.

The concentrated extracts obtained from each part of the plant, leaf, stem, root, and the whole plant, were referred to as crude solutions. These crude extracts were then subjected to fractionation using solvents of increasing polarity: hexane, ethyl acetate, acetone, methanol, and water. Following this, compound separation was carried out using thin layer chromatography (TLC). As a result, five distinct fractions were obtained from each crude extract: Hexane Fraction (HF), Ethyl Acetate Fraction (EF), Acetone Fraction (AF), Methanol Fraction (MF), and Water Fraction (WF). The different fractions derived from each plant part are listed below:

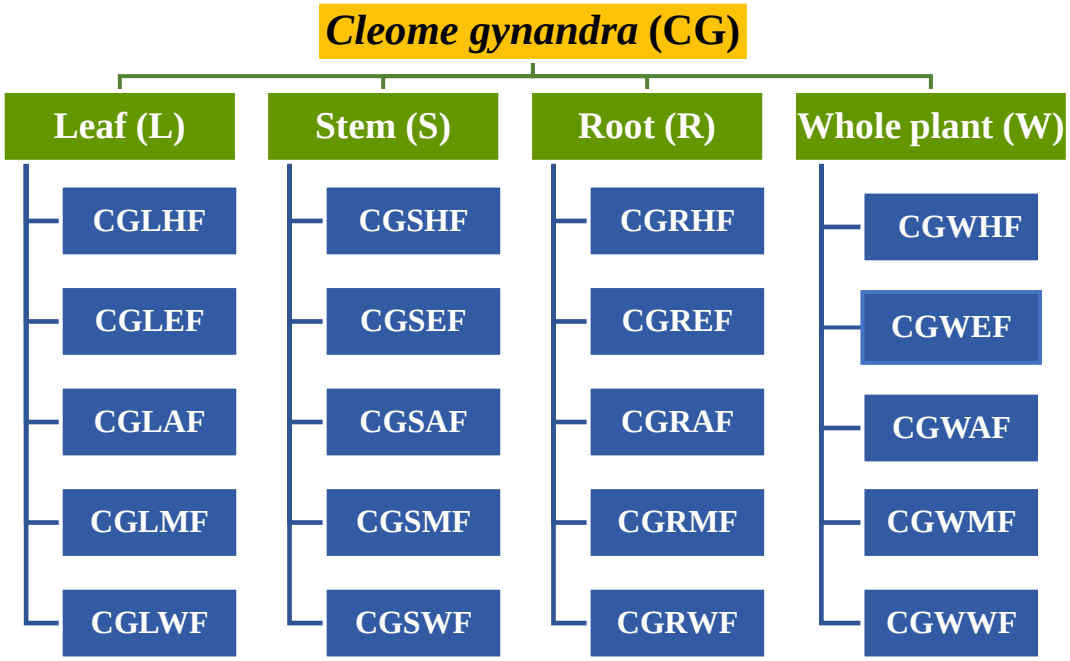

Figure 4.1: Different fractions derived from each plant part of *Cleome gynandra*

Chapter 5

INHIBITION OF UREASE ENZYME

5.1 Introduction

Urease activity is determined by measuring the amount of ammonia released during the hydrolysis of urea. This reaction is catalysed by the enzyme urease, resulting in the emission of ammonia into the atmosphere. To reduce nitrogen loss and improve its uptake by the soil, urease inhibitors are commonly used in combination with urea-based fertilizers.

To determine whether a substance effectively inhibits urease by preventing urea from binding to the enzyme's active site, its impact on the enzymatic reaction must be assessed. This is typically achieved by measuring the concentration of ammonia produced. Several analytical methods can be employed for this purpose, including colorimetric assays, conductivity analysis, and other relevant techniques.

5.1.1 Colorimetric analysis:

- **Berthelot Assay:**

  This colorimetric method was originally developed by chemist Pierre Eugene Marcellin Berthelot to detect and measure ammonia release. In this assay, ammonia reacts with phenol and Berthelot's reagent (hypochlorite) in an alkaline solution, forming a blue-colored compound known as indophenol through an oxidative phenol coupling reaction.

  The intensity of the blue color, measured using spectrophotometry, directly correlates with the concentration of ammonia present **(Kaplan et al., 1969).** This method is sensitive enough to detect ammonia in complex matrices such as blood, soil, and seawater. The stronger the color intensity, the higher the ammonia concentration. The Berthelot reaction involves two key reagents—hypochlorite and a phenolic compound, commonly a non-toxic salicylate. The blue-colored compound 5-aminosalicylate ($C_7H_7O_3N$)

exhibits strong absorbance within the wavelength range of 630–720 nm **(Michalec et al., 2016).**

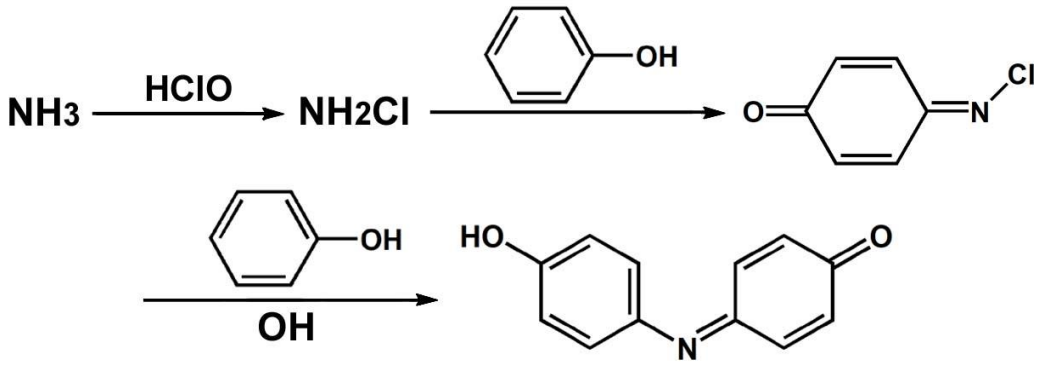

In recent years, the phenol-hypochlorite reaction has attracted renewed attention for measuring ammonia production. The addition of sodium nitroprusside as a catalyst has significantly enhanced the sensitivity of this method, allowing for the detection of ammonia at low micromolar concentrations, as described by **Chaney and Marbach (1962).** Color development in this reaction primarily involves two components: phenol combined with nitroprusside, and an alkaline solution containing hypochlorite. Various reagent combinations have been proposed—for instance, mixing alkali with phenol to produce alkaline phenate, while nitroprusside and hypochlorite are often prepared as separate solutions. In some protocols, nitroprusside and hypochlorite are pre-mixed before use. However, there are differing interpretations regarding the optimal order and timing of reagent addition, as well as inconsistencies in the recommended temperature and duration for color development **(Weatherburn, 1967).**

- **Nessler Assay:**

The Nessler assay detects ammonia and ammonium salts in solution by reacting with Nessler's reagent (potassium tetraiodomercurate) in an alkaline environment. This reaction produces an orangish-brown compound that absorbs light in the 360–480 nm wavelength range, enabling spectrophotometric determination of ammonia concentration. The color

intensity produced is directly proportional to the amount of ammonia present.

Reaction:

$$NH_3 + 2HgI_4^{2-} + 3OH^- \rightarrow OHg_2NH_2I \text{ (orangish-brown)} + 7I^- + 2H_2O$$

This method requires only a single reagent and is relatively quick and cost-effective. However, the orangish-brown product may slowly precipitate into a solid by-product, complicating spectrophotometric measurements. Additionally, the use of mercury-containing reagents introduces toxicity concerns, making the disposal of reaction waste more challenging. Despite these drawbacks, the assay remains a sensitive method for detecting ammonia in aqueous solutions **(Kolacinska et al., 2014).**

- **Phenol Red Assay:**

The phenol red assay detects ammonia by observing a color change in the solution, facilitated by the pH indicator phenol red. Phenol red indicates changes in pH, with the presence of ammonia causing an increase in pH. As a result, the solution shifts in color from yellow to pink. Ammonia in solution reacts with water in the presence of phenol red to form ammonia hydroxide, which raises the pH. This color change is most noticeable within the pH range of 6.8 to 8.2. The assay is commonly used to detect urease-producing bacteria. When urea is added to the solution, bacterial urease catalyzes urea hydrolysis, releasing ammonia and carbon dioxide, which causes the solution to turn pink. It can also be used to detect ammonia production by microorganisms in culture media. However, this method can be sensitive to variations in the concentration of phenol red and other components in the solution, which may affect the results **(Okyay et al., 2013; Ruiz-Herrera et al., 1969).**

5.1.2 Alternative Methods for Assessing Urease Activity

- **Urease Activity Using Kit Assay:**

  This is a direct and convenient method for measuring urease activity in various sample types, including bacteria, yeast, plant cells, environmental samples, and fecal matter. The assay is performed using a commercially available kit in a 96-well plate format. It relies on the Berthelot reaction to detect the ammonia produced during urea hydrolysis, with absorbance measured at 670 nm. The absorbance value is directly proportional to the urease activity present in the sample.

- **Soil Urease Activity:**

  This technique provides a precise measurement of urease activity in soil by estimating the ammonia released during urea hydrolysis. The procedure involves incubating soil samples at 37°C for 2 hours with THAM buffer [tris(hydroxymethyl)aminomethane], a urea solution, and toluene. After incubation, the sample is treated with a 2.5 M KCl solution containing the inhibitor, followed by steam distillation of a portion of the soil mixture using magnesium oxide (MgO) for 3–4 minutes. The optimal conditions for this assay include a THAM buffer at pH 9.0 and a urea concentration of 0.02 M. This method yields fast and consistent results, particularly for soils with ammonia fixation properties **(Klose et al., 1999).**

5.2 Experimental Design

The urease inhibitory activity of raw extracts from different parts of *Cleome gynandra*, including leaf, stem, root, and the entire plant, was evaluated by measuring ammonia release at 640 nm, following a modified version of the **Weatherburn method (1967)**. This assay is based on the phenol-hypochlorite reaction, originally developed by Berthelot, with slight modifications to the protocol.

The following reagents and conditions were used for the assay:

- **Standard inhibitor**: Thiourea
- **Buffer system**: Phosphate buffer at pH 8.2, with the reaction carried out at 37°C
- **Enzyme**: Urease Type IX from *Canavalia ensiformis* (Jack bean), at a concentration of 0.03 mg/mL
- **Test samples**: Raw extracts from leaf, stem, root, and whole plant, tested at concentrations ranging from 0.5 mg/mL to 2 mg/mL
- **Substrate**: Urea at concentrations of 500 µM, 1000 µM, 1500 µM, and 2000 µM
- **Incubation period**: 20 minutes

The percentage of urease inhibition was calculated using the following formula:

$$\textbf{Urease Inhibition (\%)} = 100 - [(\textbf{Test} / \textbf{Reference}) \times 100]$$

A phosphate buffer solution (pH 8.2) was prepared at 37°C, containing 10 mM potassium phosphate, 10 mM lithium chloride, and 1 mM ethylenediaminetetraacetic acid (EDTA). Urease enzyme (0.03 mg/mL) was added to this buffer, followed by 0.1 mL of the test extract from each part of the plant, at concentrations ranging from 0.5 mg/mL to 2 mg/mL. The mixture was incubated for 5 minutes at room temperature.

Urea was then added at varying concentrations (500 µM, 1000 µM, 1500 µM, and 2000 µM), and the mixture was further incubated for 20–25 minutes. After this, two color-developing solutions were sequentially added:

- **Solution A**: 0.5 g phenol and 2.5 mg sodium nitroprusside dissolved in 50 mL demineralized water
- **Solution B**: 250 mg sodium hydroxide and 820 µL of 5% sodium hypochlorite (Berthelot reagent) in 50 mL distilled water

One millilitre of each solution was added to the reaction mixture. Color development was observed for each crude plant extract, and ammonia release was measured spectrophotometrically at 640 nm. Thiourea was used as the standard urease inhibitor, where minimal color change indicated strong inhibitory activity.

5.2.1 IC_{50} Value of Crude Extracts from Different Plant Parts at Varying Substrate Concentrations

The IC_{50} value represents the concentration of a compound or biological extract needed to inhibit a biochemical reaction by 50%. It serves as an indicator of the compound's potency; the lower the IC_{50} value, the more effective the inhibitor. Typically, IC_{50} values are derived from percentage inhibition data collected through experiments, often conducted in duplicate or triplicate. A dose-response curve is plotted by graphing the percentage of inhibition against varying concentrations of the test extract. The IC_{50} is identified as the concentration corresponding to 50% inhibition, usually represented by the midpoint of the curve.

In this study, IC_{50} values for crude extracts from different parts of *Cleome gynandra* (leaf, stalk, root, and whole plant) were determined by evaluating the percentage of urease inhibition at different extract concentrations across multiple urea substrate concentrations.

5.3 Results and Discussion

The IC_{50} values for each part of the plant were determined based on the percentage of urease inhibition observed at varying urea concentrations. Among the tested extracts, the whole plant and root showed inhibitory effects comparable to that of the standard inhibitor, indicating that similar concentrations were required to achieve 50% inhibition. Urease inhibition percentages were recorded over 30 minutes, beginning with the lowest concentration of each extract.

Concentration of urea (µm)	Whole Plant IC_{50} (µg/ml)	Leaf IC_{50} (µg/ml)	Stem IC_{50} (µg/ml)	Root IC_{50} (µg/ml)	Thiourea IC_{50} (µg/ml)
500	1477.713±17.18	2654±72.11	4654±82.11	1589±17.18	1329±36.65
1000	1849±26.98	2989±41.89	4689±81.89	1908±27.78	1632±26.98
1500	2115.32±58.06	3345±63.86	5145±93.89	2354±78.98	1778±54.76
2000	2755±38.65	3987±72.54	5887±72.54	2987±87.09	1886±76.98

Table 5.1: IC_{50} Values of Crude Extracts from Different Plant Parts at Various Urea Concentrations.

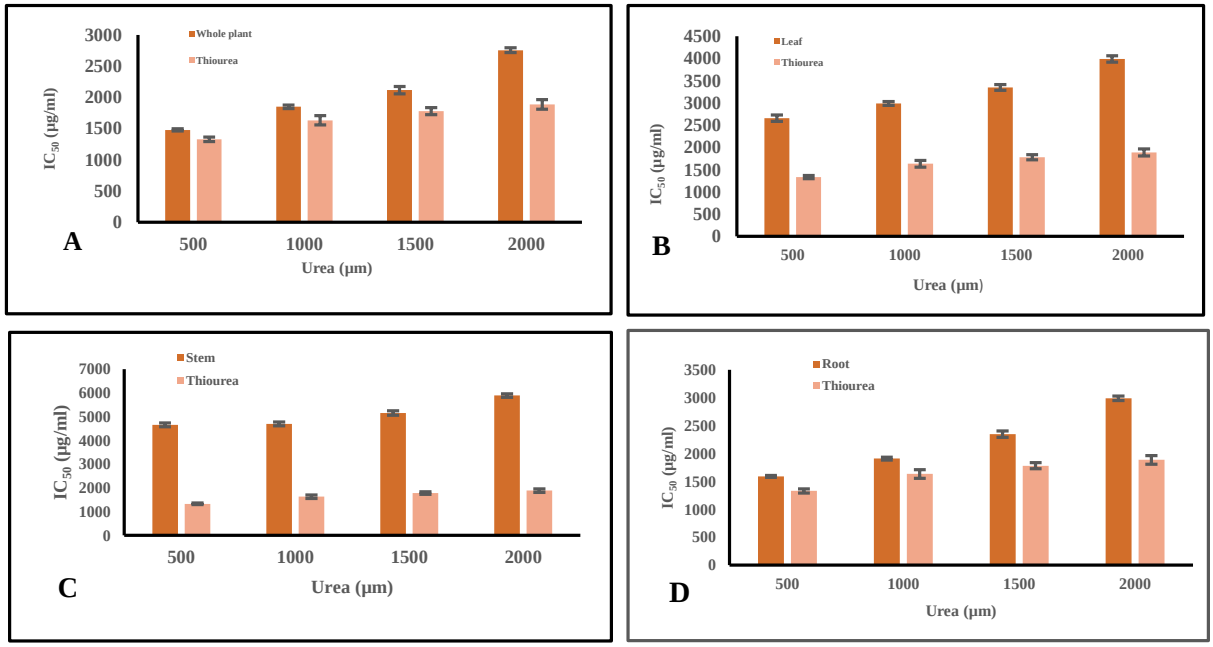

Figure 5.1: IC_{50} values of crude extract from each plant part (A) Whole plant, (B) leaf, (C) Stem and (D) Root as compared to standard thiourea.

An increase in substrate concentration leads to a corresponding rise in IC_{50} values, indicating a reduction in the inhibitory effect of the test compound. This suggests that urea competes with the inhibitor for access to the enzyme's active site. At low substrate concentrations, where the active sites are largely unoccupied, the inhibitor effectively binds to the enzyme, thereby suppressing its activity. This behavior is notably observed in Figures A and D (whole plant and root extracts),

where IC_{50} values closely match those of the standard inhibitor. As the substrate concentration increases, the competition between substrate and inhibitor becomes more pronounced. Eventually, both may interact with the enzyme concurrently, diminishing the degree of inhibition and raising the IC_{50} value. Consequently, a higher concentration of inhibitor is required to achieve 50% enzyme inhibition at elevated substrate levels. This pattern is consistently reflected in the IC_{50} plots of all plant parts, demonstrating that increased substrate availability necessitates higher inhibitory concentrations.

The equation and R^2 value of all the four datasets are:

1A: $y = 409.82x + 1024.7$, $R^2 = 0.9661$

1B: $y = 435.5x + 2155$, $R^2 = 0.9722$

1C: $y = 415.5x + 4055$, $R^2 = 0.8727$

1D: $y = 463.1x + 1049.5$, $R^2 = 0.9759$

The combined IC_{50} values of all the plant part and representation of the entire dataset have been depicted in the following figures:

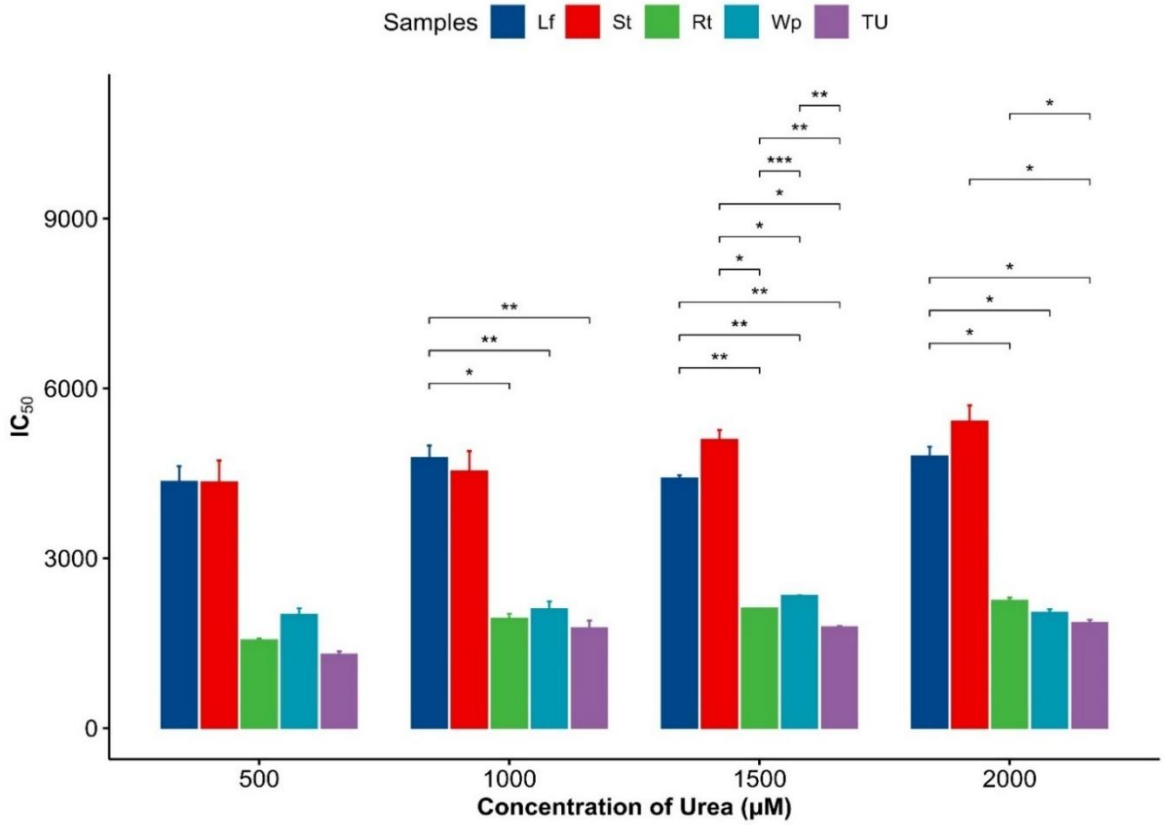

Figure 5.2: Combined IC_{50} values of crude extract of each plant parts Leaf (Lf), Stem (St), Root (Rt) and Whole plant (Wp) in comparison with Thiourea (Tu) at different urea concentrations.

At all concentrations of urea, the leaf and stem extracts exhibit a significant deviation in IC_{50} values compared to the standard inhibitor, thiourea. In contrast, the IC_{50} values for the whole plant and root extracts are not markedly different from those of the standard, indicating comparable inhibitory activity. These findings suggest that the root is the primary contributor to the overall inhibitory effect observed in the whole plant, which inherently represents a cumulative response from the leaf, stem, and root. Among these, the root demonstrates the most substantial inhibitory potential, as evidenced by its IC_{50} value closely aligning with that of thiourea. Statistical analysis further supports this observation, with an F-value of 913.7538 and a p-value of 1.02×10^{-38}, indicating

a highly significant difference among the sample groups and confirming a meaningful relationship between the test extracts and the standard inhibitor.

5.3.1 Box plot representation of the dataset

Box plots visualize differences among individual samples or groups. They are also used in descriptive statistics to clarify data analysis. Box plots represent numerical data and skewness by demonstrating data quartiles and averages **(DuToit et al., 2012).**

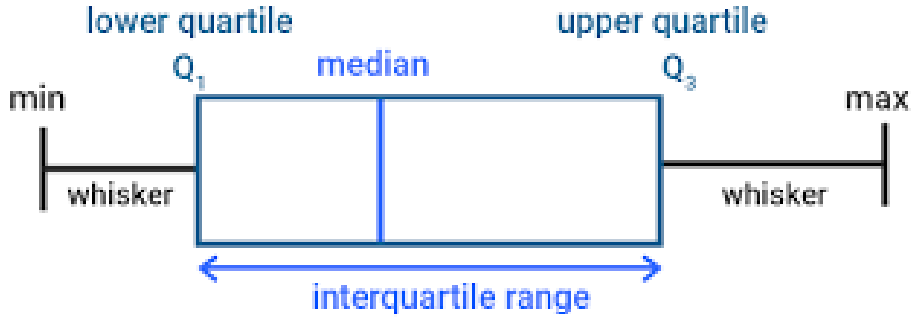

Figure 5.3: Box plot representation of five number summary

It shows five number summaries of a data set:

- Minimum score: represents the lowest score excluding the outliers
- Lower quartile range (Q1) or first quartile: one-fourth percent result fall beneath lower quartile series
- Median: it is the center of the statistics displayed by a streak that divide the box from middle into two halves. Half of the results are greater than or equal to this value and half of the scores are less than this value
- Upper quartile range (Q2) or third quartile: almost three quarters of results are beneath the upper quartile division
- Maximum score: represent highest scores, excluding the outliers
- Whiskers: the higher and minor whiskers represent results external to the central fifty percent, thus representing the lower twenty five percent scores and upper twenty five percent scores

- The interquartile range (IQR): it shows the middle fifty percent results i.e. the series amongst twenty fifth as well as seventy fifth grade (**Holmes et al., 2017**).

The box plot clearly highlights the differences among the various samples, offering insights into the median, range, and presence of outliers. It also helps assess the distribution pattern of the data whether it is normal or skewed. A distribution is considered normal when the median is centered within the box and the whiskers are of roughly equal length on both sides. Positive skewness, or rightward skew, is indicated when the median lies closer to the lower edge of the box with a longer upper whisker. Conversely, negative skewness, or leftward skew, is observed when the median is positioned nearer to the top of the box with a longer lower whisker.

The box plot indicates that both the standard inhibitor and the root extract belong to a similar group in terms of inhibitory activity. Based on this observation, further analysis was conducted on the root to evaluate which specific fraction exhibits the most effective urease inhibition.

Root samples were separated from the rest of the plant parts and five distinct fractions were obtained from the crude root residue. These included CGRHF (*Cleome gynandra* root hexane fraction), CGRREF (root ethyl acetate fraction), CGRAF (root acetone fraction), CGRMF (root methanol fraction), and CGRWF (root water fraction). Each of these fractions was subsequently evaluated for IC_{50} value determination.

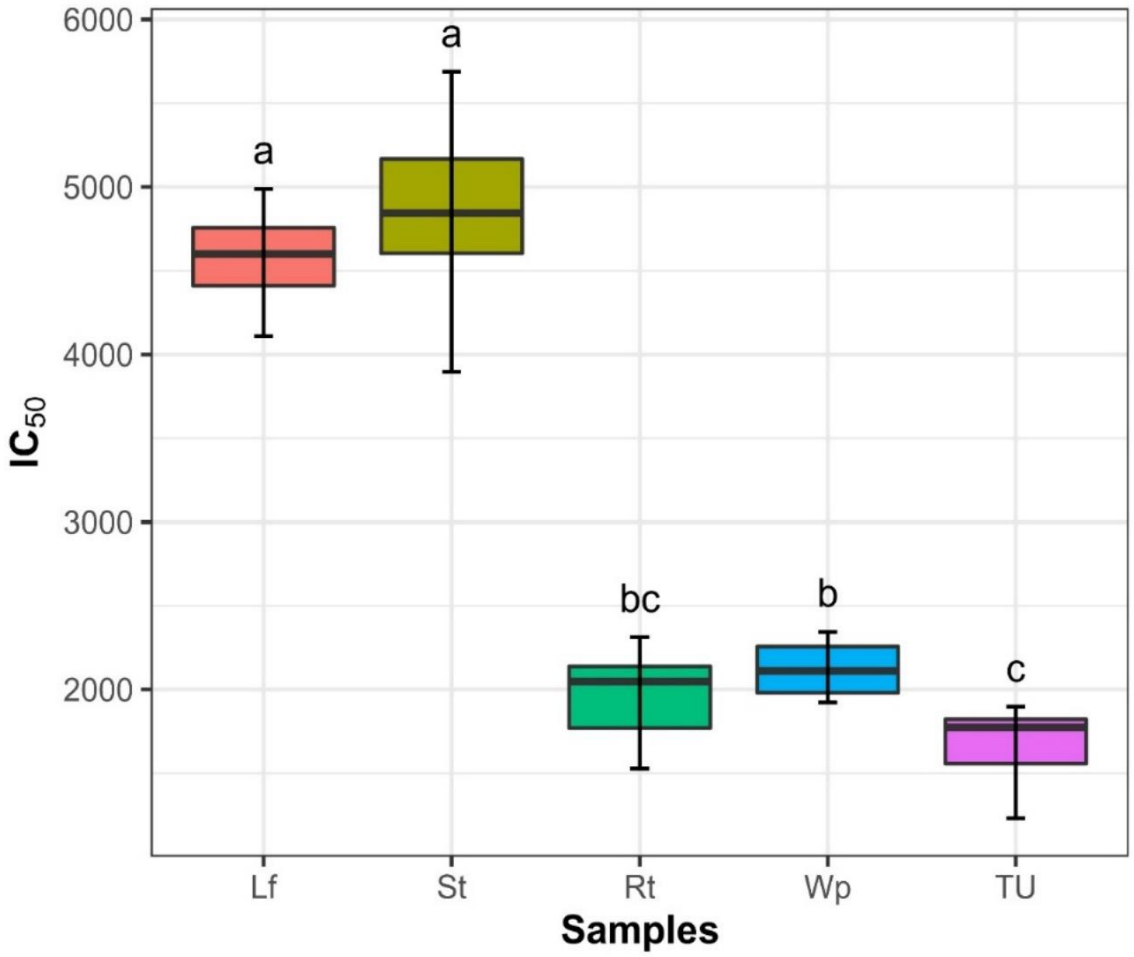

Figure 5.4: Box plot representation of the IC_{50} values of different plant parts.

5.3.2 Fraction-wise IC_{50} Values of Root Extracts at Varying Substrate Concentrations

The concentration of each root fraction required to achieve 50% inhibition of urease activity (IC_{50}) was determined by evaluating their inhibitory effects across a range of concentrations (0.5 mg/mL to 2 mg/mL) at varying urea substrate levels (500 µM, 1000 µM, 1500 µM, and 2000 µM). These results were compared to the standard inhibitor, thiourea. Notably, the acetone, methanol, and water fractions exhibited urease inhibition comparable to that of thiourea, as evidenced by similar IC_{50} values across the tested conditions.

The equation and R^2 value for all the five data set are:

2A: $y = 308.78x + 1153.3$, $R^2 = 0.9746$

2B: $y = 364.96x + 1258.2$, $R^2 = 0.9076$

2C: $y = 332.46x + 1566.7$, $R^2 = 0.9507$

2D: $y = 400.3x + 2182.3$, $R^2 = 0.9948$

2E: $y = 377.3x + 3297.3$, $R^2 = 0.9599$

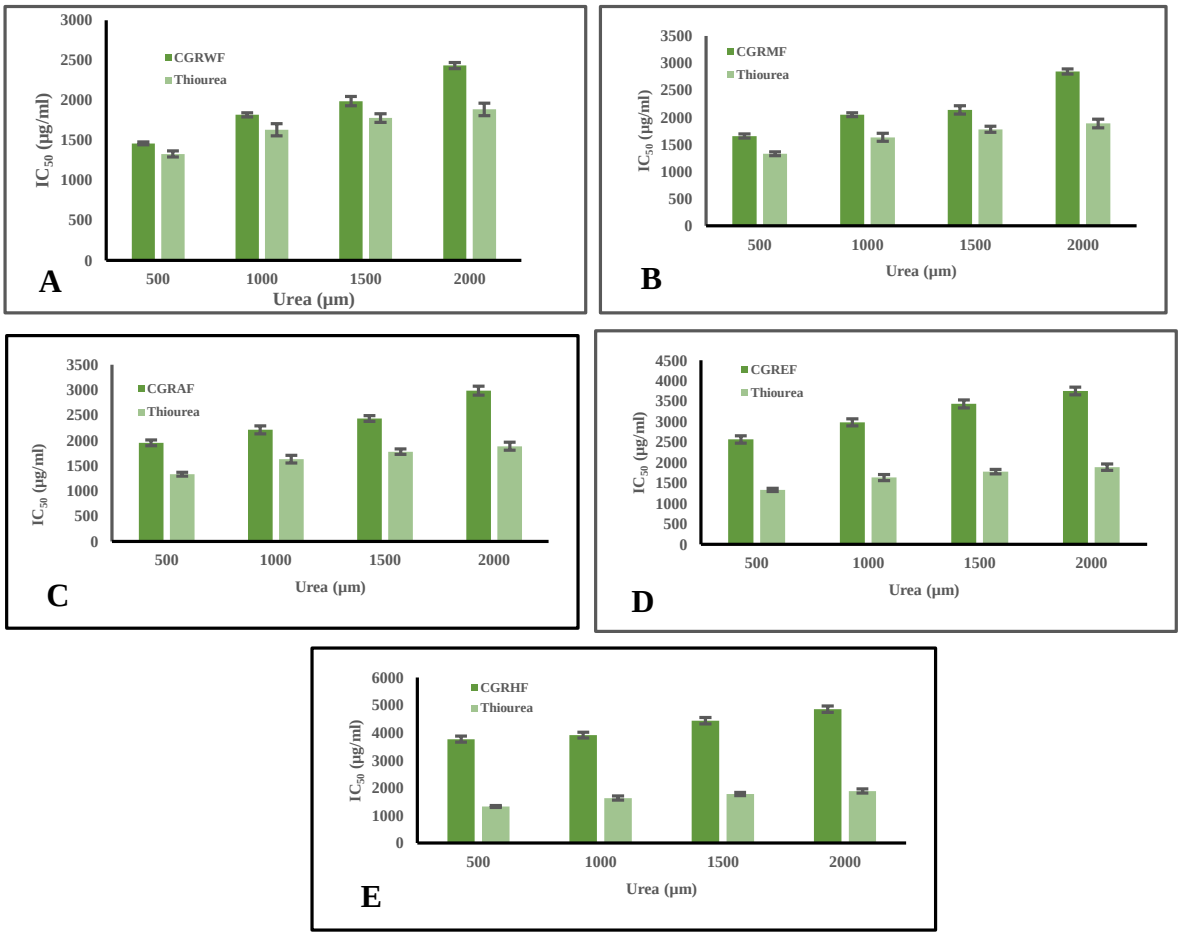

Figure 5.5: IC_{50} value of individual root water fraction (Hexane, Ethyl acetate, Acetone, Methanol and Water) at different urea concentration

The combined IC_{50} values of all the root fractions and representation of the entire dataset have been depicted in the following figures:

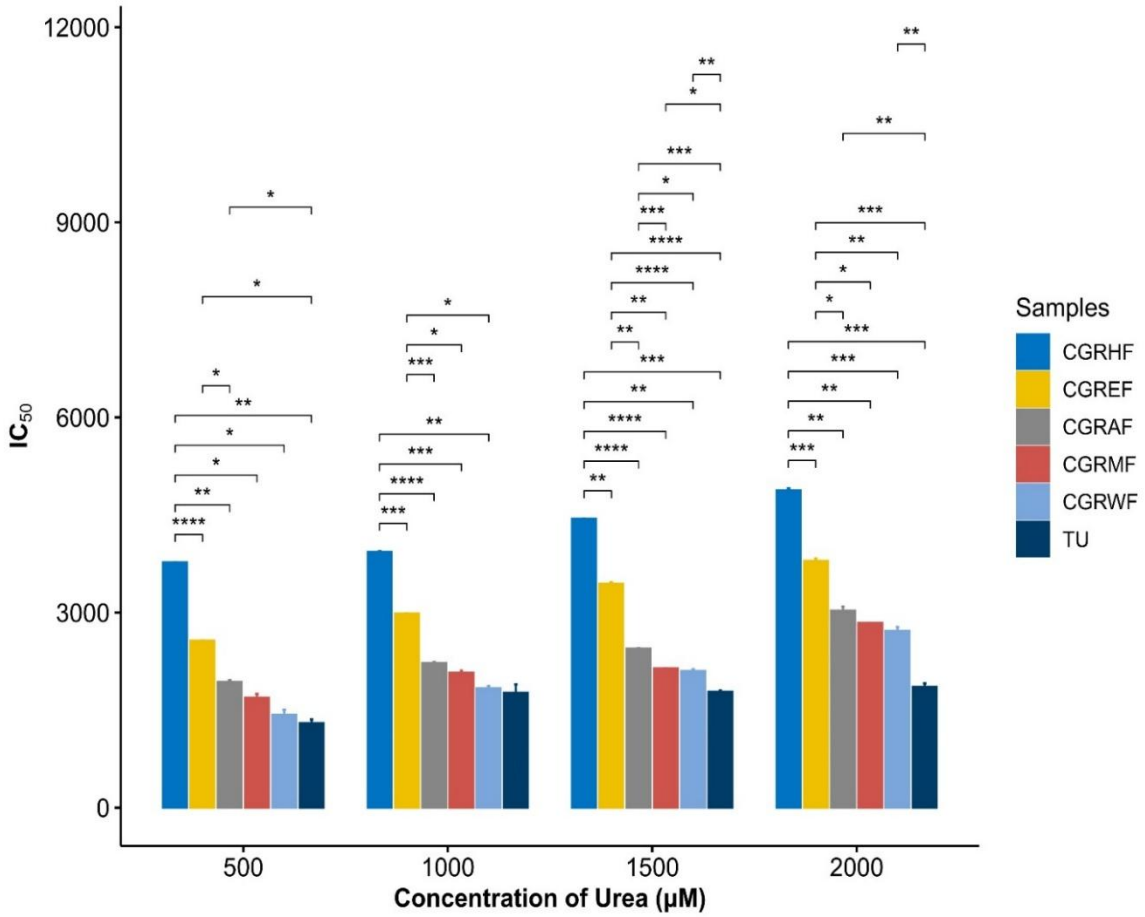

Figure 5.6: Combined IC_{50} values of all root fractions: hexane, ethyl acetate, acetone, methanol and water fractions at different urea concentrations.

5.3.3 Fraction-wise Evaluation of Inhibitory Activity

The evaluation of individual root fractions from *Cleome gynandra* revealed that the bioactive compound responsible for urease inhibition is most likely present in the water fraction. While the methanol and acetone fractions also exhibited considerable inhibitory activity compared to the standard inhibitor, thiourea, and their exact mode of inhibition warrants further investigation alongside the water fraction. In contrast, the ethyl acetate and hexane fractions showed significantly higher IC_{50} values, indicating weaker inhibition relative to the standard. Statistical analysis yielded an F-value of 5335.716 and a p-value of 1.21×10^{-64}, confirming that the differences among the sample groups are statistically significant and

suggesting a meaningful relationship between the tested fractions and the standard inhibitor.

Box plot representation of the dataset

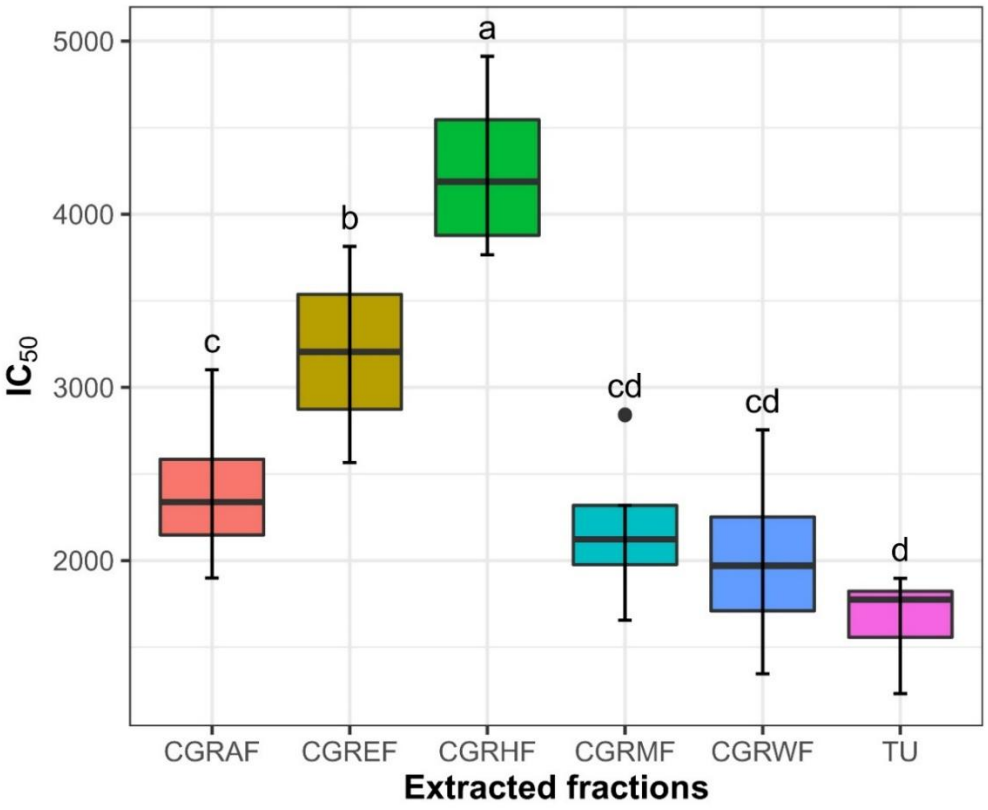

Figure 5.7: Box plot representation of the IC_{50} values of different root fractions.

The box plot clearly illustrates the variation and statistical distribution among the different root fractions. It shows that the acetone (CGRAF), methanol (CGRMF), and water (CGRWF) fractions cluster within the same category, with the water fraction demonstrating inhibitory activity comparable to the standard inhibitor, thiourea. Based on these observations, the CGRAF, CGRMF, and CGRWF fractions were selected for further enzyme kinetic studies.

5.4 Enzyme Kinetic Studies

To understand how the inhibitor is competing with the substrate to inhibit the enzyme from catalyzing a reaction it is necessary to understand the category of enzyme inhibition. The inhibitors decrease the reaction velocity of enzyme

catalyzed reaction without causing enzyme denaturation. There are certain compounds that are called activator which increases the reaction velocity without affecting the enzymes' structure. Inhibitor and activator work in a similar way by influencing reaction velocity of the enzyme. They are grouped as effector or modifiers. Activators are positive modifier while inhibitors are negative modifiers. Enzyme are capable of reducing reaction velocity either by combining with enzyme alone or with substrate-enzyme binary complex or with both (**Copeland et al 2013**).

Enzymes primarily undergo two fundamental types of inhibition:

- **Irreversible nature:** In irreversible inhibition, the inhibitor binds permanently to the enzyme's active site, typically through the formation of covalent (electrovalent) bonds. As a result, the inhibitor cannot be removed, and the enzyme remains permanently inactivated. This form of inhibition involves the persistent attachment of the inhibitor to the enzyme or catalytic protein **(Kuriyan et al., 2012).**
- **Reversible nature:** In reversible inhibition, the inhibitor binds to the enzyme's active site through weak, non-covalent interactions such as hydrogen bonds or hydrophobic forces, rather than forming covalent (electrovalent) bonds. These interactions are temporary, allowing the inhibitor to be easily removed through processes like dilution or dialysis **(Tuley et al., 2018).** Reversible inhibition is generally classified into three types:
  - **Competitive Inhibition:** Certain inhibitors closely resemble the substrate in structure, allowing them to compete for binding at the enzyme's active site. This form of inhibition is termed *competitive inhibition* and is generally reversible. Introducing an excess of substrate can displace the inhibitor from the enzyme's active site, thereby reducing or eliminating the inhibitory effect **(Cornish-Bowden et al., 2013).**

$E+I \rightleftharpoons EI$

So, $K_i = [E][I]/[EI]$, where K_i= association constant for EI complex

In presence of inhibitor during any stage of reaction, E may be present as free enzyme, E-S complex and EI complex. Since one molecule of substrate combine with one molecule of enzyme and one molecule of inhibitor with one molecule of free enzyme, concentration of total enzyme,

$E_{total} = E+ES+EI$

Or, $E_t = E(1+I/K_i)+ES$

Or, $E_t - ES = E(1+I/K_i)$

Or, $E_t - ES/(1+I/K_i) = E$

Since, $E/ES = K_m/S$

Therefore, $E_t - ES/(1+I/K_i)ES = K_m/S$

Or, $E_t - ES/ES = K_m(1+I/K_i)/S$

Or, $E_t/ES = K_m(1+I/K_i)/S + 1$

Therefore, $V_{max}/V = K_m([1+I/K_i)+S]/S$

So, $v = V_{max}[S]/K_m(1+I/K_i)+S$

Here, K_m remains increased by a factor $(1+I/K_i)$ while V_{max} remain unaffected.

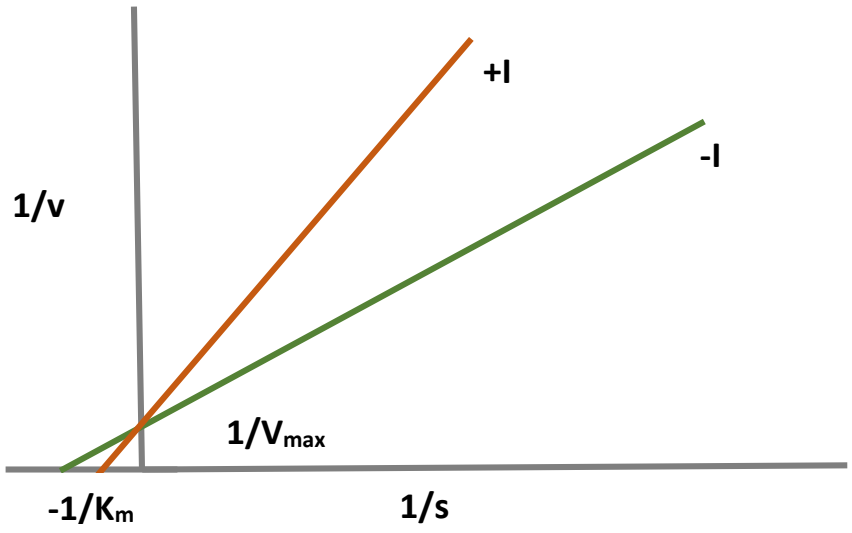

Figure 5.8: Lineweaver-Burk plot (1/v vs 1/[S]) for competitive inhibition

The 1/v vs 1/s plot of competitive inhibition. Increase in K_m indicates the affinity of enzyme for substrate which is decreased here (**Palmer et al., 2007**).

- **Non-competitive inhibition:** here the inhibitor combines at a position which is dissimilar from the substrate attaching spot. Therefore, inhibitor can combine to the free enzyme along with substrate-enzyme composite (**Palmer et al., 2007**).

  $E+I \rightleftharpoons EI \quad K_i=E.I/EI$

  And $E+S \rightleftharpoons ESI \quad K_i=(ES)I/ESI$

  Let us assume both dissociation constant K_i is same. When this K_i is same that type of inhibition is pure non-competitive inhibition. If K_i are different then it is called mixed inhibition of non-competitive type.

  In regards to non-competitive mode of inhibition,

  $E_{total}=E_t=E+ES+EI+ESI$

  Or, $v = [V_{max}(S)/ 1+I/K_i] [1/K_m+S]$

  Here V_{max} is reduced by a factor of $(1+I/K_i)$

  The double reciprocal plotting of this type of inhibition is:

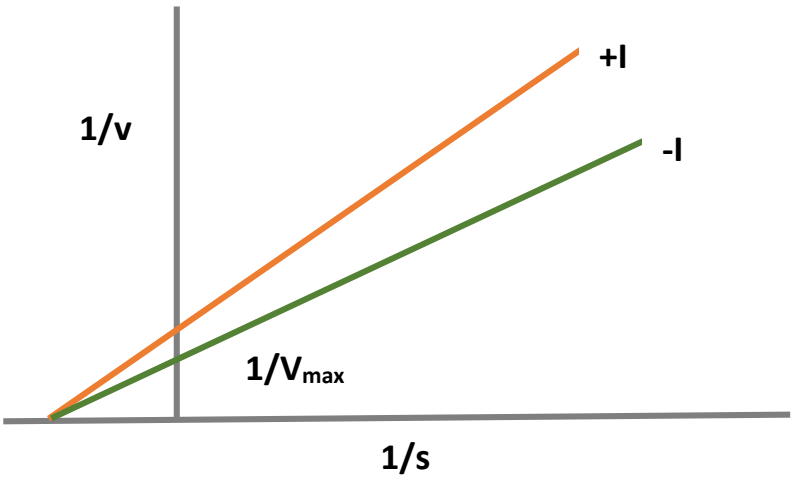

Figure 5.9: Lineweaver-Burk plot (1/v vs 1/[S]) for non-competitive inhibition

Since V_{max} is decreased the value of $1/V_{max}$ should be increased (**Tuley et al., 2018**).

- **Uncompetitive inhibition:** here the inhibitor combines with enzyme-substrate composite
    - $ES+I \rightleftharpoons ESI$

  Usually, the inhibitor cannot combine with enzyme in absence of substrate. When substrate combine with enzyme, it includes some structural changes that facilitate the binding of inhibitor with enzyme substrate complex.
    - In presence of uncompetitive inhibition,
    - $E_{total}=E_t=E+ES+ESI$
    - Or, $v=\{V_{max}/1+I/K_i\}.S/[K_m/(1+I/K_i)+S]$
    - From this equation it is seen that in presence of inhibitor both V_{max} and K_m should reduce by a factor of $(1+I/K_i)$ (**Palmer et al., 2007**).
    - The double reciprocal plotting of this type of inhibition is:

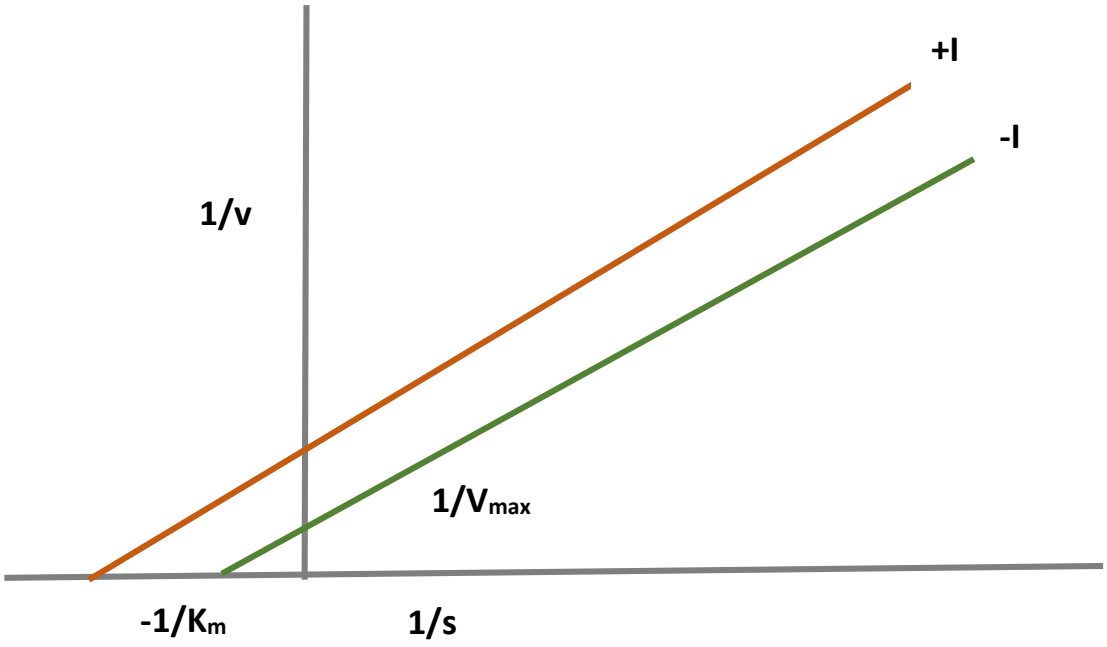

Figure 5.10: Lineweaver-Burk plot (1/v vs 1/[S]) for uncompetitive inhibition.

In the presence of an uncompetitive inhibitor (I), the enzyme's maximum velocity (V_{max}) cannot be achieved. Although the inhibitor leads to a decrease in the Michaelis constant (K_m), theoretically suggesting an increased substrate affinity, this enhanced affinity is not typically observed in practical scenarios **(Tuley et al., 2018).**

5.4.1 Double Reciprocal Plot Analysis

To determine the mode of enzyme inhibition, the Lineweaver-Burk plot, also known as the double reciprocal plot, was employed. This graphical method, introduced by Hans Lineweaver and Dean Burk in 1934, is a linear transformation of the Michaelis-Menten equation used to analyze enzyme kinetics. Historically, plotting initial velocity (v_0) against substrate concentration ($[S_0]$) made it difficult to accurately determine V_{max} and K_m, as the resulting curve was nonlinear and imprecise, particularly at low substrate concentrations **(Palmer et al., 2007).** This limitation was addressed by inverting the Michaelis-Menten equation, enabling a linear representation without the need for new methodologies.

$V_0 = V_{max}[S_0]/([S_0] + K_m)$

Or, $1/v_0 = [S_0] + K_m/V_{max}[S_0] = [S_0]/V_{max}[S_0] + K_m/V_{max}[S_0]$

Therefore, $1/v_0 = K_m/V_{max}.1/[S_0] + 1/V_{max}$ (double reciprocal equation)

This is one usage of y=mx+c which is the calculation of a linear graph; a plot of y vs x having a slope designated m and intercept designated c along the y axis (**Lineweaver et al., 1934; Greco et al., 1979**).

This can differentiate various modes of inhibition of enzyme kinetics and identify the type of inhibitors. The several methods of inhibition can be matched to the uninhibited response.

Reaction velocity was calculated in different urea concentration (from 500 μm to 2000 μm) using 0.03 mg/ml of enzyme urease and 1/v vs 1/S for *Cleome*

gynandra root water fraction, methanol fraction and acetone fraction was plotted in presence and absence of the fractions to determine the kinetic parameters $K_m$and V_{max}.

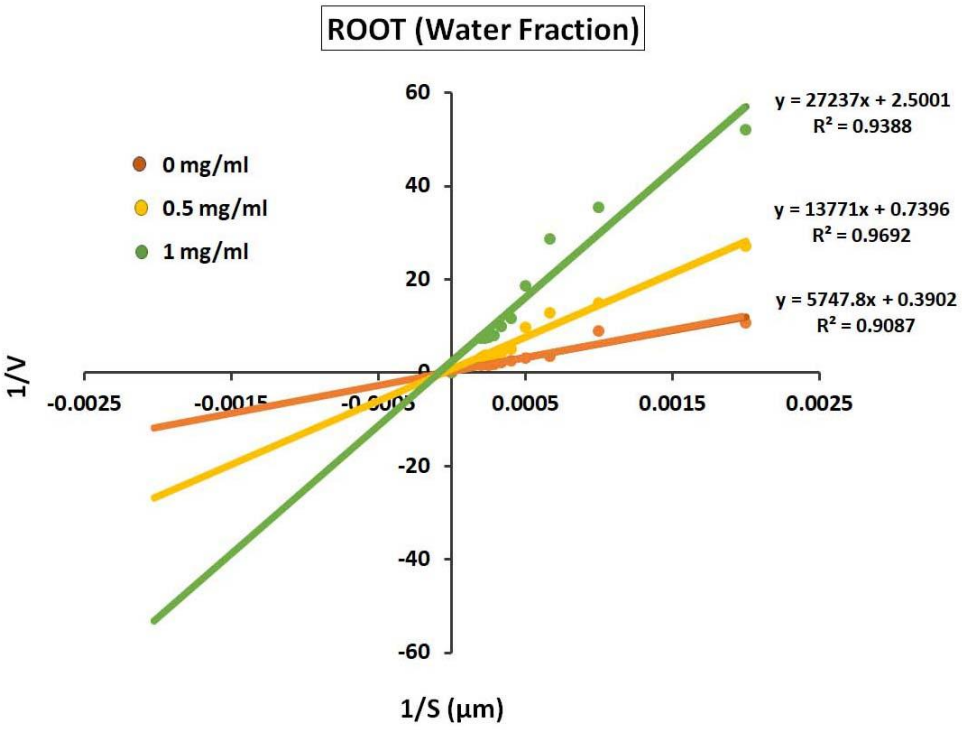

Figure 5.11: Lineweaver-Burk Plot (1/v vs 1/[S]) of root water fraction at different inhibitor concentrations.

The reciprocals of substrate concentration and reaction velocity (per unit time) were plotted for root fractions at concentrations of 0.5 mg/mL and 1 mg/mL. The data point at 0 mg/mL represents the baseline reaction velocity in the absence of the inhibitor.

Inhibitor (mg/ml)	V_{max} (µm/min)	K_m (µm)	K_i (µg/ml)
0	1.5165±0.17	10749±0.92	-
0.5	0.8216±0.19	10506±0.18	558.659±0.45
1	0.512±1.14	10033±0.19	184.911±0.73

Table 5.2: V_{max}, K_m, and K_i Values for the Root Water Fraction in the presence or absence Inhibitor.

V_{max} and K_i are:

Inhibition factor (α)=1+[I]/K_i

Or, K_i= [I]/ α-1

α = V_{max} during lack of inhibitor/V_{max} in occurrence of inhibitor

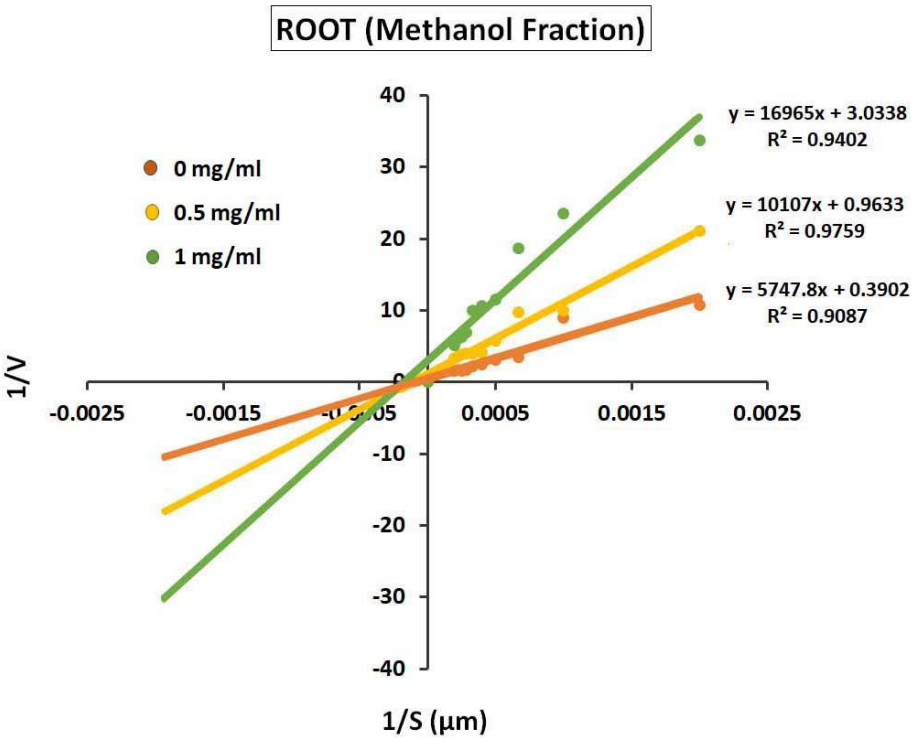

Figure 5.12: Lineweaver-Burk Plot (1/v vs 1/[S]) of root methanol fraction at different inhibitor concentrations.

Similar plotting was done for root methanol fraction with the corresponding Vmax, K_m, and Ki are:

Inhibitor (mg/ml)	V_{max} (µm/min)	K_m (µm)	K_i (µg/ml)
0	1.5165±0.17	10749±0.92	-
0.5	1.0380±0.23	10492±0.13	159.33±0.66
1	0.9627±2.86	10730±1.87	147.34±0.21

Table 5.3: Vmax, K_m, and Ki Values for the Root Methanol Fraction in the presence or absence Inhibitor.

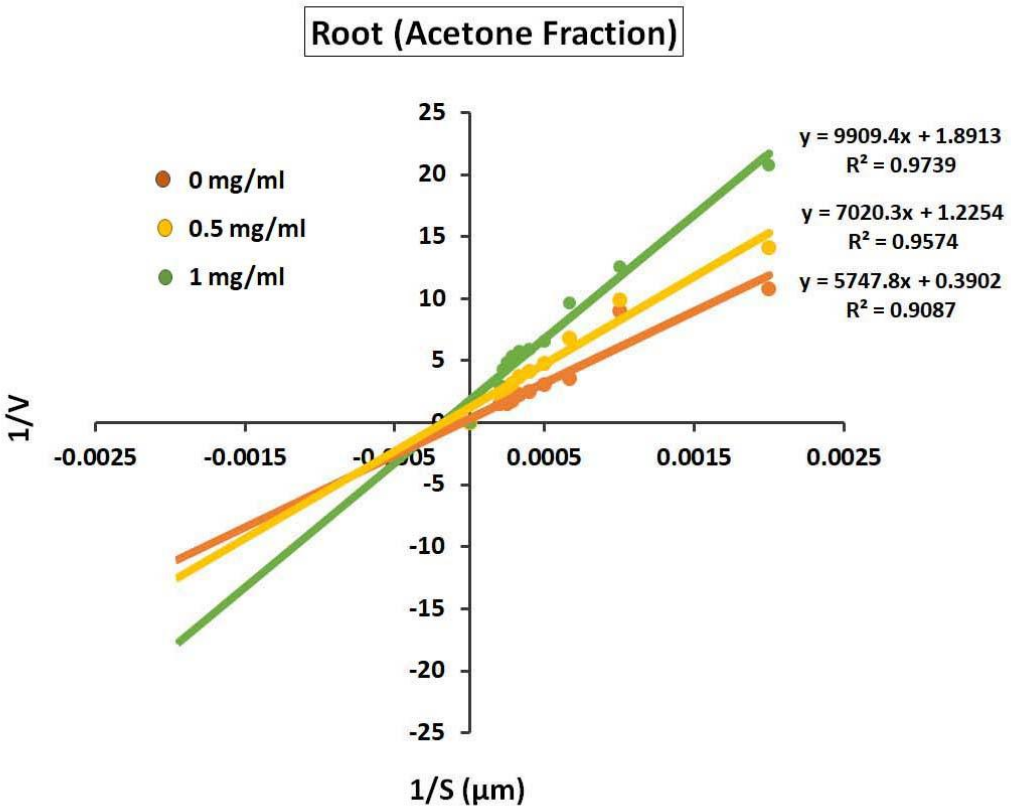

Figure 5.13: Lineweaver-Burk Plot (1/v vs 1/[S]) of root acetone fraction at different inhibitor concentrations.

A double reciprocal plot for the root acetone fraction is similarly constructed to determine the mode of inhibition.

Inhibitor (mg/ml)	V_{max} (µm/min)	K_m (µm)	K_i (µg/ml)
0	1.5165±0.17	10749±0.92	-
0.5	0.8160±0.33	10572±0.99	259.60±0.98
1	0.5627±0.79	10730±0.76	233.75±0.63

Table 5.4: Vmax, K_m, and Ki Values for the Root Acetone Fraction in the presence or absence Inhibitor.

Kinetic analysis revealed a non-competitive mode of inhibition, characterized by a consistent $K_m$value and a reduction in V_{max} as the inhibitor concentration increased. The inhibition constant (K_i) represents the strength of the interaction

between the enzyme and the inhibitor, with a lower K_i indicating a higher binding affinity **(Bisswanger et al., 2017).** In non-competitive inhibition, the inhibitor effectively reduces the overall enzyme activity, leading to a decline in V_{max}, while K_m remains unaffected since the inhibitor and substrate bind independently without interfering with each other's binding sites.

These findings indicate that *Cleome gynandra* holds strong potential as a natural source of urease inhibitors. Previous studies have highlighted the role of water-soluble bioactive compounds in plants with urease-inhibitory properties. Such compounds are often polyphenols, flavonoids, or antioxidant molecules known for their beneficial health effects **(Modolo et al., 2015).**

In our study, the root water fraction demonstrated the highest urease inhibitory activity, leading us to focus on identifying the bioactive constituents specifically present in this fraction. Compounds that are water-soluble, easily absorbed, and rapidly transported within biological systems are of particular interest. Therefore, the subsequent chapters will delve into the characterization of these compounds, exploring their molecular interactions and behaviour under dynamic biological conditions.

Chapter 6

6.1 HR-LCMS ANALYSIS TO IDENTIFY THE BIOACTIVE COMPOUNDS

The most potent part of the plant, the root of *Cleome gynandra* (methanol, acetone, and water fraction) having the maximum urease inhibiting activity was assessed through high-resolution liquid chromatography-mass spectrometry (HR-LCMS). The analysis was performed using Agilent instruments from the United States of America, including the UHPLC Infinity 1290 system, Nano HPLC Infinity 1260 with chip stacking, and an iFunnel Q-TOF 6550 mass spectrometer using column particulars- ZORBAX column family eclipse plus HPLC C18 column, tapered bore 2.1x150 mm, 5-micron acquired from Indian Institute of Technology Bombay (SAIF).

Mass spectrometry acquisition parameters included a lower mass range of 150 m/z and an upper limit of 1200 m/z, with a scan rate of one spectrum per second. The accurate mass data was obtained using the 6200 Series TOF/6500 Series Q-TOF model (version B.05.01, B5125.3).

The system was equipped with a vapor phase chromatograph operating at 250°C, with a carrier gas flow of 13 psi/min. A Hip sampler (Model G4226A) was used with a sample injection volume of 3.00 µl, an auxiliary flow rate of 100 µl/min, and a flush volume of 5.0 µl. The total runtime was 30 minutes.

Ionization was performed using dual Jet Stream ESI technology in both positive and negative ion modes. Operating conditions were maintained at a column pressure of up to 1200 bar, a flow rate of 0.3 ml/min, a column temperature of 35°C, and a discharge speed of 100 ml/min in a 30-minute stop-flow mode.

Main Features of HR-LCMS:

- Screening of several thousand analytes, including amino acid, fatty acid, lipid, phenolic compounds, flavonoids, alkaloids, aromatic compounds, carotenoids, etc., in a single run.

- Capable of detecting, identifying, and quantifying compounds at very low concentrations.
- Facilitates the generation of molecular formulas for unknown bioactive compounds.
- Allows for the determination of chemical structures and properties.

Among the tested fractions, the water, methanol, and acetone root extracts exhibited the most significant urease enzyme inhibition. Consequently, the bioactive compounds present in these fractions were selected for further analysis.

6.2 Results of HR-LCMS Analysis

6.2.1 HR-LCMS Spectrum of the Purified Root Water Fraction of *C. gynandra*

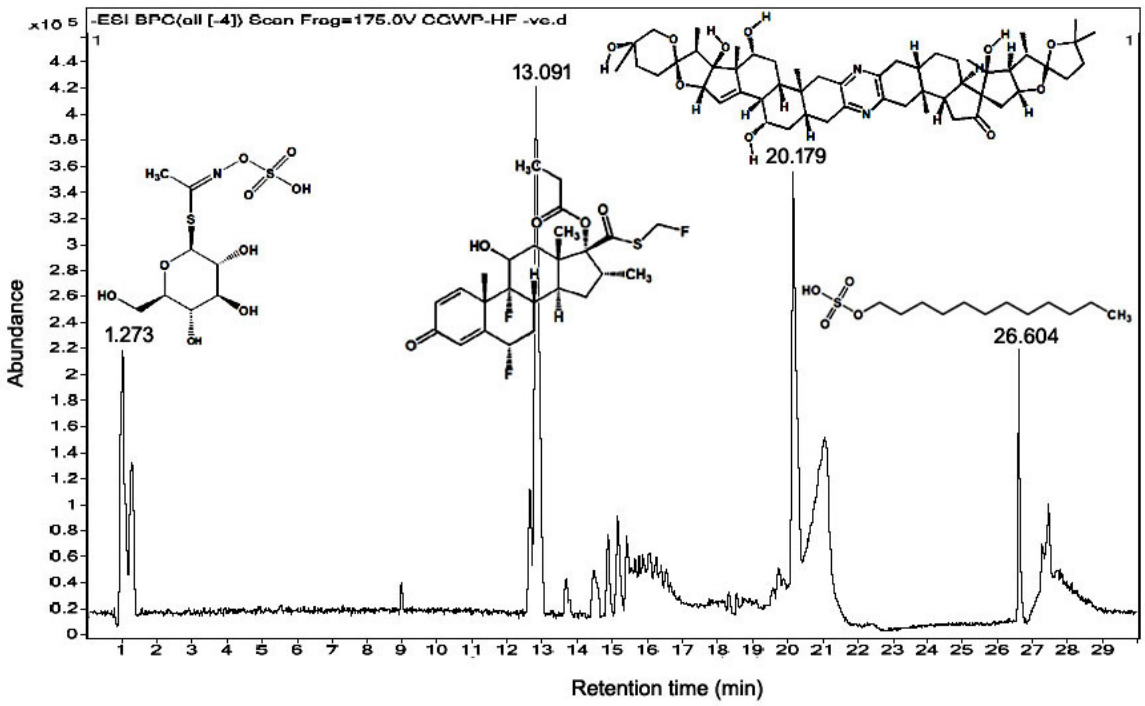

Figure 6.1: HR-LCMS spectra of purified *Cleome gynandra* root water fraction.

The water fraction exhibited several distinct sharp peaks with retention times at 1.237 min, 12.867 min, 20.179 min, and 26.604 min, corresponding to the compounds Glucocapparin (GCP), Fluticasone Propionate (FP), Ritterizine A (RA), and Lauryl Hydrogen Sulphate (LHS), respectively.

Retention time refers to the duration a specific biomolecule takes to travel through the chromatography column and reach the detector. This parameter is crucial for separating molecules within a complex mixture and plays a significant role in identifying and quantifying analytes.

- **Glucocapparin -** It is a type of glucosinolate, a prominent group of secondary metabolites commonly found in cruciferous crops such as cabbage, mustard, and radish and others. These compounds represent the most bioactive constituents of the Brassicaceae family, as well as a few closely related plant families. Glucosinolate profiling in *Cleome gynandra* has revealed its potential medicinal benefits. The concentration of methyl glucosinolate, also known as glucocapparin, can vary depending on the extraction method used and and the developmental stage of the plant **(Mano et al., 2024).** Previous studies have reported high levels of methyl glucosinolates in the seeds of *Cleome gynandra* and *Cleome spinosa*. Additionally, glucocapparin has also been reported in *Isomeris arborea*, a member of the Capparaceae family **(Blua et al., 1986).**
- **Fluticasone Propionate (FP) -** It is a distinctive androstane-based glucocorticoid known for its potent anti-inflammatory properties. It has been widely and effectively used in the treatment of asthma and is considered a cost-efficient therapeutic option. In patients with persistent asthma, the use of fluticasone propionate has been associated with significant improvements in quality of life. Interestingly, this compound has also been identified in the methanolic leaf extract of the tomato plant (*Solanum lycopersicum* L.) **(Johnson et al., 1998).**
- **Ritterazine A:** It is a cytotoxic steroidal alkaloid known to trigger apoptosis in cancer cells. In 1990, Fusetani's research group identified approximately 26 ritterazine compounds from *Ritterella tokioka* extracts. These compounds have demonstrated significant anticancer activity against various cancer

types, including renal, breast, brain, lung, prostate, and colon cancers **(Lee et al., 2009).**

- **Lauryl Hydrogen Sulfate - It** is an anionic surfactant known for its protein-denaturing properties. It has been reported to inhibit a range of both enveloped and non-enveloped viruses by disrupting viral envelopes or denaturing capsid and envelope proteins. Notably, it is non-toxic to various cultured cell lines at concentrations effective enough to inactivate viruses such as Human Immunodeficiency Virus-1 (HIV-1), herpes simplex virus, and human papillomavirus in vitro. Due to these antiviral properties, it has been proposed as a promising microbicide for the prevention of sexually transmitted infections **(Piret et al., 2002).**

6.2.2 HR-LCMS Spectrum of the Purified Root Methanol Fraction of *Cleome gynandra*

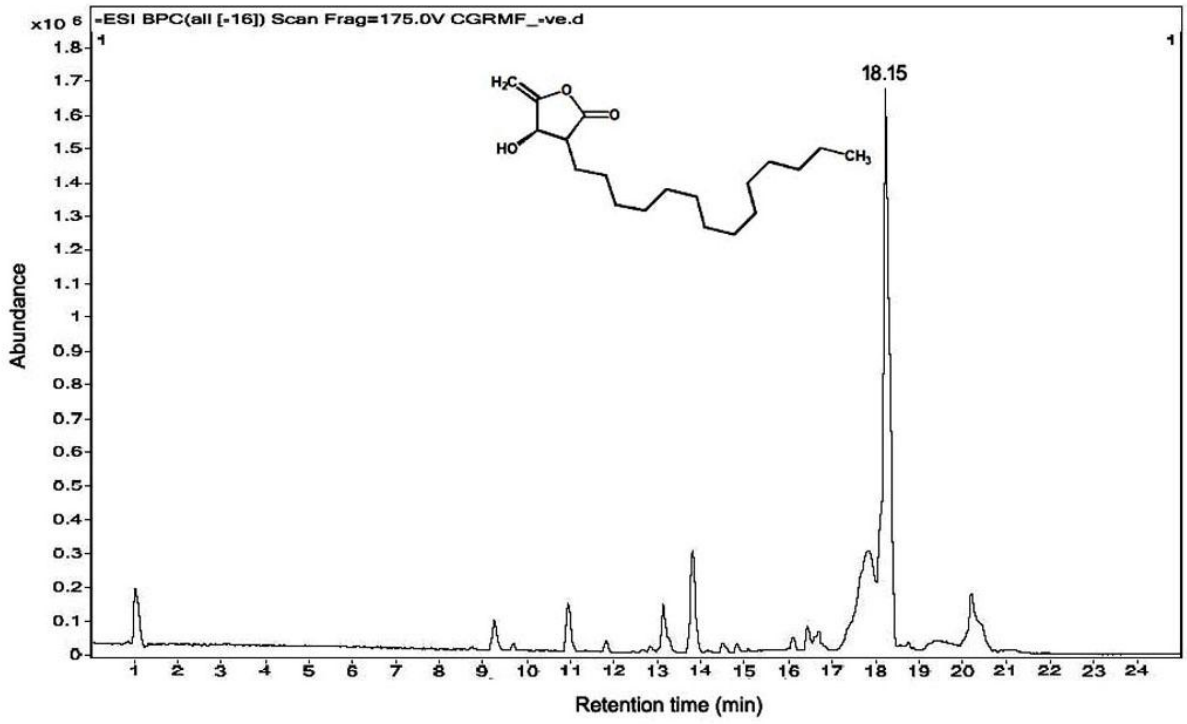

Figure 6.2: HR-LCMS spectra of purified *Cleome gynandra* root methanol fraction.

HR-LCMS spectra of the purified methanolic root extract of *Cleome gynandra* revealed a single prominent peak, corresponding to the compound Obtusilactone A, with a retention time of 18.15 minutes.

- **Obtusilactone A (OA):** This bioactive compound, isolated from *Cinnamomum kotoense*, demonstrates significant anticancer potential. It induces double-stranded DNA breakage and activates the DNA damage response through apoptosis. Exposure to OA leads to cell cycle arrest at both the S and G1 phases. This compound also stimulates the production of reactive oxygen species (ROS), which in turn activate signaling pathways involved in DNA repair, checkpoint control, and programmed cell death **(Wang et al., 2010).** Beyond its anticancer potential, OA also supports mineral deposition in the extracellular matrix of bone marrow-derived mesenchymal stem cells (BMSCs). As a result, it shows promise in stimulating osteoprogenitor cells and enhancing bone regeneration via BMSCs **(Lin et al., 2018).**

6.2.3 HR-LCMS spectrum of the purified root acetone fraction of *C. gynandra*

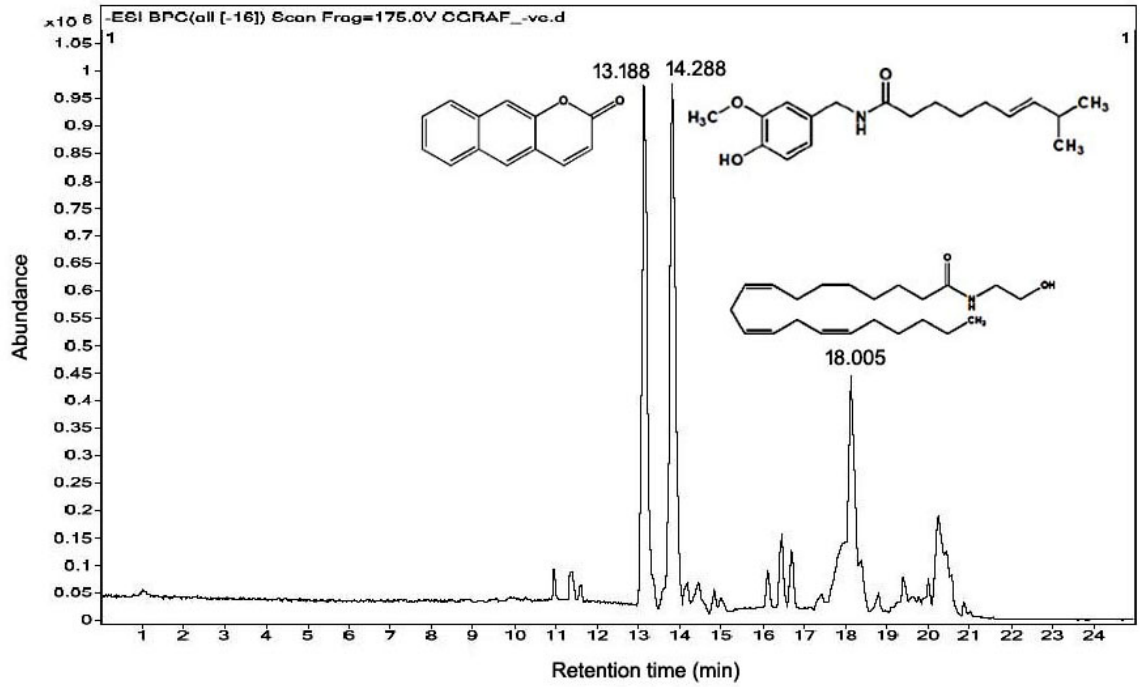

Figure 6.3: HR-LCMS spectra of purified *Cleome gynandra* root acetone fracion.

HR-LCMS analysis of the purified acetone fraction displayed three prominent peaks at retention times of 13.18, 14.28, and 18.00 minutes, corresponding to benzocoumarin, capsaicin, and dihomo-γ-linolenoyl-ethyl acetate, respectively.

- **Benzocoumarins:** These coumarin derivatives exhibit a wide range of biological activities, including anti-leukotriene, antimicrobial, anti-tumor, antioxidant, anticoagulant, and analgesic effects. They are naturally occurring flavonoids are widely found throughout the plant kingdom and have also demonstrated anti-diabetic potential. The leaves of *Murraya alata* Drake (Rutaceae) were found to contain 33 different coumarin derivatives in its 95% aqueous extract. The biosynthesis and natural evolution of benzocoumarin compounds have shown promising antioxidant and lipid-lowering activities **(Lv et al., 2015).** The lipid-dropping activity and lipoprotein lipase (LPL) activity of various benzocoumarin products lipoprotein lipase (LPL), have been investigated in vivo using Triton-based models. Moreover, coumarin-based selective estrogen receptor modulators (SERMs) and coumarin-estrogen hybrids have emerged as potential therapeutic agents in the treatment of breast cancer, a disease that has become a leading cause of cancer-related deaths among American women, second only to bronchogenic carcinoma **(Lv et al., 2014).**
- **Capsaicin:** It is a chili pepper extract with notable analgesic properties. First isolated by Christian Bucholz in 1816, it has long been used in homeopathic medicine to alleviate burning pain **(Sharma et al., 2013).** Over the years, its therapeutic applications have expanded to include the treatment of various painful conditions, such as:
  - Non-diabetic nerve pain
  - Nerve pain resulting from varicella-zoster virus infection
  - Chronic joint pain due to cartilage degeneration

- Recurrent pain in muscles, ligaments, and tendons that recovers every three months
- Postoperative neuropathic pain following breast surgery
- Burning mouth syndrome
- Treatment of OAB (overactive bladder) condition
- Gastrointestinal discomfort or pain related to gastropathy
- Postoperative or post-anesthesia nausea and vomiting
- Treatment of pruritus (generalized skin itchiness)
- Postoperative sore throat
- Treatment of swallowing disorders, including dysphagia
- Management of mucositis caused by chemotherapy and radiotherapy

Capsaicin alleviates pain by triggering an influx of calcium ions, which desensitizes afferent neurons. This influx impairs mitochondrial function, thereby reducing the activity of these sensory nerves (Fitzgerald et al., 1983). Hence these plant-based compounds have shown promising potential in the management and alleviation of various diseases.

- **Dihomo-γ-linolenoyl-ethyl acetate:** studies have shown administration of ethyl dihomo-y-linolenate in rabbits could deliver a technique for cumulative biosynthesis of prostaglandin E with no accumulation of blood clot or thrombus due to high platelet count, resulting in blood pressure drop. Increased levels of prostaglandin E1 may offer therapeutic benefits in certain disease conditions **(Needleman et al., 1980).**

  The *Cleome* genus has been recognized as a rich source of bioactive compounds, including essential oils, flavonoids, phenolic compounds, and alkaloids, all of which contribute significantly to the treatment of various disease conditions. Among the different solvent fractions, the aqueous extract demonstrated the most potent urease inhibitory activity. This finding prompted further investigation into the interaction between the bioactive

constituents of the water extract and the catalytic site of the target enzyme. Aqueous extraction is often preferred over organic solvent-based methods due to its accessibility, cost-effectiveness, and safety. Additionally, the use of water as a solvent aligns with environmentally friendly practices, making it a more sustainable option **(Gallina et al., 2022).**

Chapter 7

MOLECULAR DOCKING STUDY

7.1 Structure Based Design – Docking

It is a computational method that predicts the conformation of bonding between protein and ligand as well as determines the free energies for binding of small ligand molecules to their target protein. Proteins and nucleic acids can interact with small ligand fragments to form macromolecular complexes, which play significant roles in regulating protein function, either enhancing or inhibiting their biological activity. Docking studies are carried out to gain insights into the mechanisms of inhibition and the specific modes of interaction between ligands and target proteins. These studies help determine the most favorable orientation and binding affinity of a ligand within the enzyme's active site **(Lengauer et al., 1996).** Depending on the various kinds of ligands, docking studies can be classified into the following categories:

- Enzyme–DNA/RNA docking
- Two enzyme molecules docking

There are various software programs that are used for molecular docking analysis such as

- AutoDock
- GOLD
- FlexX
- DOCK

The principal step in molecular docking is the study of probable protein conformity and alignments of the protein combined through ligands. This is followed by the application of a scoring function, which evaluates the most favorable binding position. Selecting an appropriate X-ray crystallographic structure from the Protein Data Bank (PDB) is a vital process followed by extraction of the bound ligand and identifying the active site of the protein. All

docking software uses specific algorithms to determine the protein's active site by allowing the ligand to bind at different regions of the protein, ultimately identifying the optimal binding conformation of the ligand–protein complex **(Kitchen et al., 2004).**

There are few basic common terms that are related to docking study:

- **Receptor:** It is a large protein molecule found either on the cell membrane or inside the cell, which selectively interacts with specific ligand molecules, leading to functional responses and, sometimes structural changes **(Kearsley et al., 1994).**
- **Ligand:** A ligand is a molecule that specifically binds to its corresponding receptor to induce changes in biological processes. Typically, ligands are small molecules such as drugs, hormones, neurotransmitters, plant metabolites, or antigens. They may also be organic compounds in the context of enzyme-enzyme interaction studies **(Kearsley et al., 1994).**
- **Dock**: It is a computational approach that employs monoatomic modeling to visualize the interaction between a specific ligand and the catalytic site of a target enzyme, facilitating the identification of the most favorable binding orientation and position.
- **Dock pose:** A ligand may bind to a protein in multiple positions, each characterized by different conformations and orientations **(Arcon et al., 2021).**
- **Mode of binding:** Refers to the specific docking configuration adopted once the ligand and protein have successfully bound in an appropriate conformation.
- **Scoring of docked complexes:** This process involves assessing a particular docked pose by calculating the sum of favorable molecular interactions, such as hydrogen bonds and hydrophobic interactions. Each pose is evaluated based on its similarity to the target molecule, considering

factors like shape and ionic properties, and assigned a docking score that identifies the most energetically favorable conformation. A high docking score for a particular ligand suggests that it theoretically has strong binding potential **(Arcon et al., 2021).**

- **Rank:** Ligands are classified based on their calculated binding free energy and favorable interactions with their corresponding receptors. After the docking process is completed, the ligands are ranked according to their docking scores. This ranking is then utilized to guide further development and biological research, focusing on the combinations predicted to demonstrate the greatest activity **(Kitchen et al., 2004).**
- **Pose predictions:** This process involves selecting the most favorable pose from multiple binding modes, based on the lowest energy. It defines the optimal position and conformation of the ligand in its docked form, accounting for its flexible nature **(Kearsley et al., 1994).**
- **Predicting affinity:** This pertains to the most energetically favorable pose of a ligand, which may include multiple poses. It involves comparing the affinity scores of different molecules and assigning them a relative ranking **(Arcon et al., 2021).**

Essential Requirements for Docking Analysis:

- **Crystal structure of the receptor:** The receptor of interest must be resolved using experimental techniques such as single crystal X-ray diffraction or NMR (nuclear magnetic resonance), with the structure obtained from the Protein Data Bank. The resolution of the receptor structure plays a crucial role for accurate docking analysis and reliable results. In general, a resolution greater than 2Å is preferable for better docking outcomes. Another important factor called factor-B that represents the attenuation of scattering of X-ray and neutron due to thermal motion. A low B-factor suggests well-ordered coordinates, while a high B-factor

points to more flexible coordinates. Therefore, a thorough understanding of the protein-ligand interactions is essential for accurate docking studies **(Arcon et al., 2021).**

- **Homology modeling of the receptor and threading techniques:** When the crystal structure of the target receptor is unavailable, structure prediction methods such as homology modeling and threading can be utilized. Threading, or fold recognition, involves evaluating whether the target amino acid sequence aligns well with any known monomeric peptides in structural databases. In contrast, homology or comparative modeling relies on the sequence similarity between the target enzyme and at least one known structure **(Lengauer et al., 1996).**
- **Combination of Ligands of Interest:** Binding of selected ligands to a target protein structure enables the identification and comparison of potential binding sites. Characterizing these sites across different ligands can offer valuable insights for designing new ligands or for docking predicted ligand molecules **(Arcon et al., 2021).**

Basic Steps in Docking:

Docking generally follows a three-stage process, irrespective of the specific software or protocol used **(Lengauer et al., 1996):**

a) Ligand Preparation: In the initial step, duplicate structures should be excluded. The operational program must be configured to define parameters such as nucleation charge, structural isomers, isomer generation, and the initiation of 3D structures for each peptide molecule.

b) Protein Preparation: This step involves the addition of hydrogen atoms and subsequent protein minimization using appropriate software. All water molecules, except those within the catalytic domain, should be removed. The receptor structure must be carefully validated by checking for errors and ensuring

that all residues in the catalytic region are complete. The receptor must be thoroughly prepared by checking for errors and verifying that all residues in the catalytic site are complete. If metal atoms are present, their atomic types and charges should be accurately assigned. Any metal ion bonds should be removed, and necessary adjustments made to the atomic charges, including accounting for the cationic charge. These preparations ensure the receptor is ready for the docking process.

c) Protein-Ligand Docking: In grid-based docking, once the receptor and ligands are properly prepared, grid files are generated using specialized grid-receptor software. The grid box is generally centered on the peptide molecule bound to the receptor's catalytic domain. In some cases, the protein's active site is first identified for docking of the prepared ligand. protein or enzyme. These values are compared with those of known receptor-bound ligands to assess whether the ligand of interest effectively targets the catalytic domain. Different conformations of each compound are stored as docked poses, ranked by docking score functions, and further analyzed for their interactions with the receptor. The docking results are then correlated with the known functional activities of the compounds in the dataset.

7.2 Experimental design

The crystal structure of the target enzyme, jack bean urease (*Canavalia ensiformis*), the first plant urease was obtained from the RCSB Protein Data Bank (PDB) [PDB ID: 4H9M] via http://www.rcsb.org/. To analyze its interaction with selected complexes within a 3D domain, computational docking was carried out using the open-source tool AutoDock Vina (http://vina.scripps.edu/), implemented through UCSF Chimera version 1.17.3 **(Pettersen et al., 2004).**

In this docking study, ligands were selected based on biologically active compounds present in the root water extract of *Cleome gynandra*, which

exhibited the highest inhibitory activity against jack bean urease. The compounds chosen for analysis were glucocapparin (PubChem ID: 21600408), fluticasone propionate (PubChem ID: 444036), dodecyl sulfate (PubChem ID: 8778), and thiourea (PubChem ID: 2723790). Their 3D structures were retrieved from the PubChem database (http://pubchem.ncbi.nlm.nih.gov/) in Structured Data Format (SDF).During receptor preparation, particular attention was given to preserving the dynamic region containing the nickel metal ion, which served as the primary focus. Subsequent steps included the removal of multicomponent molecular crystals, addition of polar hydrogen atoms, and computation of charges based on electron density. The catalytic domain of the enzyme was defined using a cubic grid box with dimensions of 20 Å on each side, centered at coordinates X: 19.0670, Y: -56.3270, and Z: 21.3340.

For docking models, nine top binding poses were generated by extending the default standards for the remaining constraints. These docked conformations were evaluated based on their binding affinities and docking scores (in kcal/mol), and interaction patterns were analyzed using tools such as LIGPLUS+ v2.2.8 **(Laskowski & Swindells, 2011),** the Protein-Ligand Interaction Profiler **(Salentin et al., 2015)** and PyMOL **(Schrödinger, 2017).** The final docked complex between receptor and ligand was selected based on the pose with the lowest binding energy. Lastly, the grounding of docking and physical minimization of the selected compounds and enzymes was carried out using UCSF Chimera version 1.17.3, enabling comprehensive setup for subsequent molecular docking analyses**.**

7.3 Results and Discussion

The molecular docking analysis was employed to predict the binding mechanisms of ligands that inhibit the target enzyme and to explore their interactions at the molecular level. Bioactive compounds identified in the *Cleome gynandra* root

water extract was selected based on their high potential to inhibit urease activity, as determined by HR-LCMS.

7.3.1 Computational Molecular Docking Results of Glucocapparin (GCP)

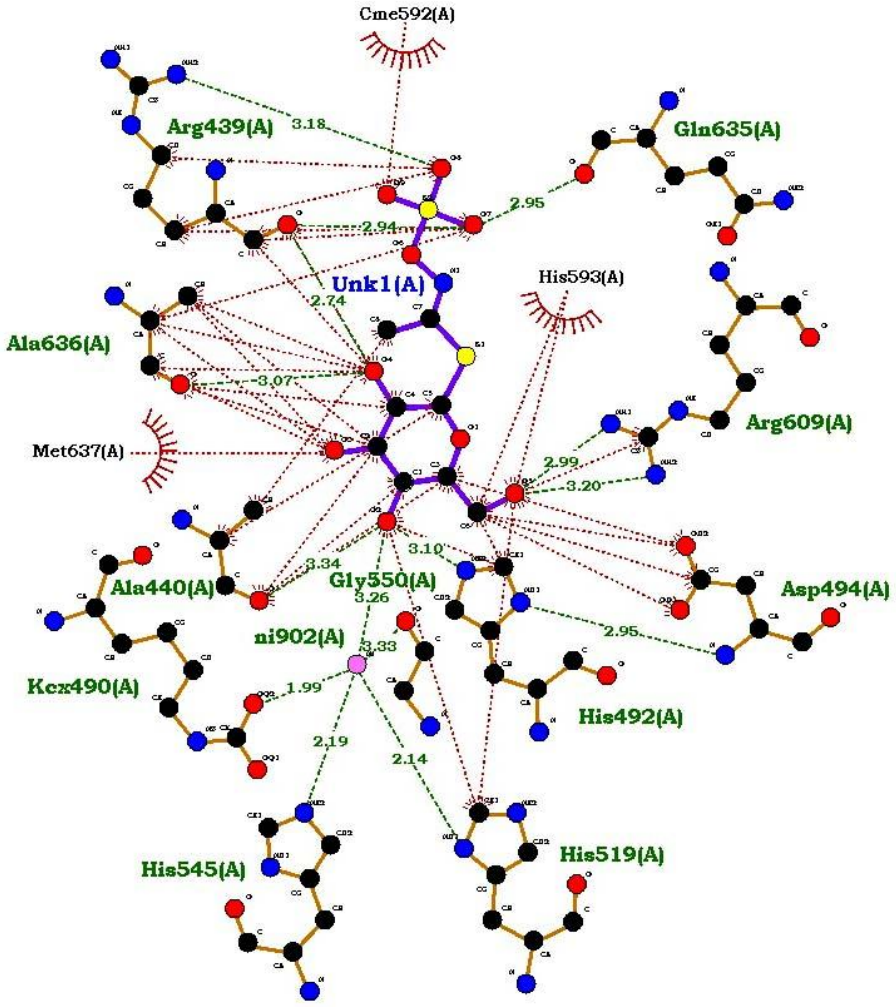

Figure 7.1: Molecular interactions of Glucocapparin (GCP) with catalytic site of urease using LIGPLUS^{+} V.2.2.8

The result of the computational molecular docking revealed that the compound GCP associate with the jack bean urease enzyme having the least docked affinity of -6.6 Kilocal/mol. This interaction of GCP with the active site of urease involved via hydrogen bonding with amino acids Histide-492, Arginine-609, Glutamine-635, Arginine-439, Alanine-636 and Glycine-550. This is enclosed by hydrophobic contact with Alanine-440, Histidine-593, Methionine-637 and Carboxymethylethanolamine-592.

➢ **2D ligand-receptor interaction diagrams of Glucocapparin:**

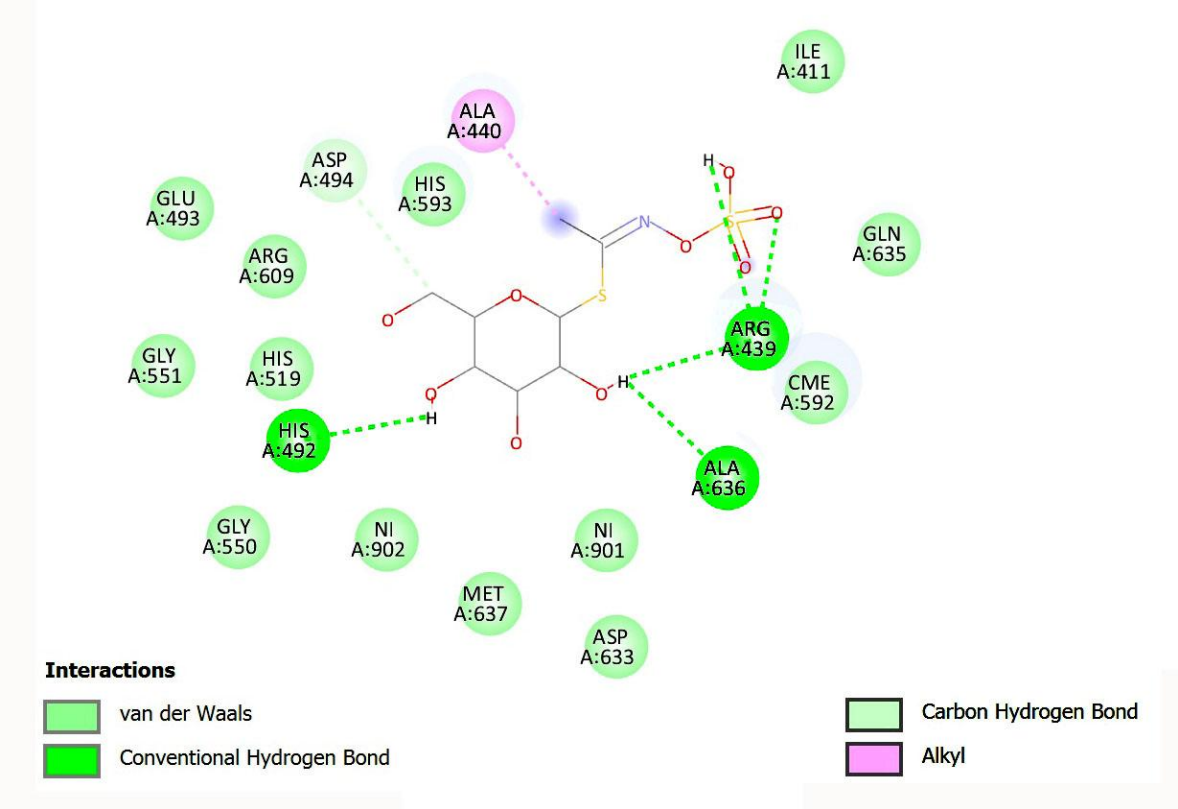

Figure 7.2: Jack bean urease-GCP complex interaction in 2-D diagram using UCSF chimera 1.17.3

The contact of glucocapparin along with amino acids Histidine-492, Alanine-636, Arginine-609 and Arginine-439 are resilient and noticeable hydrogen contact compared to others.

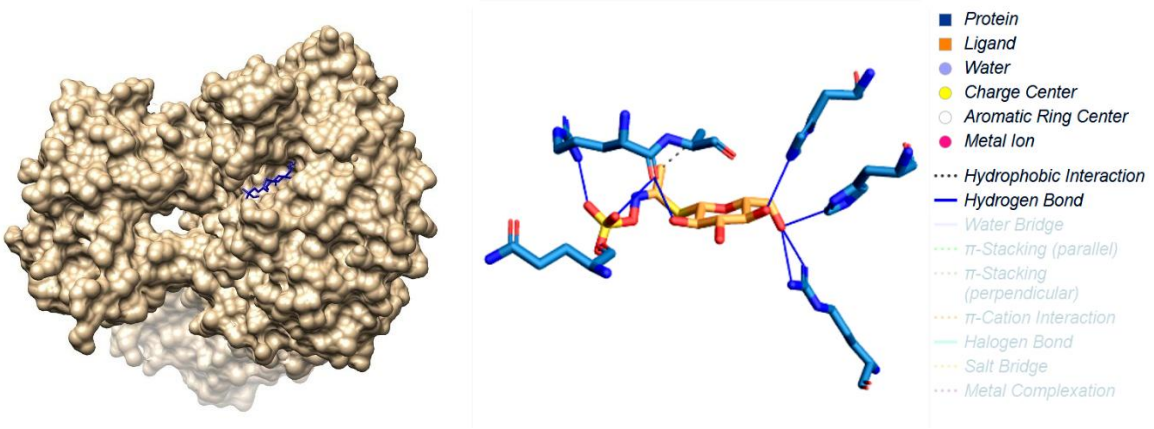

Figure 7.3: Plausible mode of binding of GCP with the conserved nickel enclosing active site flap of jack bean urease

Probable binding manners with nickel preserved catalytic position fold of JBU showing strong and noticeable hydrogen bonding. The interaction of GCP with nickel ion 902 was also conserved by a hydrogen bonding interaction with the participation of amino acids Histidine-519, Histidine-545 and Lysine nz-carboxylic acid -490.

7.3.2 Computational Molecular Docking Results of Fluticasone Propionate (FP)

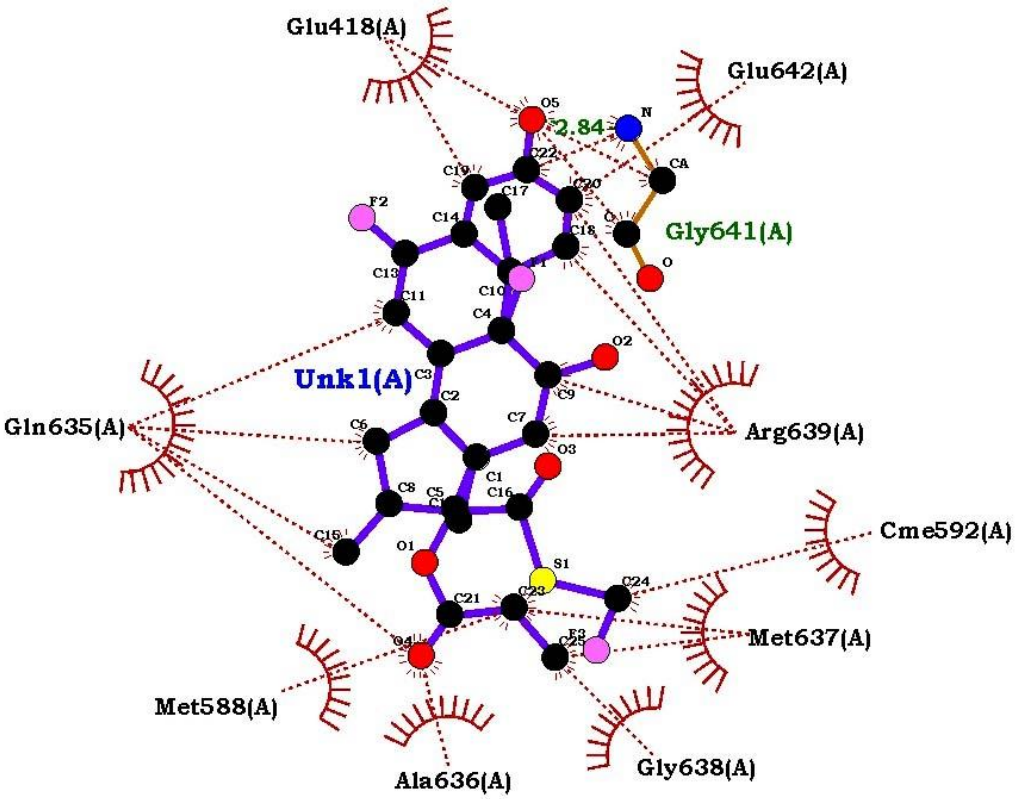

Figure 7.4: Molecular interactions of FP with catalytic site of urease using LIGPLUS^{+} V.2.2.8

Fluticasone propionate (FP) makes only one strong hydrogen bonding with amino result of -6.0 Kilocal/mol.

- **2D ligand-receptor interaction diagrams of Fluticasone propionate:**

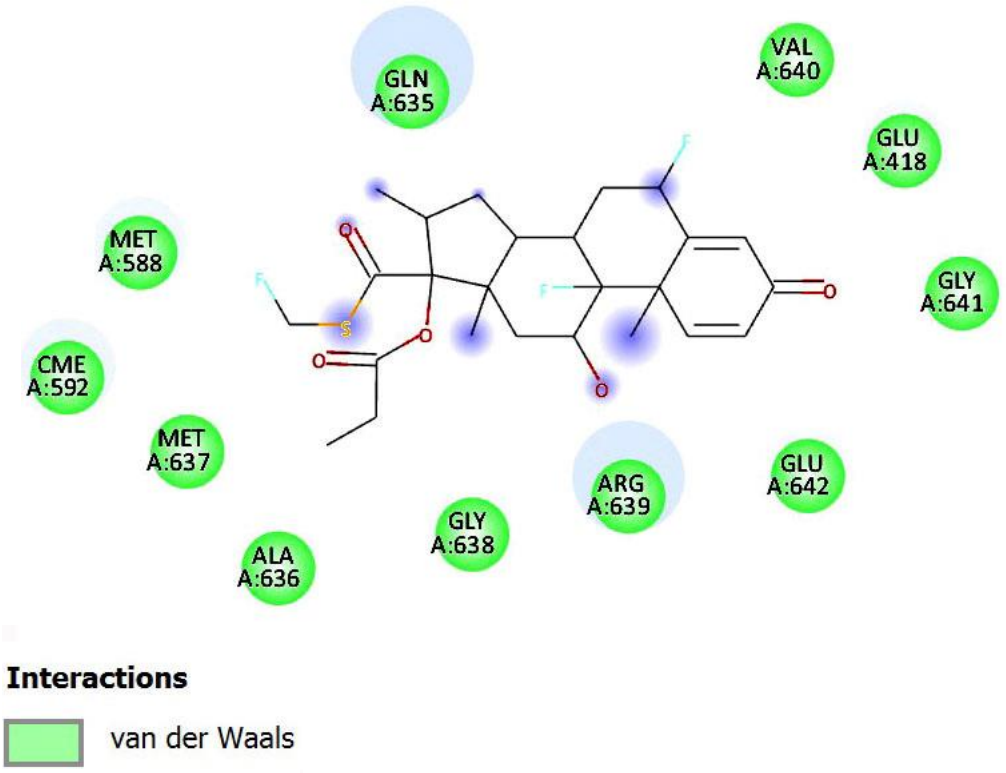

Figure 7.5: Jack bean urease-FP complex interaction in 2-D diagram using UCSF chimera 1.17.3

Besides making a single strong hydrogen bonding with GLY-641 residue it makes other hydrophobic interaction with amino acids Glutamic acid-418, Glutamine-635, Arginine-639, Glycine-638, Glutamic acid-642, Methionine-588, Methionne-637, Alanine-636 and Carboxymethylethanolamine -638.

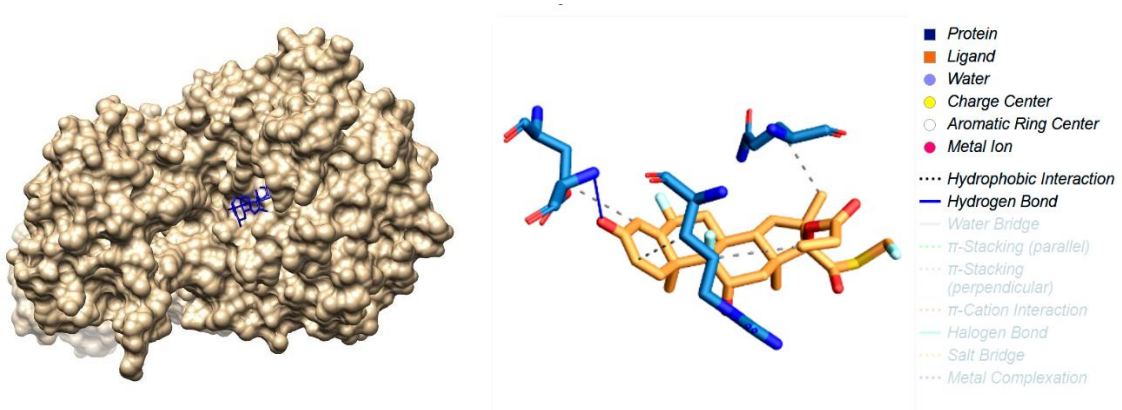

Figure 7.6: Plausible mode of binding of FP with the conserved nickel enclosing active site flap of jack bean urease

Probable binding methods with metal ion preserved catalytic binding pocket of urease enzyme with FP has more prominent visibility of single hydrogen bonding surrounded by hydrophobic interactions.

7.3.3 Computational Molecular Docking Results of Lauryl Hydrogen Sulfate (LHL)

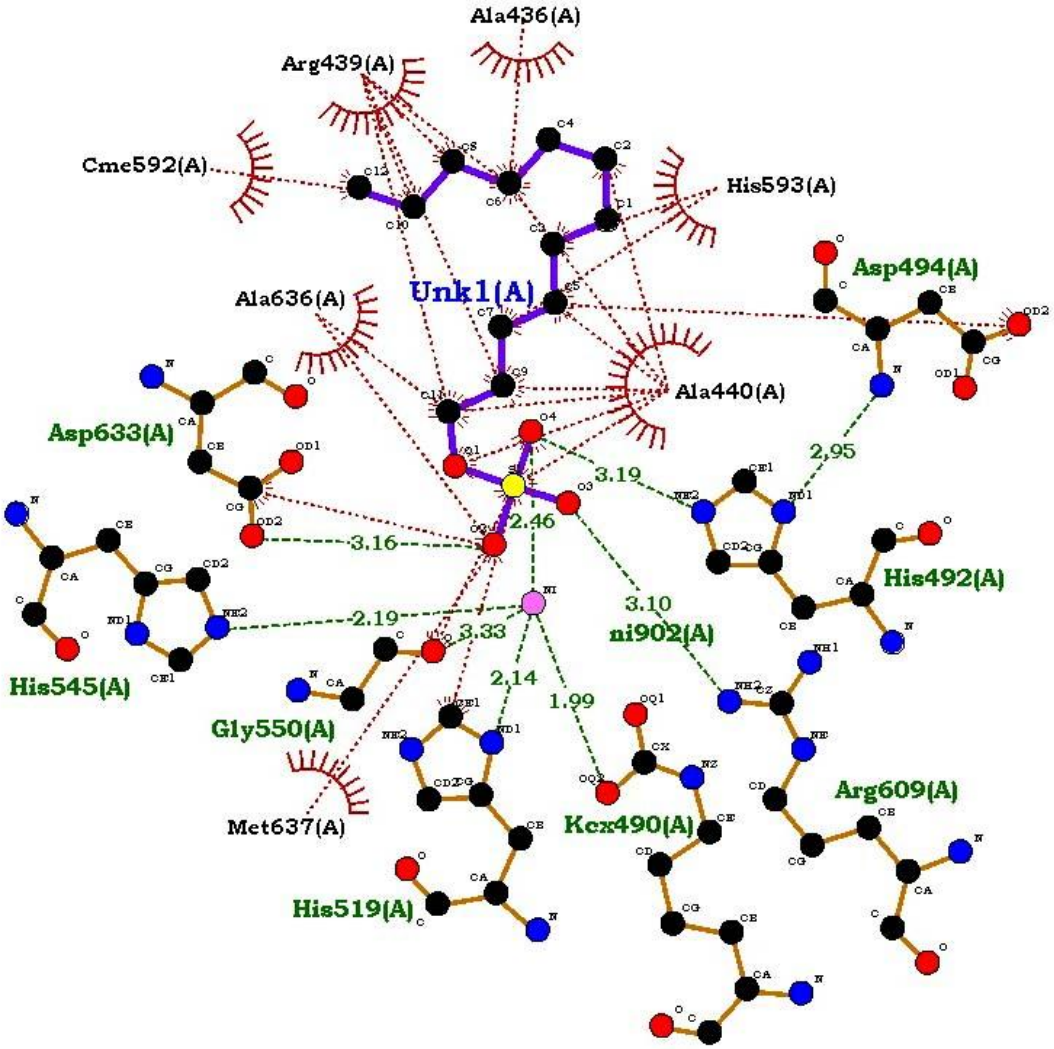

Figure 7.7: Molecular interactions of LHS with catalytic site of urease using LIGPLUS^{+} V.2.2.8

Lauryl hydrogen sulphate (LHS) has made three resilient hydrogen contacts with amino acids Alanine-440, Arginine-609 and Aspartate-633 in the binding pocket of jack bean urease. The resultant docking score was found to be -4.4kcal/mol.

➢ **2D ligand-receptor interaction diagrams of Lauryl hydrogen sulfate:**

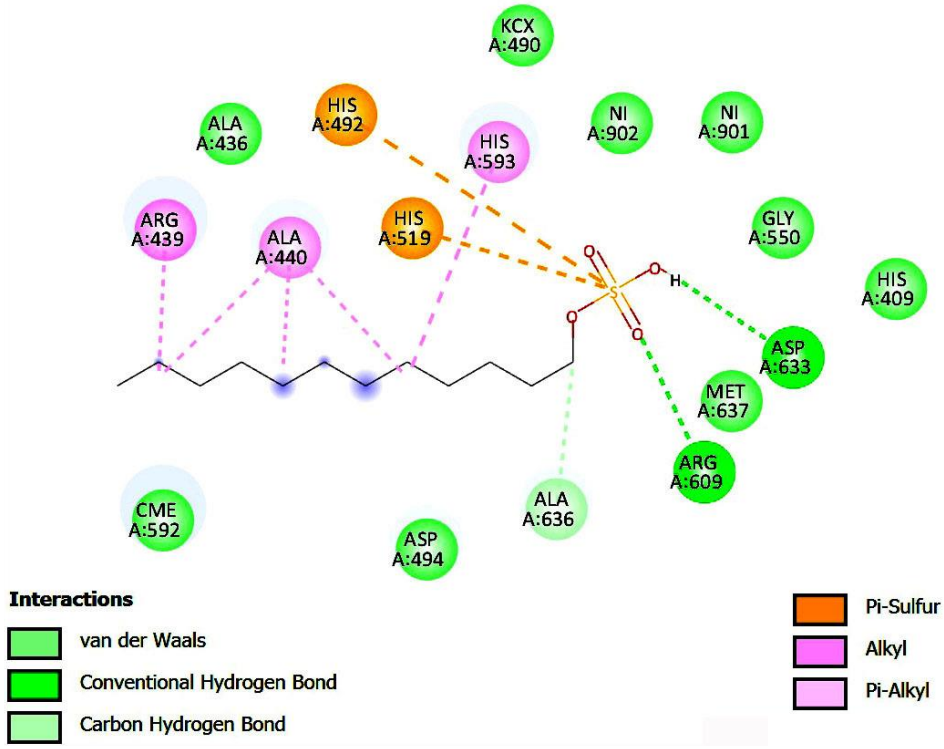

Figure 7.8: Jack bean urease-LHS complex interaction in 2-D diagram using UCSF chimera 1.17.3

An exclusive non-covalent interaction among a sulfur atom and pi-system was also detected with Histidine-492 and Histidine-519 amino acid units in the urease's catalytic site.

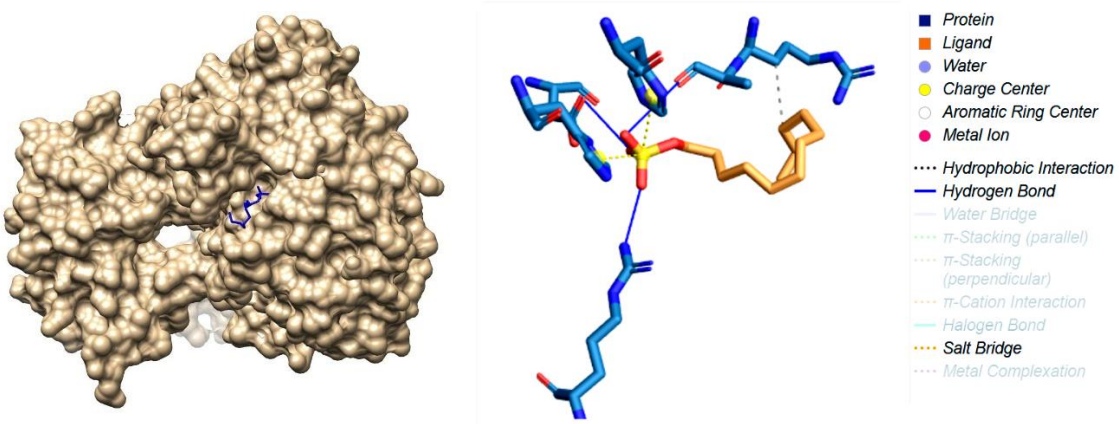

Figure 7.9: Plausible mode of binding of LHS with the conserved nickel enclosing active site flap of jack bean urease

The contact of the ligand with the receptor showing the unique pi-sulfur interaction along with hydrogen bonding and salt bridges. The binding of ligand usually induces a conformational change in the receptor for maximizing energetically advantageous connections with the compound of interest.

7.3.4 Computational molecular docking result of Thiourea, standard inhibitor

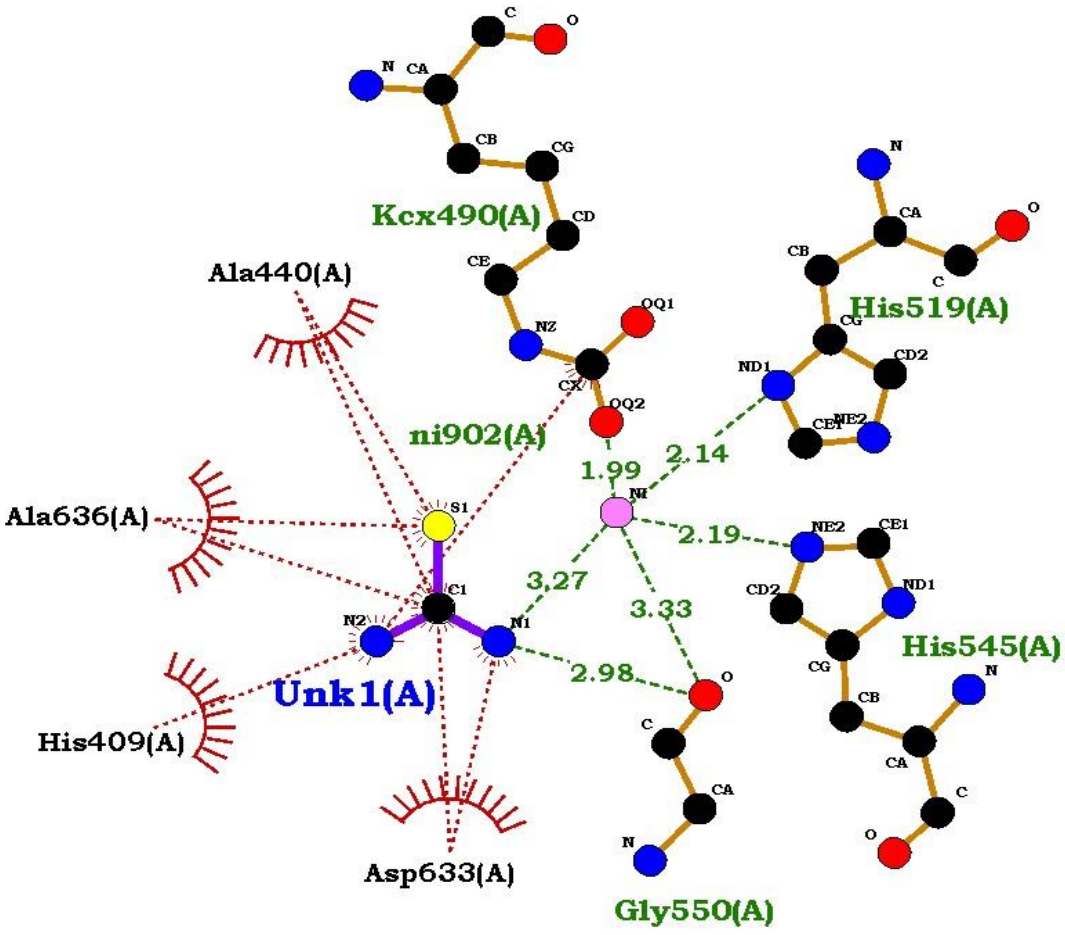

Figure 7.10: Molecular interactions of Thiourea with catalytic site of urease using LIGPLUS^{+} V.2.2.8

The standard urease inhibitor thiourea have revealed the formation of double hydrogen bonds through Histidine-409 and Glycine-550 of urease protein.

➢ **2D ligand-receptor interaction diagrams of Thiourea:**

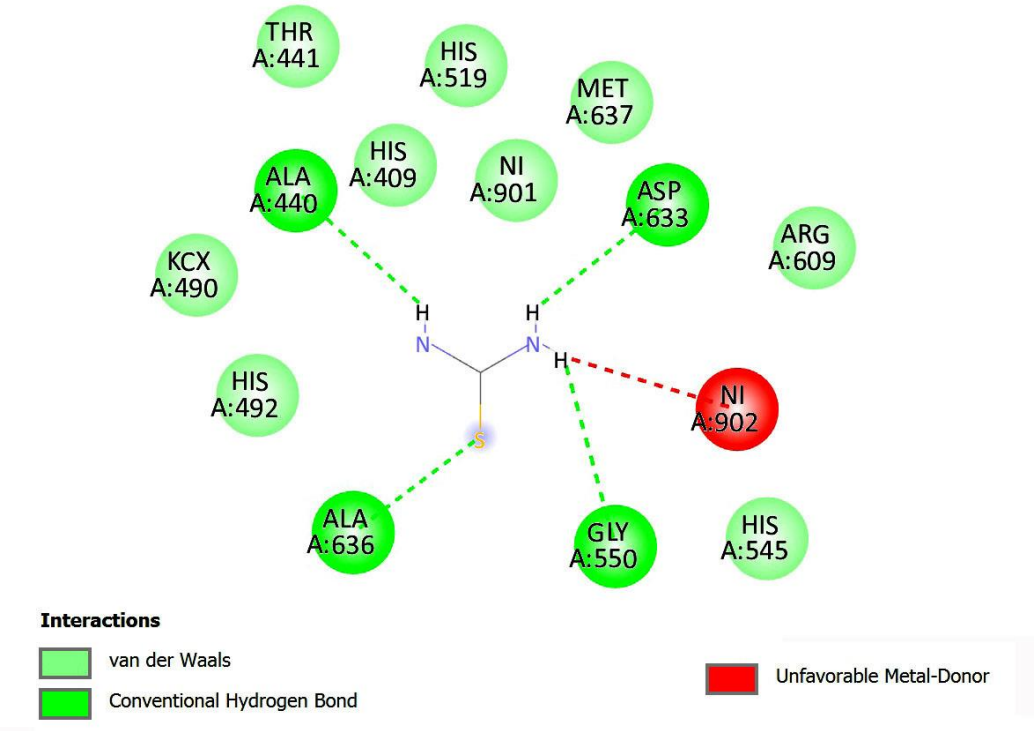

Figure 7.11: Jack bean urease-Thiourea complex interaction in 2-D diagram using UCSF chimera 1.17.3

Besides forming two hydrogen bonding with two amino acids, it involves hydrophobic connections with amino acids Alanine-440, Alanine-636 and Aspartate-633. The resultant docking score was found to be -3.0 Kcal/mol.

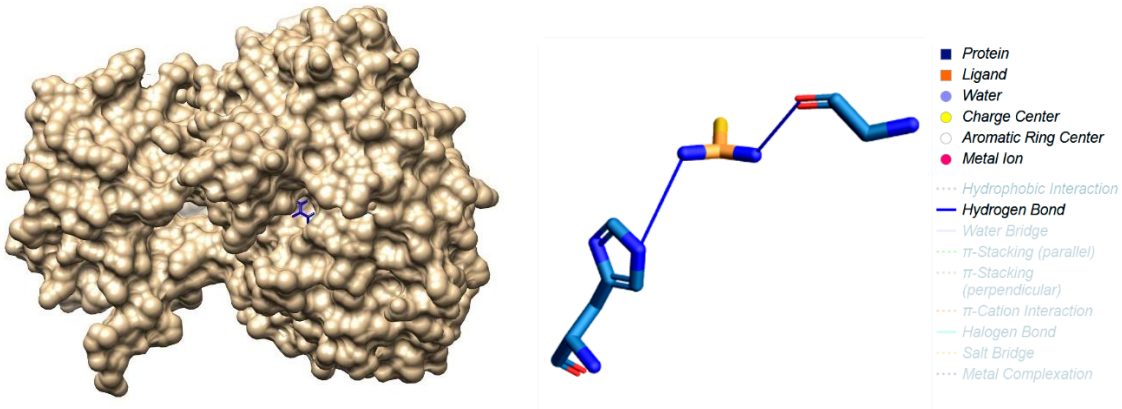

Figure 7.12: Plausible mode of binding of Thiourea with the conserved nickel enclosing active site flap of jack bean urease

The predicted binding patterns of different ligands, typically involving the formation of hydrogen bonds and hydrophobic interactions, enable bioactive molecules to securely attach within the binding pocket of the specific metalloprotein.

Docking technology enables the prediction of various critical parameters, such as the binding mode and affinity of active ligands. A primary objective is to identify the lowest-energy conformations arising from ligand–receptor interactions, a process that has yielded valuable and reliable insights. Understanding how ligands geometrically bind to urease, leading to its inhibition, is a significant aspect of such studies. Previous research has also identified specific amino acid residues within urease that interact with ligands and contribute to reduced enzymatic activity **(Hassan et al., 2017; Zolghadr et al., 2022; Ahmad et al., 2023d).**

Chapter 8

MOLECULAR DYNAMIC SIMULATIONS

8.1 Introduction

Molecular dynamics (MD) simulation is a computational approach used to track the movement of atoms within proteins or other molecular structures over time, based on the fundamental principles of physics that govern atomic interactions. In MD simulations, the dynamic relationship between a ligand and a protein is assessed within an environment designed to mimic the conditions of the human body. This allows for real-time observation of how molecules interact at different binding sites or residues across varying timeframes (**Karplus et al., 2002**).

Water molecules play a crucial role in these simulations, significantly influencing the nature of protein-ligand interactions and contributing to accurate modelling of protein-drug binding. Energy minimization and free energy calculations are utilized to monitor conformational changes during molecular contact. This approach provides valuable insights into molecular behavior at the atomic level under varying mechanical stresses, simulating real cellular conditions.

To further increase the reliability and precision of these simulations, the system is typically immersed in a large volume of water molecules (**Schlick et al., 1996**). Advances in molecular modeling, energy computation, docking algorithms, and chemical simulation tools continue to refine MD techniques, making them increasingly powerful for studying complex molecular interactions.

8.1.1 Molecular Modeling

Molecular modeling is a rapidly evolving technique in the field of computational biology. It encompasses a range of processes, including visualization, analysis, manipulation, and simulation of molecular assemblies, with a focus on understanding their mechanical and chemical properties. This approach facilitates the construction of biomolecular structures by utilizing geometric coordinates

obtained from experimental techniques such as nuclear magnetic resonance (NMR) or single-crystal X-ray diffraction. When experimental configurations are unavailable, molecular structures can be predicted using algorithmic programs that assign X, Y, and Z coordinates to atoms based on prior knowledge of their conformations. The three primary methods of molecular modeling include **Ab initio modeling**, threading, and homology modeling (**Ishida et al., 2011**).

➢ **Intermolecular Interactions and Force Fields**

In molecular docking simulations, the classical equation of motion must be solved iteratively. This equation is typically expressed as:

$$\mathbf{m_i r_i = f_i}$$

Here, f_i represents the force acting on an atom, which is derived from the potential energy function $U(r_n)$, where r_n denotes the complete set of 3N atomic coordinates.

The potential energy is defined by a functional form often referred to as the *force field*, which describes how atomic interactions contribute to the overall energy. This force field encompasses both bonded and non-bonded interactions, that is, covalent bonds and non-covalent forces between atoms and molecules. These interactions collectively help model the physical behavior of molecular systems **(Mayo et al., 1990).**

➢ **Calculation of Time Series**

Understanding time-dependent mechanisms is crucial for analyzing the dynamic behavior of biomolecular interactions over a temporal scale. Time series analysis typically involves metrics such as Root Mean Square Deviation (RMSD), Root Mean Square Fluctuation (RMSF), and Radius of Gyration (RG). These parameters, along with their respective methods of calculation, help capture the progressive structural changes that occur during molecular simulations.

RMSD measures the overall deviation of atomic positions over time, providing insights into the structural stability or instability of the system throughout the simulation. RMSF assesses the flexibility of individual residues, indicating how much each residue fluctuates during the simulation. The Radius of Gyration calculates the root mean square distance of the atoms from the molecule's center of mass, offering a sense of the system's compactness and conformational fluctuation **(Gullingsrud et al., 1999).**

- **Software commonly used for molecular dynamics simulations includes:**
- Assisted Model Building with Energy Refinement **(AMBER)**
- Chemistry at HARvard Molecular Mechanics **(CHARMM)**
- GROningen MOlecular Simulation **(GROMOS)**

8.2 Process

Molecular dynamics simulation typically involves three main steps (**Miao et al., 2001**):

I. Model Selection:

The initial step involves choosing an appropriate model system for the simulation. While complete molecular structures are often available, any missing regions must be reconstructed, and correct protonation states must be assigned to ensure biological relevance. It is essential to account for every relevant atom, as any excluded components will not be considered in subsequent simulation steps.

The finalized structure should be compatible with commonly used formats, such as the Protein Data Bank (PDB) and Protein Structure File (PSF). Generally, simulations begin by retrieving the crystal structure of the molecule from the Protein Data Bank (PDB). Key structural information includes atom names, residue names and IDs, chain identifiers, connectivity, temperature or B-factors, and fragment identifiers.

II. Energy Minimization, Heating, and Equilibration:

In this phase, the structural equilibrium of the system is evaluated using the selected force field, with the initial temperature set to zero. This is achieved by solving Newton's laws of motion. During this step, the number of iterations required to reach equilibrium is also defined, typically set to 5000 by default.
Once equilibrium is established, the system is gradually heated by adjusting atomic velocities and simulation box dimensions. This heating process continues until the system stabilizes at the desired temperature, ensuring that no significant fluctuations in structural properties occur over time.

Preparing the System for Energy Minimization: The structural energy of the system is calculated using principles based on Newtonian mechanics, often represented through the force field or energy potential. . To achieve a more stable, lower-energy configuration, the molecular structure is adjusted through a process known as energy minimization. Several methods are available to perform this minimization effectively:

- Sharp steepest descent (used for highly controlled systems)
- Conjugate acclivity (very proficient, required for massive structures)
- Broyden-Fletcher-Goldfarb-Shanno (BGFS) (iterative quasi-newton inconstant standard system)

When using a solvent box in molecular dynamics simulations, periodic boundary conditions are essential to simulate an effectively infinite system. Specific atoms can be designated as fixed to remain immobile during the simulation, which helps constrain certain regions of the molecular model. Nevertheless, all atoms, whether fixed or not, are considered during energy calculations.

To enhance the accuracy of the simulation, translational and rotational motion removers are used. The translational remover eliminates overall system

translation, while the rotational remover corrects for global rotational motion throughout the molecular dynamics run.

Topology Files: Topology files define the types of atoms present, enabling the identification of different elements and molecular orbital environments. These files also assign atomic charges and establish connectivity between atoms within the molecular system.

Parameter Files: Parameter files contain the force field coefficients necessary for calculating the energy of molecular interactions. This includes bond energies, non-bonded interactions (such as van der Waals and electrostatic forces), angle bending energy, and torsional energy. Additionally, they provide the parameters required for accurate energy estimation.

Solvation: Solvation is a critical step, as most biological processes occur in aqueous environments. The presence of solvent molecules significantly influences molecular configuration, electronic properties, and binding energy calculations. Therefore, accounting for solvation effects is essential for realistic molecular simulations.

III. Production course with examination:

During the production phase of molecular dynamics simulation, the system is subjected to stimulation under defined conditions, including constant temperature and volume (NVT ensemble) and constant temperature and pressure (NPT ensemble). This phase generates the full trajectory data over a specified simulation time. Appropriate time steps are defined for the simulation, and the resulting trajectory files are thoroughly analyzed to extract key characteristics of interest.

The simulation spans a range of time scales from microseconds to milliseconds, though millisecond-scale simulations are computationally intensive. Unlike in

vitro experiments, molecular simulations operate at femtosecond resolution, generating extensive conformational data. Transitioning from femtoseconds to milliseconds enables the exploration of a wide array of molecular states, potentially uncovering novel biological insights **(Jabbarzadeh et al., 2018; Badar et al., 2022).**

8.3 Experimental Setup

Evaluating the stability of receptor-ligand complexes over time, both in the presence and absence of the compound of interest, is crucial, and molecular dynamics (MD) simulation serves as a powerful tool for obtaining such time-dependent insights. In this study, three individual molecular dynamic simulations were conducted

Model preparation was performed using UCSF Chimera version 1.17.3. Simulations were conducted using GROMACS version 2024.2. Ligand topology files were obtained through SwissPharm. The physiography files for the protein, as well as ligands, were created through CHARMM27 (Chemistry at Harvard Molecular Mechanics 27) force field, which provides detailed atomistic definitions.

Solvation was performed using the TIP3P three-site water model within a triclinic crystal system. Sodium and chloride ions were subsequently added to neutralize the system. Energy minimization was carried out using the steepest descent algorithm.

The receptor-ligand complex was then subjected to a two-step equilibration process. The first step was conducted under NVT conditions (constant number of particles, volume, and temperature), followed by NPT conditions (constant number of particles, pressure, and temperature). The Berendsen thermostat was employed to regulate temperature during both phases. Each equilibration step was run for 100 picoseconds with 50,000 steps. The final molecular dynamics

simulation was executed for 20 nanoseconds, consisting of 10,000,000 steps under periodic boundary conditions to assess the stability and fluctuations of the protein in the presence of a nickel ion. All other simulation parameters were kept at default settings.

Post-simulation analyses were performed using UCSF Chimera (v1.17.3) and VMD (Visual Molecular Dynamics). Structural stability and flexibility were assessed using Root Mean Square Deviation (RMSD), Root Mean Square Fluctuation (RMSF), and Radius of Gyration (Rg). Data visualization and graphing were conducted using Grace Software.

8.4 In vivo ADMET Studies

The ADMET (Absorption, Distribution, Metabolism, Excretion, and Toxicity) profile plays a crucial role in evaluating the pharmacokinetic (PK) properties of drug candidates. These parameters help determine how a drug behaves within a biological system and are essential for assessing its viability. The evaluation of drug-likeness was conducted based on the established criteria proposed by Lipinski et al.

Biologically active compounds were first converted into their canonical SMILES (Simplified Molecular Input Line Entry System) format to facilitate computational analysis. These structures were then analyzed using the SwissADME web tool **(Bakchi et al., 2022),** which provided key pharmacokinetic data including the number of hydrogen bond donors and acceptors, rotatable bonds, and the topological polar surface area (TPSA).

Furthermore, potential toxicological effects, including organ-specific toxicity and other safety endpoints, were predicted using the ProTox-II tool **(Banerjee et al., 2018).** The suitability of each compound as a drug candidate was determined through a computed metric known as the drug score. A higher drug score reflects

a greater probability of the compound being considered a viable therapeutic agent.

8.5 Results and Discussion

The binding modes of inhibitors, isolated from the aqueous root fraction of *Cleome gynandra* and exhibiting a non-competitive inhibition mechanism, were predicted using molecular docking analysis. These docked complexes were subsequently validated through molecular dynamics (MD) simulations conducted over a 20 ns timeframe. The simulation trajectories were analyzed to assess the structural stability of the enzyme–substrate complexes by evaluating parameters such as root-mean-square deviation (RMSD), root-mean-square fluctuation (RMSF), and radius of gyration (Rg) over the entire simulation period.

8.5.1 Root Mean Square Deviation (RMSD) Analysis of the Urease–GCP Complex

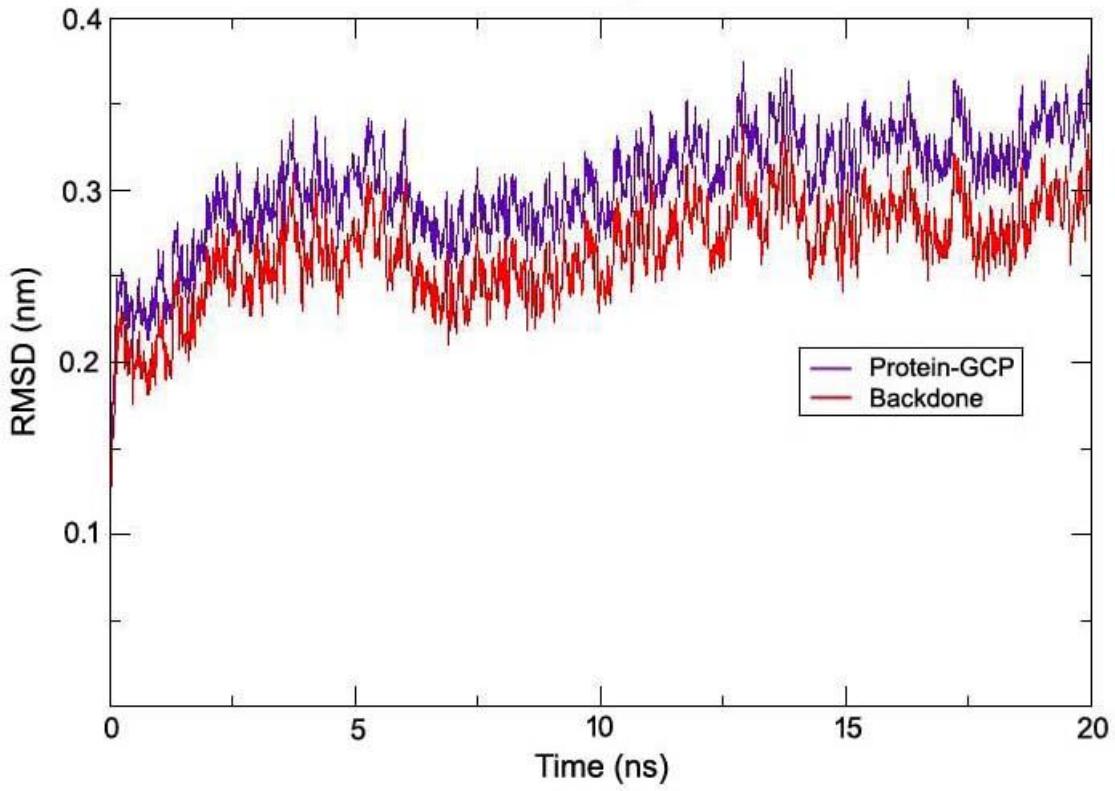

Figure 8.1: Root-mean-square deviation analysis of urease in complex with the ligand Glucocapparin (GCP).

Structural variations between the core protein backbone of urease and the urease–glucocapparin (GCP) complex were analyzed over various time intervals using using molecular dynamics simulation trajectories. Root Mean Square Deviation (RMSD) analysis was employed to assess the stability of the complex throughout the simulation. The urease–glucocapparin complex showed consistent deviations in the range of ~0.30–0.35 nm between 5 and 15 nanoseconds, gradually stabilizing around ~0.37 nm until the end of the 20-nanosecond simulation.

8.5.2 Root Mean Square Deviation (RMSD) Analysis of the Urease–FP Complex

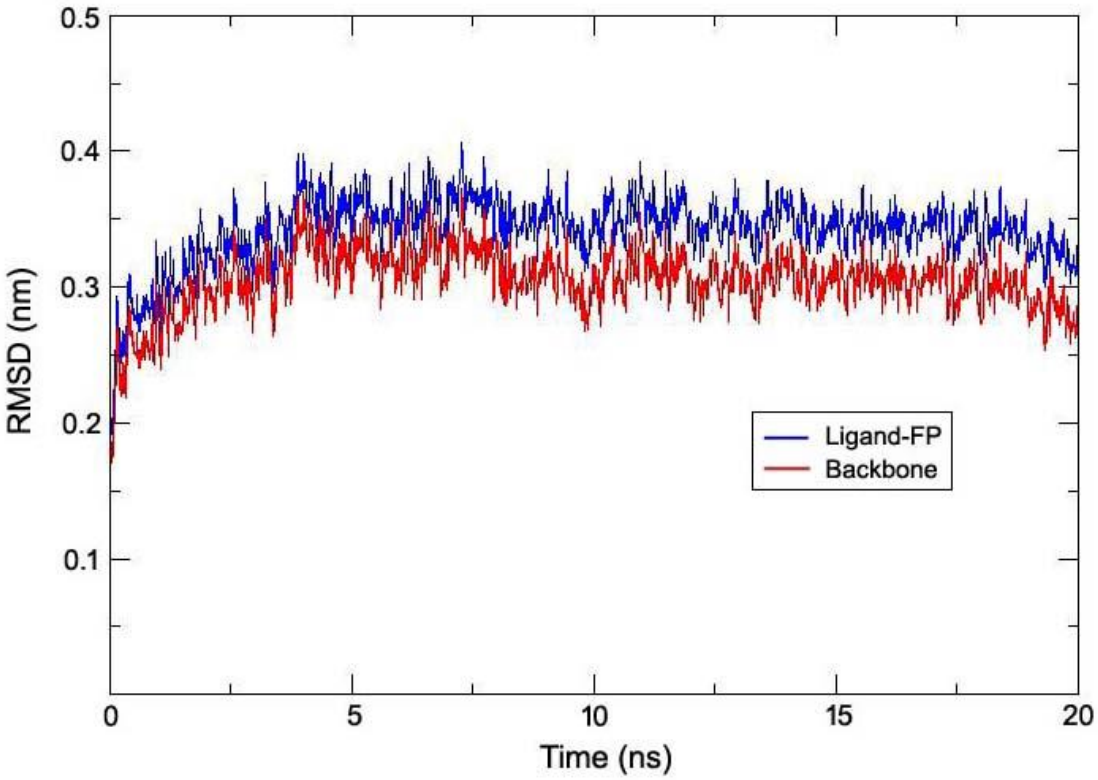

Figure 8.2: Root mean square deviation analysis of urease with ligand Fluticasone propionate (FP)

RMSD (Root Mean Square Deviation) measures the average distance between corresponding atoms, commonly those in the protein backbone, throughout the simulation. It reflects the structural deviation between the initial and final conformations of the system over time. In this study, the urease–fluticasone propionate complex maintained an RMSD range of approximately 0.35 to 0.38 nm during the 5 to 15 nanosecond interval, indicating a relatively stable conformation.

8.5.3 Root Mean Square Deviation (RMSD) Analysis of the Urease–LHS Complex

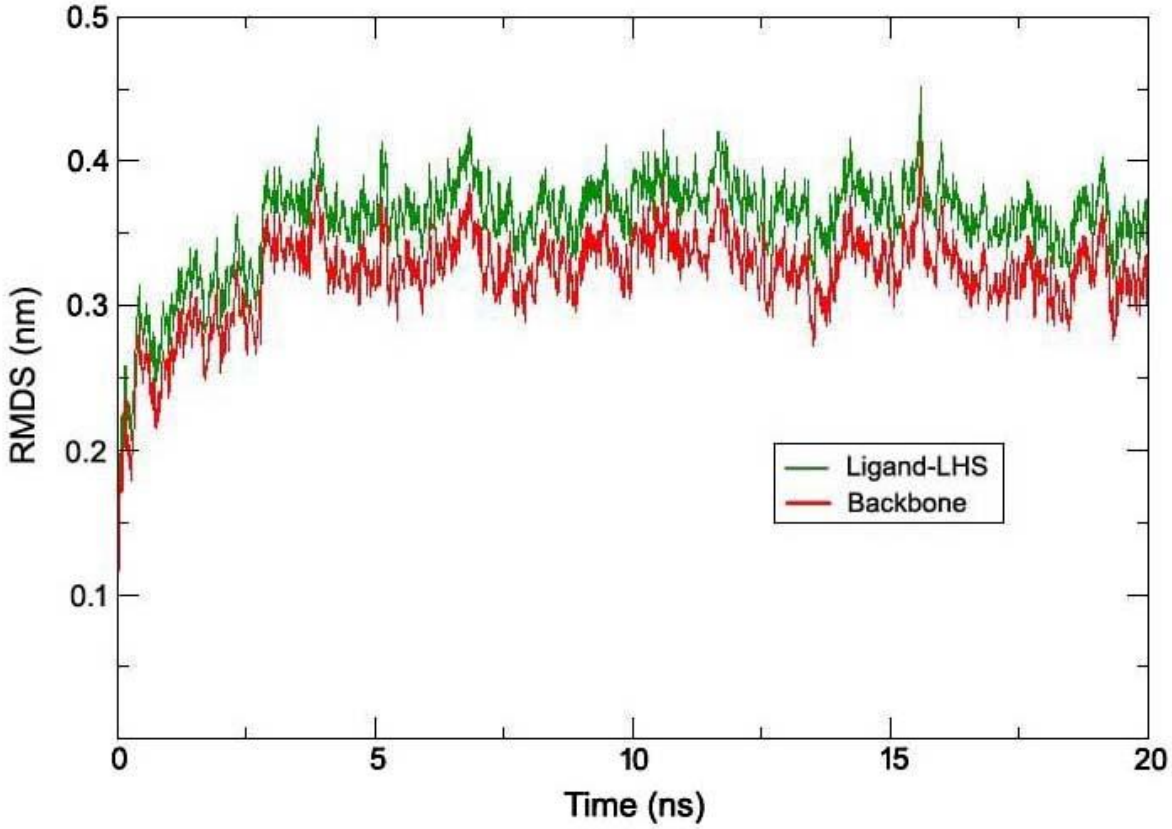

Figure 8.3: Root mean square deviation analysis of urease with ligand Lauryl hydrogen sulfate (LHS)

RMSD (Root Mean Square Deviation) consolidates the extent of deviations between calculated values and reference data into a single, quantifiable metric. RMSD values are always non-negative, with a value of zero, though practically unattainable, indicating a perfect fit to the data. Lower RMSD values are generally preferred, as they reflect closer agreement with the reference. However, comparisons across different datasets can be misleading, since RMSD is dependent on the scale of the values involved. In the case of urease–lauryl hydrogen sulfate, RMSD values were observed to range between approximately 0.40 and 0.45 nanometers over a similar time series.

8.5.4 Root Mean Square Fluctuation (RMSF) and Radius of Gyration (Rg)

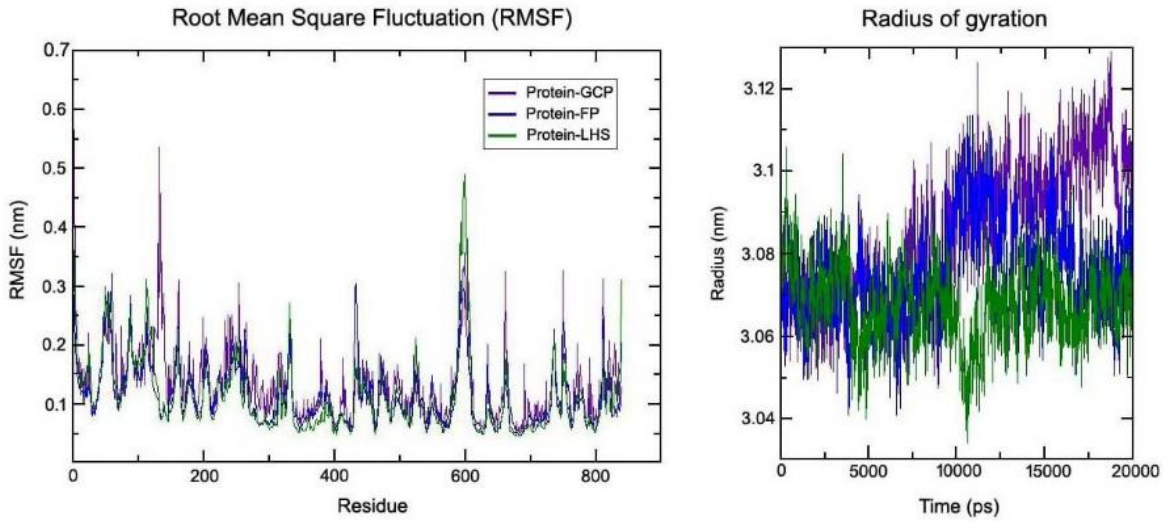

Figure 8.4: Stability of jack bean urease structure at the time of interaction with Glucocapparin (GCP), Fluticasone propionate (FP), and Lauryl hydrogen sulfate (LHS) based on root mean square fluctuation and radius of gyration.

Root mean square fluctuation (RMSF) was employed to evaluate the mobility of individual atoms or residues throughout the simulation, providing a measure of the flexibility within specific regions of the protein. Higher RMSF values typically correspond to more flexible regions, such as loops, while lower values indicate structurally stable elements like α-helices and β-sheets **(Martinez et al., 2015).** The RMSF is calculated as the average displacement of atoms from a reference structure, which is commonly the time-averaged position of each atom throughout the simulation.

In the case of the urease protein, notable fluctuations were observed in the residue regions 5–110, 160–265, 435–540, and 600–665, suggesting the presence of flexible loop regions. Conversely, the remaining segments of the protein displayed structural rigidity and stability throughout the simulation. Thus, RMSF analysis effectively highlights the most dynamic regions of a protein, offering

valuable insight into the behaviour and flexibility of amino acid residues during molecular dynamics simulations.

The Radius of Gyration (Rg) analysis was conducted to evaluate the compactness of the urease protein during its interaction with the respective ligand. Rg measures the average distance of the protein's atoms from its centre of mass, offering insight into the structural integrity and folding behaviour of the protein throughout the molecular dynamics (MD) simulation.

Lower Rg values suggest that the protein remains compact and structurally stable, with atoms positioned closer to the centre of mass. In contrast, higher Rg values indicate structural expansion or flexibility, reflecting atomic displacement away from the protein's core **(Lobanov et al., 2008).** Therefore, Rg is a useful parameter in monitoring protein stability and conformational dynamics under varying simulation conditions.

In the present analysis, the Rg plot revealed that the urease–ligand complex-maintained values consistently between ~ 30.2–31.3nm. This relatively narrow and stable range implies that the enzyme retained a compact structure and experienced minimal conformational deviation during the simulation, supporting its stability in the ligand-bound state.

The minor fluctuations observed in the molecular dynamics (MD) simulation trajectories suggested that the protein–ligand complexes maintained structural stability throughout the simulation. Notably, the urease–glucocapparin complex exhibited greater stability compared to the other ligands, maintaining a strong and consistent binding interaction with the protein during the entire simulation.

8.5.5 Drug-Likeness and Pharmacokinetic Properties of Potential Inhibitors in the Root Water Fraction of *Cleome gynandra*

The SwissADME analysis results for each compound identified in the root water fraction of *Cleome gynandra* are presented in tabular form:

Compounds	**PubChem Id**	**Mol. weight**	**Rotational bonds**	**Log P_0/w**	**TPSA**	**ROS violation**
Glucocapparin	21600408	333.34	5	1.17	199.79	0
Fluticasone propionate	444036	500.57	6	3.66	105.97	1; violation:MW>500
Lauryl hydrogen sulphate	8778	266.4	12	2.88	71.98	0

Table 8.1: Dug-likely properties of the identified inhibitors from *Cleome gynandra* roots

Compounds	**GI absorption**	**BBB permeant**	**Pgp substrate**	**CYP1A2 inhibitor**	**CYP2C19 inhibitor**	**CYP2C9 inhibitor**	**CYP3A4 inhibitor**
Glucocapparin	Low activity	none	yes	no	no	no	no
Fluticasone propionate	Low activity	none	yes	no	no	no	yes
Lauryl hydrogen sulfate	High activity	none	no	no	no	yes	no

Table 8.2: Pharmacokinetic characteristics of the identified inhibitors from *Cleome gynandra* roots. GI for gastrointestinal, BBB for blood-brain-barrier, pgp for P-glycoprotein, CYP for cytochrome P.

The Lipinski Rule of Five is commonly applied in drug discovery to assess the drug-likeness of compounds. It is based on four key physicochemical properties. A potential drug candidate is typically considered acceptable if it satisfies these criteria, allowing for no more than one violation **(Rai et al., 2023):**

- Lower than 500 Dalton molecular mass
- The total number of proton acceptors should be less than 10
- The total number of proton donors should be less than 5
- The calculated value of the N-octanol-water partition coefficient (log P_0/w) of less than 5

Among the three active compounds, glucocapparin adheres to Lipinski's Rule of Five and exhibits a significantly lower log P_0/w value compared to FP and LHS, while also displaying no detectable toxic properties.

Pharmacokinetic analyses have provided valuable insights into the solubility, lipophilicity, permeability, and enzyme-related metabolic stability of the compounds. The ADMET profiles highlight important characteristics of the biologically active components present in the root water extract of the spider plant. Among the three compounds studied, GCP exhibits the most promising drug-like properties, showing low toxicity and minimal adverse effects compared to FP and LHS.

Chapter 9

DISCUSSION AND LIMITATIONS OF THE STUDY

9.1 Discussion

Healthy soil is fundamental to agriculture and plays a vital role in global crop production. Urea fertilizer, a primary source of nitrogen, is extensively used by farmers to enhance crop yield and support plant health. As nitrogen is the primary limiting nutrient, urea remains the most widely applied fertilizer worldwide, significantly impacting food security and agricultural productivity. However, urea is rapidly broken down by the enzyme urease, which is naturally present in soil and produced by various soil microorganisms. This breakdown releases ammonia and carbon dioxide, and if ammonia is not quickly incorporated into the soil, it escapes into the atmosphere as a gas, leading to nitrogen loss. This nitrogen loss poses a significant global challenge. Thereby, the use of urease inhibitors has gained considerable importance in reducing or slowing the nitrogen loss process, improving the efficiency of urea fertilizer. These inhibitors help to reduce urease-induced ammonia formation on the soil surface, thereby enhancing crop plants' nitrogen uptake. It is essential, however, that the inhibitors do not cause any harm to the environment while fulfilling their role. For this reason, plant-derived inhibitors are gaining attention for their potential to benefit both crop production and the environment.

In this study, we investigated the urease-inhibitory potential of *Cleome gynandra*, a widely distributed weed from the Cleomaceae family, closely related to Brassicaceae. Sequential solvent extraction of various plant parts revealed that the root exhibited the strongest inhibitory effect against jack bean urease, surpassing the activity observed in the leaf and stem.

To further evaluate the root's urease-inhibiting potential, a colorimetric assay was performed using varying concentrations of root-derived solvent fractions. Among

five solvent fractions, hexane, ethyl acetate, acetone, methanol, and water, the water extract showed the highest inhibition, even compared to the standard inhibitor thiourea, followed by the methanol and acetone extracts. These three fractions were subsequently selected for enzyme kinetics studies.

Lineweaver-Burk (double reciprocal) plots were used to analyse the mode of inhibition. Results indicated non-competitive inhibition, where the inhibitor binds to a site distinct from the active site, interacting with both free enzyme and the enzyme-substrate complex. This interaction reduced the maximum reaction velocity (Vmax) without affecting the Michaelis constant (K_m), confirming non-competitive inhibition. The inhibition constant (K_i) represented the binding affinity between the enzyme and the inhibitor.

High Resolution-Liquid Chromatography & Mass Spectrometry (HR-LCMS) analysis of the root fractions identified several bioactive compounds. In the acetone fraction, benzocoumarin, capsaicin, and dihomo-γ-linolenoyl ethyl acetate were detected at retention times 13.18, 14.28, and 18.00 minutes, respectively. The methanol fraction showed obtusilactone A at 18.15 minutes. The water fraction revealed several peaks, notably glucocapparin (GCP), fluticasone propionate (FP), ritterizine A (RA), and lauryl hydrogen sulfate (LHS), detected at 1.237, 12.867, 20.179, and 26.604 minutes, respectively. Given the high urease inhibition shown by the water fraction and the significance of water-soluble bioactives **(Gallina et al., 2022),** we focused on the interactions between these compounds and the enzyme's catalytic site.

Computational docking studies revealed that glucocapparin exhibited the strongest binding affinity with urease, with a docking score of -6.6 kcal/mol. It formed stable hydrogen bonds with key catalytic residues, His492, Ala636, Arg609, and Arg439, which are known to be crucial in urease activity **(Hassan et al., 2017; Zolghadr et al., 2022; Ahmad et al., 2023d).**

Molecular dynamics simulations further confirmed the stability of the glucocapparin-urease complex. Root mean square deviation (RMSD), root mean square fluctuation (RMSF), and radius of gyration (Rg) analyses showed consistent structural stability, with fluctuations remaining within the acceptable threshold (0.3 nm). Glucocapparin maintained a strong and stable interaction with the enzyme throughout the simulation period.

Finally, ADMET profiling suggested that glucocapparin possesses favourable drug-like characteristics and promising pharmacokinetic properties compared to other compounds. These findings highlight glucocapparin as a strong candidate for future development as a urease inhibitor.

9.2 Limitation of the Study:

The development of a practical and efficient urease inhibitor is accompanied by certain challenges and limitations, such as:

- **Effectiveness and longevity:** The inhibitor must maintain its activity over an extended period to effectively prevent ammonia volatilization. A short-lived effect would reduce its practical applicability, requiring frequent reapplication and ultimately reducing its overall efficiency and value.
- **Stability and specificity:** The inhibitor must be stable under various environmental conditions and exhibit high specificity toward the target enzyme. It must not interact with other proteins, as such non-specific interactions could lead to undesirable side effects.
- **Proper formulation and integration:** Enhancing the formulation of the inhibitor and effectively integrating the compound of interest into agricultural practices remains a significant challenge. Effective integration is crucial for reducing nitrogen losses and enhancing nitrogen use efficiency in crop production.

- **Lack of large-scale studies:** Conducting large-scale research requires sophisticated and often expensive infrastructure, which may not be readily available. Consequently, current studies are typically confined to examining the structure-activity relationships of a narrow group of compounds, rather than investigating the entire spectrum of potential urease inhibitors.

Further experimental research is necessary to comprehensively assess the environmental impact of these inhibitors, especially regarding their role in ammonia and nitrous oxide emissions. Our study revealed limitations in their practical use within agriculture and underscored the lack of insight into their long-term effects on soil microbial communities. Additionally, understanding how these inhibitors degrade during storage and under field conditions is crucial to maintaining their long-term efficacy.

9.3 Future Scopes of the Study:

Secondary metabolites from plants across various classes hold significant potential to inhibit urease activity. This insight can be applied to develop innovative, non-toxic, and cost-effective urease inhibitors, which could improve the quality of life for both humans and environment. Such inhibitors have the potential to combat diseases or enhance the quality and yield of agricultural crops.

A promising direction for future research is exploring the combined effects of urease and nitrification inhibitors. Urease inhibitors work by blocking the enzyme's active site, slowing the breakdown of urea and reducing nitrogen loss to the atmosphere. In contrast, nitrification inhibitors target soil enzymes involved in nitrification and denitrification, helping to control nitrogen loss through nitrous oxide emissions and nitrate leaching in soil. Therefore, a combined use of these two inhibitors along with urea fertilizer can help in further reduction of nitrogen loss from the soil and limiting greenhouse gas (GHG)

emissions. The European Union (EU) has already targeted a 20% decrease in GHG release by the year 2020 and a subsequent decrease to 40% by the end of 2030 as compared to the level of emission in 1990 **(Knodt et al., 2018).** It is likely that regulations requiring the combined use of these inhibitors will be implemented soon to help achieve these emission reduction goals. Continued research and development are critical to assess the effectiveness and shelf life of existing urease inhibitors.

In our study, we have explored a novel source of urease inhibitors from *Cleome gynandra* root extract. This research should be expanded to develop synthetic inhibitors with improved properties and effective formulations suitable for agricultural applications. A comprehensive evaluation of their safety, potential environmental risks, and impacts on the food chain is essential before widespread use.

Chapter 10

References

1. Ahmad, I., Chaudhary, B. A., Ashraf, M., Uzair, M., & Janbaz, K. H. (2012). Vernonione, a new urease inhibitory carvotacetone derivative from Vernonia cinerascens. Journal of the Chemical Society of Pakistan, 34(3).
2. Ahmad, I., Chaudhary, B. A., Janbaz, K. H., Uzair, M., & Ashraf, M. (2011). Urease inhibitors and antioxidants from Vernonia cinerascens.
3. Ahmad, I., Fatima, I., Afza, N., Malik, A., Lodhi, M. A., & Choudhary, M. I. (2008). Urease and serine protease inhibitory alkaloids from Isatis tinctoria. Journal of Enzyme Inhibition and Medicinal Chemistry, 23(6), 918-921.
4. Ahmad, M., Muhammad, N., Ahmad, M., Arif Lodhi, M., Mahjabeen, Jehan, N., ... & Iqbal Choudhary, M. (2008). Urease inhibitor from Datisca cannabina linn. Journal of Enzyme Inhibition and Medicinal Chemistry, 23(3), 386-390.
5. Ahmad, S., Abdul Qadir, M., Ahmed, M., Imran, M., Yousaf, N., Wani, T. A., ... & Muddassar, M. (2023). Exploring the potential of propanamide-sulfonamide based drug conjugates as dual inhibitors of urease and cyclooxygenase-2: biological and their in silico studies. Frontiers in Chemistry, 11, 1206380.
6. Ahmad, V. U., Hussain, J., Hussain, H., Jassbi, A. R., Ullah, F., Lodhi, M. A., ... & Choudhary, M. I. (2003). First natural urease inhibitor from Euphorbia decipiens. Chemical and pharmaceutical bulletin, 51(6), 719-723.
7. Ahmed, M., Rauf, M., Mukhtar, Z., & Saeed, N. A. (2017). Excessive use of nitrogenous fertilizers: an unawareness causing serious threats to

environment and human health. *Environmental Science and Pollution Research*, *24*, 26983-26987.

8. Ajaiyeoba, E. O. (2000). Phytochemical and antimicrobial studies of Gynandropsis gynandra and Buchholzia coriaceae extracts. African journal of Biomedical research, 3(3), 161-165.
9. Ajaiyeoba, E. O., Onocha, P. A., & Olarenwaju, O. T. (2001). In vitro anthelmintic properties of Buchholzia coriaceae and Gynandropsis gynandra extracts. Pharmaceutical biology, 39(3), 217-220.
10. Akhtar, N., Saleem, M., Riaz, N., Ali, M. S., Yaqoob, A., Nasim, F. U. H., & Jabbar, A. (2013). Isolation and characterization of the chemical constituents from Plumeria rubra. Phytochemistry letters, 6(2), 291-298.
11. Akhtar, N., Saleem, M., Riaz, N., Ali, M. S., Yaqoob, A., Nasim, F. U. H., & Jabbar, A. (2013). Isolation and characterization of the chemical constituents from Plumeria rubra. Phytochemistry letters, 6(2), 291-298.
12. Ali, M., Latif, A., Zaman, K., Arfan, M., Maitland, D., Ahmad, H., & Ahmad, M. (2014). Anti-ulcer xanthones from the roots of Hypericum oblongifolium Wall. Fitoterapia, 95, 258-265.
13. Alley, M. M., & Vanlauwe, B. (2009). *The role of fertilizers in integrated plant nutrient management*. International fertilizer industry Association.
14. Ambrose, J. F., Kistiakowsky, G. B., & Kridl, A. G. (1950). Inhibition of urease by sulfur compounds. Journal of the American Chemical Society, 72(1), 317-321.
15. Amtul, Z., Siddiqui, R. A., & Choudhary, M. I. (2002). Chemistry and mechanism of urease inhibition. Current medicinal chemistry, 9(14), 1323-1348.
16. Arcon, J. P., Turjanski, A. G., Martí, M. A., & Forli, S. (2021). Biased docking for protein–ligand pose prediction. Protein-ligand interactions and drug design, 39-72.

17. Arfan, M., Ali, M., Ahmad, H., Anis, I., Khan, A., Choudhary, M. I., & Shah, M. R. (2010). Urease inhibitors from Hypericum oblongifolium WALL. Journal of Enzyme Inhibition and Medicinal Chemistry, 25(2), 296-299.
18. Arfan, M., Amin, H., Khan, I., Shah, M. R., Shah, H., Khan, A. Z., ... & Khan, M. A. (2012). Molecular simulations of bergenin as a new urease inhibitor. Medicinal Chemistry Research, 21, 2454-2457.
19. Ayaz, M., ARIF LODHI, M. U. H. A. M. M. A. D., Riaz, M., -UL-HAQ, A. Z. H. A. R., Malik, A., & Iqbal Choudhary, M. (2006). Novel urease inhibitors from Daphne oleoids. Journal of Enzyme Inhibition and Medicinal Chemistry, 21(5), 527-529.
20. Azwanida, N. N. (2015). A review on the extraction methods use in medicinal plants, principle, strength and limitation. Med aromat plants, 4(196), 2167-0412.
21. Badar, M. S., Shamsi, S., Ahmed, J., & Alam, M. A. (2022). Molecular dynamics simulations: concept, methods, and applications. In Transdisciplinarity (pp. 131-151). Cham: Springer International Publishing.
22. Bafoev, A. X., Rajabboev, A. I., Niyozov, S. A., Bakhshilloev, N. K., & Mahmudov, R. A. (2022). Significance and classification of mineral fertilizers. *Texas Journal of Engineering and Technology*, *5*, 1-5.
23. Bakchi, B., Krishna, A. D., Sreecharan, E., Ganesh, V. B. J., Niharika, M., Maharshi, S., ... & Shaik, A. B. (2022). An overview on applications of SwissADME web tool in the design and development of anticancer, antitubercular and antimicrobial agents: a medicinal chemist's perspective. Journal of Molecular Structure, 1259, 132712.
24. Bala, A., Kar, B., Haldar, P. K., Mazumder, U. K., & Bera, S. (2010). Evaluation of anticancer activity of Cleome gynandra on Ehrlich's

Ascites Carcinoma treated mice. Journal of Ethnopharmacology, 129(1), 131-134.

25. Banerjee, P., Eckert, A. O., Schrey, A. K., & Preissner, R. (2018). ProTox-II: a webserver for the prediction of toxicity of chemicals. Nucleic acids research, 46(W1), W257-W263.
26. Banu, K. S., & Cathrine, L. (2015). General techniques involved in phytochemical analysis. International journal of advanced research in chemical science, 2(4), 25-32.
27. Belgasem, F. F. B., & Salleh, H. M. (2015). Characterization of Recombinant Enzymes. *Recombinant Enzymes-From Basic Science to Commercialization*, 41-60.
28. Benini, S., Cianci, M., Mazzei, L., & Ciurli, S. (2014). Fluoride inhibition of Sporosarcina pasteurii urease: structure and thermodynamics. JBIC Journal of Biological Inorganic Chemistry, 19, 1243-1261.
29. Bianucci, M., Maestro, M., & Walde, P. (1990). Bell-shaped curves of the enzyme activity in reverse micelles: a simplified model for hydrolytic reactions. *Chemical physics*, *141*(2-3), 273-283.
30. Bisswanger, H. (2017). Enzyme kinetics: principles and methods. John Wiley & Sons.
31. Blanco-Canqui, H., & Lal, R. (2009). Crop residue removal impacts on soil productivity and environmental quality. *Critical reviews in plant science*, *28*(3), 139-163.
32. Blua, M. J., & Hanscom, Z. (1986). Isolation and characterization of glucocapparin in Isomeris arborea Nutt. Journal of chemical ecology, 12, 1449-1458.
33. Boon, B., & Laudelout, H. (1962). Kinetics of nitrite oxidation by Nitrobacter winogradskyi. *Biochemical Journal*, *85*(3), 440.
34. Bremner, J. M. (1995). Recent research on problems in the use of urea as a nitrogen fertilizer. *Fertilizer research*, *42*, 321-329.

35. Bremner, J. M., & Douglas, L. A. (1971). Inhibition of urease activity in soils. Soil Biology and Biochemistry, 3(4), 297-307.
36. Bremner, J. T. (1965). Organic forms of nitrogen. *Methods of Soil Analysis: Part 2 Chemical and Microbiological Properties*, *9*, 1238-1255.
37. Brown, G. D., Liang, G. Y., & Sy, L. K. (2003). Terpenoids from the seeds of Artemisia annua. Phytochemistry, 64(1), 303-323.
38. Brown, P. D., & Morra, M. J. (2009). Brassicaceae tissues as inhibitors of nitrification in soil. Journal of agricultural and food chemistry, 57(17), 7706-7711.
39. Bugg, T. D. (2012). *Introduction to enzyme and coenzyme chemistry*. John Wiley & Sons.
40. Byrnes, B. H., Savant, N. K., & Craswell, E. T. (1983). Effect of a urease inhibitor phenyl phosphorodiamidate on the efficiency of urea applied to rice. Soil Science Society of America Journal, 47(2), 270-274.
41. Cabrera, M. L., Kissel, D. E., & Bock, B. R. (1991). Urea hydrolysis in soil: Effects of urea concentration and soil pH. *Soil Biology and Biochemistry*, *23*(12), 1121-1124.
42. Cameron, K. C., Di, H. J., & Moir, J. L. (2013). Nitrogen losses from the soil/plant system: a review. *Annals of applied biology*, *162*(2), 145-173.
43. Cantarella, H., Otto, R., Soares, J. R., & de Brito Silva, A. G. (2018). Agronomic efficiency of NBPT as a urease inhibitor: A review. Journal of advanced research, 13, 19-27.
44. Carocho, M., & CFR Ferreira, I. (2013). The role of phenolic compounds in the fight against cancer–a review. Anti-Cancer Agents in Medicinal Chemistry (Formerly Current Medicinal Chemistry-Anti-Cancer Agents), 13(8), 1236-1258.
45. Caruso, P. B., & Ligabue-Braun, R. (2024). Historical hallmarks in urease study. In *Ureases* (pp. 15-24). Academic Press.

46. Chaney, A. L., & Marbach, E. P. (1962). Modified reagents for determination of urea and ammonia. Clinical chemistry, 8(2), 130-132.
47. Chen, W. W., Niepel, M., & Sorger, P. K. (2010). Classic and contemporary approaches to modeling biochemical reactions. *Genes & development*, *24*(17), 1861-1875.
48. Chen, X., Li, H., Tian, L., Li, Q., Luo, J., & Zhang, Y. (2020). Analysis of the physicochemical properties of acaricides based on Lipinski's rule of five. Journal of computational biology, 27(9), 1397-1406.
49. Chen, Y., Liao, J., Chen, M., Huang, Q., & Lu, Q. (2015). Gossypol: new class of urease inhibitors, molecular docking and inhibition assay. J Chem Pharm Res, 7(1), 10-15.
50. Chrisman, M. A., Goldcamp, M. J., Rhodes, A. N., & Riffle, J. (2023). Exploring Michaelis–Menten kinetics and the inhibition of catalysis in a synthetic mimic of catechol oxidase: An experiment for the inorganic chemistry or biochemistry laboratory. *Journal of Chemical Education*, *100*(2), 893-899.
51. Ciurli, S., Benini, S., Rypniewski, W. R., Wilson, K. S., Miletti, S., & Mangani, S. (1999). Structural properties of the nickel ions in urease: novel insights into the catalytic and inhibition mechanisms. *Coordination Chemistry Reviews*, *190*, 331-355.
52. Cooper, G. M. (2000). The central role of enzymes as biological catalysts. Sinauer Associates.
53. Copeland, R. A. (2013). Evaluation of enzyme inhibitors in drug discovery: a guide for medicinal chemists and pharmacologists. John Wiley & Sons.
54. Cornish-Bowden, A. (2013). Fundamentals of enzyme kinetics. John Wiley & Sons.
55. Da Fonseca, A. B., Santos, C., Nunes, A. P. P., Oliveira, D. P., De Melo, M. E. A., Takayama, T., ... & Guelfi, D. (2023). Urease inhibitors

technologies as strategy to mitigate agricultural ammonia emissions and enhance the use efficiency of urea-based fertilizers. Scientific Reports, 13(1), 22739.

56. Das, M., Bickers, D. R., & Mukhtar, H. (1984). Plant phenols as invitro inhibitors of glutathione S-transferase (s). Biochemical and biophysical research communications, 120(2), 427-433.
57. Delgado, A., Quemada, M., & Villalobos, F. J. (2016). Fertilizers. *Principles of agronomy for sustainable agriculture*, 321-339.
58. Díaz-Sánchez, Á. G., Alvarez-Parrilla, E., Martínez-Martínez, A., Aguirre-Reyes, L., Orozpe-Olvera, J. A., Ramos-Soto, M. A., ... & de la Rosa, L. A. (2016). Inhibition of urease by disulfiram, an FDA-approved thiol reagent used in humans. Molecules, 21(12), 1628.
59. Díaz-Sánchez, Á. G., Alvarez-Parrilla, E., Martínez-Martínez, A., Aguirre-Reyes, L., Orozpe-Olvera, J. A., Ramos-Soto, M. A., ... & de la Rosa, L. A. (2016). Inhibition of urease by disulfiram, an FDA-approved thiol reagent used in humans. Molecules, 21(12), 1628
60. Dixon, N. E., Riddles, P. W., Gazzola, C., Blakeley, R. L., & Zerner, B. (1980). Jack bean urease (EC 3.5. 1.5). V. On the mechanism of action of urease on urea, formamide, acetamide, N-methylurea, and related compounds. *Canadian Journal of Biochemistry*, *58*(12), 1335-1344.
61. Dobermann, A. R. (2005). Nitrogen use efficiency-state of the art. *Agronomy--Faculty Publications*, 316.
62. Doelman, P., & Haanstra, L. (1986). Short-and long-term effects of heavy metals on urease activity in soils. Biology and Fertility of Soils, 2, 213-218.
63. Dunn, B. E., Campbell, G. P., Perez-Perez, G. I., & Blaser, M. J. (1990). Purification and characterization of urease from Helicobacter pylori. *Journal of Biological Chemistry*, *265*(16), 9464-9469.

64. DuToit, S. H., Steyn, A. G. W., & Stumpf, R. H. (2012). Graphical exploratory data analysis. Springer Science & Business Media.
65. Elçin, Y. M., & Saçak, M. (1996). Acrylamide grafted poly (ethylene terephthalate) fibers activated by glutaraldehyde as support for urease. *Applied biochemistry and biotechnology*, *60*, 19-32.
66. Fahey, J. W., Stephenson, K. K., Wade, K. L., & Talalay, P. (2013). Urease from Helicobacter pylori is inactivated by sulforaphane and other isothiocyanates. Biochemical and biophysical research communications, 435(1), 1-7.
67. Fierer, N., Carney, K. M., Horner-Devine, M. C., & Megonigal, J. P. (2009). The biogeography of ammonia-oxidizing bacterial communities in soil. *Microbial ecology*, *58*, 435-445.
68. Firestone, M. K. (1982). Biological denitrification. *Nitrogen in agricultural soils*, *22*, 289-326.
69. Fishbein, W. N., & Carbone, P. P. (1965). Urease Catalysis: II. Inhibition of the enzyme by hydroxyurea, hydroxylamine, and acetohydroxamic acid. Journal of Biological Chemistry, 240(6), 2407-2414.
70. Fitzgerald, M. (1983). Capsaicin and sensory neurones—a review. Pain, 15(1-4), 109-130.
71. Fixen, P. E., & West, F. B. (2002). Nitrogen fertilizers: meeting contemporary challenges. *Ambio: a journal of the human environment*, *31*(2), 169-176.
72. Forster, S. S. D., Cripps, A. C., & Smith-Carington, A. (1982). Nitrate leaching to groundwater. *Philosophical transactions of the royal society of London. B, Biological Sciences*, *296*(1082), 477-489.
73. Fowler, D., Coyle, M., Skiba, U., Sutton, M. A., Cape, J. N., Reis, S., ... & Voss, M. (2013). The global nitrogen cycle in the twenty-first century. *Philosophical Transactions of the Royal Society B: Biological Sciences*, *368*(1621), 20130164.

74. Franzke, A., Lysak, M. A., Al-Shehbaz, I. A., Koch, M. A., & Mummenhoff, K. (2011). Cabbage family affairs: the evolutionary history of Brassicaceae. Trends in plant science, 16(2), 108-116.
75. Freney, J. R., Simpson, J. R., & Denmead, O. T. (1981). Ammonia volatilization. *Ecological Bulletins*, 291-302.
76. Frink, C. R., Waggoner, P. E., & Ausubel, J. H. (1999). Nitrogen fertilizer: retrospect and prospect. *Proceedings of the National Academy of Sciences*, *96*(4), 1175-1180.
77. Gagnon, B., Ziadi, N., & Grant, C. (2012). Urea fertilizer forms affect grain corn yield and nitrogen use efficiency. *Canadian Journal of Soil Science*, *92*(2), 341-351.
78. Gale, G. R. (1965). Inhibition of urease by hydroxyurea. Biochemical Pharmacology, 14(5), 693-698.
79. Gallina, L., Cravotto, C., Capaldi, G., Grillo, G., & Cravotto, G. (2022). Plant extraction in water: Towards highly efficient industrial applications. Processes, 10(11), 2233.
80. Gasser, J. K. R. (1964). Urea as a fertilizer.
81. Ge, H. M., Huang, B., Tan, S. H., Shi, D. H., Song, Y. C., & Tan, R. X. (2006). Bioactive oligostilbenoids from the stem bark of Hopea exalata. Journal of natural products, 69(12), 1800-1802.
82. Gee, P. T. (2011). Unleashing the untold and misunderstood observations on vitamin E. Genes & nutrition, 6(1), 5-16.
83. Glew, R. S., Amoako-Atta, B., Ankar-Brewoo, G., Presley, J., Chuang, L. T., Millson, M., ... & Glew, R. H. (2009). Non-cultivated plant foods in West Africa: Nutritional analysis of the leaves of three indigenous leafy vegetables in Ghana. Food, 3(1), 39-42.
84. Glibert, P. M., Seitzinger, S., Heil, C. A., Burkholder, J. M., Parrow, M. W., Codispoti, L. A., & Kelly, V. (2005). Eutrophication. *Oceanography*, *18*(2), 198.

85. Goldstein, L., Levy, M., & Shemer, L. (1983). Kinetics of multilayer immobilized enzyme-filter reactors: behavior of urease-filter reactors in different buffers. *Biotechnology and Bioengineering*, *25*(6), 1485-1499.
86. Gould, W. D., Cook, F. D., & Bulat, J. A. (1978). Inhibition of urease activity by heterocyclic sulfur compounds. Soil Science Society of America Journal, 42(1), 66-72.
87. Gowele, V. F., Kinabo, J., Jumbe, T., Kirschmann, C., Frank, J., & Stuetz, W. (2019). Provitamin A carotenoids, tocopherols, ascorbic acid and minerals in indigenous leafy vegetables from Tanzania. Foods, 8(1), 35.
88. Greco, W. R., & Hakala, M. T. (1979). Evaluation of methods for estimating the dissociation constant of tight binding enzyme inhibitors. The Journal of biological chemistry, 254(23), 12104-12109.
89. Gullingsrud, J. R., Braun, R., & Schulten, K. (1999). Reconstructing potentials of mean force through time series analysis of steered molecular dynamics simulations. Journal of Computational Physics, 151(1), 190-211.
90. Hargrove, W. L. (1988). Soil, environmental, and management factors influencing ammonia volatilization under field conditions. *Ammonia volatilization from urea fertilizers. Alabama, National Fertilizer Development Center*, 17-36.
91. Harmon, K. M., & Niemann, C. (1949). The competitive inhibition of the urease-catalyzed hydrolysis of urea by phosphate. J. biol. Chem, 177(2), 601-605.
92. Hassan, S. T., & Švajdlenka, E. (2017). Biological evaluation and molecular docking of protocatechuic acid from Hibiscus sabdariffa L. as a potent urease inhibitor by an ESI-MS based method. Molecules, 22(10), 1696.
93. Heinrich, M., Appendino, G., Efferth, T., Fürst, R., Izzo, A. A., Kayser, O., ... & Viljoen, A. (2020). Best practice in research–overcoming

common challenges in phytopharmacological research. Journal of Ethnopharmacology, 246, 112230.

94. Herbert, R. A. (1999). Nitrogen cycling in coastal marine ecosystems. *FEMS microbiology reviews*, *23*(5), 563-590.
95. Holmes, A., Illowsky, B., & Dean, S. (2017). Introductory Business Statistics 2e. OpenStax.
96. Huang, M., Cui, P., Zhou, J., Liu, C., & Wang, Y. (2023). Theoretical study on the inhibition mechanisms of heavy metal ions on urease activity. Chemosphere, 345, 140416.
97. Huang, T. C., & Chen, D. H. (1991). Kinetic study of urease-catalysed urea hydrolysis. *Journal of Chemical Technology & Biotechnology*, *52*(4), 433-444.
98. Hutchinson, H. B., & Miller, N. J. (1912). The direct assimilation of inorganic and organic forms of nitrogen by higher plants. *The Journal of Agricultural Science*, *4*(3), 282-302.
99. Ingle, K. P., Deshmukh, A. G., Padole, D. A., Dudhare, M. S., Moharil, M. P., & Khelurkar, V. C. (2017). Phytochemicals: Extraction methods, identification and detection of bioactive compounds from plant extracts. Journal of Pharmacognosy and Phytochemistry, 6(1), 32-36.
100. Ishida, H., & Agag, T. (Eds.). (2011). Handbook of benzoxazine resins. Elsevier.
101. Isleib, J. (2017). A quick look at the nitrogen cycle and nitrogen fertilizer sources–Part 2. *Michigan State 677 University Extension*.
102. Jabbarzadeh Kaboli, P., Ismail, P., & Ling, K. H. (2018). Molecular modeling, dynamics simulations, and binding efficiency of berberine derivatives: A new group of RAF inhibitors for cancer treatment. PLoS One, 13(3), e0193941.

103. Jabri, E., Carr, M. B., Hausinger, R. P., & Karplus, P. A. (1995). The crystal structure of urease from Klebsiella aerogenes. *Science*, *268*(5213), 998-1004.
104. Jamil, F., Mukhtar, H., Fouillaud, M., & Dufossé, L. (2022). Rhizosphere signaling: Insights into plant–rhizomicrobiome interactions for sustainable agronomy. *Microorganisms*, *10*(5), 899.
105. Jiang, N., Doseff, A. I., & Grotewold, E. (2016). Flavones: from biosynthesis to health benefits. Plants, 5(2), 27.
106. Jickells, T., Baker, A. R., Cape, J. N., Cornell, S. E., & Nemitz, E. (2013). The cycling of organic nitrogen through the atmosphere. *Philosophical Transactions of the Royal Society B: Biological Sciences*, *368*(1621), 20130115.
107. Johnson, M. (1998). Development of fluticasone propionate and comparison with other inhaled corticosteroids. Journal of allergy and clinical immunology, 101(4), S434-S439.
108. Jones, C. A., Koenig, R. T., Ellsworth, J. W., Brown, B. D., & Jackson, G. D. (2007). Management of urea fertilizer to minimize volatilization. *MSU Extension*, 1-12.
109. Kaplan, A. (1969). The determination of urea, ammonia, and urease. Methods of biochemical analysis, 17, 311-324.
110. Karplus, M., & McCammon, J. A. (2002). Molecular dynamics simulations of biomolecules. Nature structural biology, 9(9), 646-652.
111. Kazmi, M. H., Fatima, I., Malik, A., Iqbal, L., Latif, M., & Afza, N. (2011). Sorbicins A and B, new urease and serine protease inhibitory triterpenes from Sorbus cashmiriana. Journal of Asian natural products research, 13(12), 1081-1086.
112. Kearsley, S. K., Underwood, D. J., Sheridan, R. P., & Miller, M. D. (1994). Flexibases: a way to enhance the use of molecular docking methods. Journal of computer-aided molecular design, 8, 565-582.

113. Khan, K. M., Rahim, F., Wadood, A., Kosar, N., Taha, M., Lalani, S., ... & Choudhary, M. I. (2014). Synthesis and molecular docking studies of potent α-glucosidase inhibitors based on biscoumarin skeleton. European journal of medicinal chemistry, 81, 245-252.
114. Khan, S. S., Khan, A., Khan, A., Wadood, A., Farooq, U., Ahmed, A., ... & Erdemoglu, N. (2014). Urease inhibitory activity of ursane type sulfated saponins from the aerial parts of Zygophyllum fabago Linn. Phytomedicine, 21(3), 379-382.
115. Khan, W. N., Lodhi, M. A., Ali, I., Azhar-Ul-Haq, Malik, A., Bilal, S., & Choudhary, M. I. (2006). New natural urease inhibitors from Ranunculus repens. Journal of enzyme inhibition and medicinal chemistry, 21(1), 17-19.
116. Kiss, S., Simihăian, M., Kiss, S., & Simihăian, M. (2002). Organic Compounds Tested for Evaluation of Their Inhibiting Effect on Soil Urease Activity, Urea Hydrolysis, Ammonia Volatilization, and Nitrous Oxide Emission. Improving Efficiency of Urea Fertilizers by Inhibition of Soil Urease Activity, 43-178.
117. Kitchen, D. B., Decornez, H., Furr, J. R., & Bajorath, J. (2004). Docking and scoring in virtual screening for drug discovery: methods and applications. Nature reviews Drug discovery, 3(11), 935-949.
118. Klose, S., & Tabatabai, M. A. (1999). Urease activity of microbial biomass in soils. Soil Biology and Biochemistry, 31(2), 205-211.
119. Klose, S., & Tabatabai, M. A. (2000). Urease activity of microbial biomass in soils as affected by cropping systems. *Biology and fertility of soils*, *31*, 191-199.
120. Knodt, M., & Ringel, M. (2018, July). The European Commission as a policy shaper–harder soft governance in the Energy Union. In The European Commission in turbulent times (pp. 181-206). Nomos Verlagsgesellschaft mbH & Co. KG.

121. Knowles, R. (1982). Denitrification. *Microbiological reviews*, *46*(1), 43-70.
122. Kobashi, K., Hase, J. I., & Uehara, K. (1962). Specific inhibition of urease by hydroxamic acids. Biochimica et biophysica acta, 65(2), 380-383.
123. Kobashi, K., TERASHIMA, N., TAKEBE, S., & HASE, J. I. (1978). A new method of determination of hydroxamic acid by its urease inhibition and application to biochemical studies. The Journal of Biochemistry, 83(1), 287-293.
124. Kolacinska, K., & Koncki, R. (2014). A novel optoelectronic detector and improved flow analysis procedure for ammonia determination with Nessler's reagent. Analytical Sciences, 30(10), 1019-1022.
125. Kori, M. L., Gaur, K., & Dixit, V. K. (2009). Investigation of immunomodulatory potential of Cleome gynandra Linn. Asian J Pharm Clin Res, 2(1), 35-9.
126. Krajewska, B., & Zaborska, W. (2007). Jack bean urease: The effect of active-site binding inhibitors on the reactivity of enzyme thiol groups. Bioorganic chemistry, 35(5), 355-365.
127. Krajewska, B., Leszko, M., & Zaborska, W. (1988). Immobilization of urease for dialysate regeneration system of artificial kidney. *Post. Fiz. Med*, *23*, 115-130.
128. Kubo, J., Lee, J. R., & Kubo, I. (1999). Anti-Helicobacter pylori agents from the cashew apple. Journal of Agricultural and Food Chemistry, 47(2), 533-537.
129. Kumar, S., & Kayastha, A. M. (2010). Inhibition studies of soybean (Glycine max) urease with heavy metals, sodium salts of mineral acids, boric acid, and boronic acids. Journal of Enzyme Inhibition and Medicinal Chemistry, 25(5), 646-652.

130. Kuriyan, J., Konforti, B., & Wemmer, D. (2012). The molecules of life: Physical and chemical principles. WW Norton & Company.
131. Ladd, J. N., & Jackson, R. B. (1982). Biochemistry of ammonification. *Nitrogen in agricultural soils*, *22*, 173-228.
132. Laskowski, R. A., & Swindells, M. B. (2011). LigPlot+: multiple ligand–protein interaction diagrams for drug discovery.
133. Lee, S., LaCour, T. G., & Fuchs, P. L. (2009). Chemistry of trisdecacyclic pyrazine antineoplastics: The cephalostatins and ritterazines. Chemical reviews, 109(6), 2275-2314.
134. Lees, H., & Simpson, J. R. (1957). The biochemistry of the nitrifying organisms. 5. Nitrite oxidation by Nitrobacter. *Biochemical Journal*, *65*(2), 297.
135. Lehtovirta-Morley, L. E. (2018). Ammonia oxidation: ecology, physiology, biochemistry and why they must all come together. *FEMS microbiology letters*, *365*(9), fny058.
136. Lengauer, T., & Rarey, M. (1996). Methods for predicting molecular complexes involving proteins. Current opinion in structural biology.
137. Leszko, M. J., Kot, M., & Zaborska, W. (1995). The enthalpimetric determination of the KM and v (max) of the urease-urea system from a single enzyme reaction progress curve. *Polish Journal of Chemistry*, *69*(12), 1704-1717.
138. Li, A. N., Li, S., Zhang, Y. J., Xu, X. R., Chen, Y. M., & Li, H. B. (2014). Resources and biological activities of natural polyphenols. Nutrients, 6(12), 6020-6047.
139. Lin, L., Lin, H., Bai, S., Zheng, L., & Zhang, X. (2018). Bone marrow mesenchymal stem cells (BMSCs) improved functional recovery of spinal cord injury partly by promoting axonal regeneration. Neurochemistry international, 115, 80-84.

140. Lin, Y. H., Chen, C. Y., Chou, L. Y., Chen, C. H., Kang, L., & Wang, C. Z. (2017). Enhancement of bone marrow-derived mesenchymal stem cell osteogenesis and new bone formation in rats by obtusilactone A. International journal of molecular sciences, 18(11), 2422.
141. Lineweaver, H., & Burk, D. (1934). The determination of enzyme dissociation constants. *Journal of the American chemical society*, *56*(3), 658-666.
142. Ling, N., Wang, T., & Kuzyakov, Y. (2022). Rhizosphere bacteriome structure and functions. *Nature communications*, *13*(1), 836.
143. Lippard, S. J. (1995). At last—the crystal structure of urease. *Science*, *268*(5213), 996-997.
144. Lobanov, M. Y., Bogatyreva, N. S., & Galzitskaya, O. V. (2008). Radius of gyration as an indicator of protein structure compactness. Molecular Biology, 42, 623-628.
145. Lodhi, M. A., Hussain, J., Abbasi, M. A., Jassbi, A. R., Choudhary, M. I., & Ahmad, V. U. (2006). A new Bacillus pasteurii urease inhibitor from Euphorbia decipiens. Journal of Enzyme Inhibition and Medicinal Chemistry, 21(5), 531-535.
146. Loes, A. N., Ruyle, L., Arvizu, M., Gresko, K. E., Wilson, A. L., & Deutch, C. E. (2014). Inhibition of urease activity in the urinary tract pathogen Staphylococcus saprophyticus. Letters in applied microbiology, 58(1), 31-41.
147. Lv, H. N., Tu, P. F., & Jiang, Y. (2014). Benzocoumarins: isolation, synthesis, and biological activities. Mini Reviews in Medicinal Chemistry, 14(7), 603-622.
148. Lv, H. N., Wang, S., Zeng, K. W., Li, J., Guo, X. Y., Ferreira, D., & Jiang, Y. (2015). Anti-inflammatory coumarin and benzocoumarin derivatives from Murraya alata. Journal of natural products, 78(2), 279-285.

149. Maia, L. B., & Moura, J. J. (2014). How biology handles nitrite. *Chemical Reviews*, *114*(10), 97.
150. Majekodunmi, S. O. (2015). Review of extraction of medicinal plants for pharmaceutical research. Merit Res J Med, 3, 521-527.
151. Mano, J., Dicko, C., Ouédraogo, J. C. W., & Bonzi-Coulibaly, Y. L. (2024). Glucosinolate profiling in Cleome gynandra L. aerial parts based on two extraction methods. Canadian Journal of Chemistry, 103(1), 27-36.
152. Mansoor, F., Anis, I., Khan, A., Marasini, B. P., Choudhary, M. I., & Shah, M. R. (2014). Urease inhibitory constituents from Daphne retusa. Journal of Asian Natural Products Research, 16(2), 210-215.
153. Martinez, R., Blasina, A., Hallin, J. F., Hu, W., Rymer, I., Fan, J., ... & Murray, B. W. (2015). Mitotic checkpoint kinase Mps1 has a role in normal physiology which impacts clinical utility. PLoS One, 10(9), e0138616.
154. Martins, M. B. F., Cruz, M. E. M., Cabral, J. M., & Kennedy, J. F. (1987). Urease immobilization on an alkylamine derivative of titanium (IV)-porous silica: Kinetics and operational stability. *Journal of Chemical Technology & Biotechnology*, *39*(3), 201-213.
155. Matsumoto, K. (1992). Beverages by Immobilized Acid Urease. *Industrial application of immobilized biocatalysts*, *16*, 255.
156. Mayo, S. L., Olafson, B. D., & Goddard, W. A. (1990). DREIDING: a generic force field for molecular simulations. Journal of Physical chemistry, 94(26), 8897-8909.
157. Mazzei, L., Musiani, F., & Ciurli, S. (2017). Urease.
158. McCarty, G. W., Bremner, J. M., & Lee, J. S. (1990). Inhibition of plant and microbial ureases by phosphoroamides. Plant and soil, 127, 269-283.
159. McDonald, A. G., & Tipton, K. F. (2023). Enzyme nomenclature and classification: the state of the art. *The FEBS journal*, *290*(9), 2214-2231.

160. McNear Jr, D. H. (2013). The Rhizosphere-Roots. *Soil and Everything In*.
161. ME Trenkel, T. (2021). Slow-and controlled-release and Stabilized Fertilizers: an option for enhancing nutrient use effiiency in agriculture. International Fertilizer Industry Association (IFA).
162. Mekonnen, E., Kebede, A., Nigussie, A., Kebede, G., & Tafesse, M. (2021). Isolation and characterization of urease-producing soil bacteria. *International journal of microbiology*, *2021*(1), 8888641.
163. Meyer, F. (1998). A bridging coordination mode of urea and carbamate at a dinuclear nickel (II) centre. *Chemical Communications*, (15), 1555-1556.
164. Miao, J., Hodgson, K. O., & Sayre, D. (2001). An approach to three-dimensional structures of biomolecules by using single-molecule diffraction images. Proceedings of the National Academy of Sciences, 98(12), 6641-6645.
165. Michalec, M., Granica, M., Bzura, J., Koncki, R., Matuszkiewicz-Rowińska, J., & Tymecki, Ł. (2016). Optoelectronic detectors and flow analysis systems for determination of dialysate urea nitrogen. Sensors and Actuators B: Chemical, 226, 563-569.
166. Miflin, B. J., & Lea, P. J. (1976). The pathway of nitrogen assimilation in plants. *Phytochemistry*, *15*(6), 873-885.
167. Mishra, S. S., Moharana, S. K., & Dash, M. R. (2011). Review on Cleome gynandra. International journal of research in Pharmacy and chemistry, 1(3), 681-689.
168. Mobley, H. L. (2001). Urease. *Helicobacter pylori: physiology and genetics*, 177-191.
169. Mobley, H. L., & Hausinger, R. P. (1989). Microbial ureases: significance, regulation, and molecular characterization. *Microbiological reviews*, *53*(1), 85-108.

170. Modolo, L. V., de Souza, A. X., Horta, L. P., Araujo, D. P., & de Fatima, A. (2015). An overview on the potential of natural products as ureases inhibitors: A review. Journal of Advanced Research, 6(1), 35-44.
171. Moyo, M., Amoo, S. O., Aremu, A. O., Gruz, J., Šubrtová, M., Jarošová, M., & Doležal, K. (2018). Determination of mineral constituents, phytochemicals and antioxidant qualities of Cleome gynandra, compared to Brassica oleracea and Beta vulgaris. Frontiers in Chemistry, 5, 128.
172. Na, G., He, C., Zhang, S., Tian, S., Bao, Y., & Shan, Y. (2023). Dietary isothiocyanates: Novel insights into the potential for cancer prevention and therapy. International Journal of Molecular Sciences, 24(3), 1962.
173. Narendhirakannan, R. T., Subramanian, S., & Kandaswamy, M. (2007). Anti-inflammatory and lysosomal stability actions of Cleome gynandra L. studied in adjuvant induced arthritic rats. Food and Chemical Toxicology, 45(6), 1001-1012.
174. Needleman, P., Whitaker, M. O., Wyche, A., Watters, K., Sprecher, H., & Raz, A. (1980). Manipulation of platelet aggregation by prostaglandins and their fatty acid precursors: pharmacological basis for a therapeutic approach. Prostaglandins, 19(1), 165-181.
175. Ngan, L. T. M., Moon, J. K., Shibamoto, T., & Ahn, Y. J. (2012). Growth-inhibiting, bactericidal, and urease inhibitory effects of Paeonia lactiflora root constituents and related compounds on antibiotic-susceptible and-resistant strains of Helicobacter pylori. Journal of agricultural and food chemistry, 60(36), 9062-9073.
176. Ni, B., Lu, S., & Liu, M. (2012). Novel multinutrient fertilizer and its effect on slow release, water holding, and soil amending. *Industrial & engineering chemistry research*, *51*(40), 12993-13000.
177. Ninfa, A. J., Ballou, D. P., & Benore, M. (2009). *Fundamental laboratory approaches for biochemistry and biotechnology*. John Wiley & Sons.

178. Ohyama, T. (2010). Nitrogen as a major essential element of plants. *Nitrogen Assim. Plants*, *37*, 1-17.
179. Okyay, T. O., & Rodrigues, D. F. (2013). High throughput colorimetric assay for rapid urease activity quantification. Journal of microbiological methods, 95(3), 324-326.
180. Olech, Z., Zaborska, W., & Kot, M. (2014). Jack bean urease inhibition by crude juices of Allium and Brassica plants. Determination of thiosulfinates. Food chemistry, 145, 154-160.
181. Omondi, E. O., Engels, C., Nambafu, G., Schreiner, M., Neugart, S., Abukutsa-Onyango, M., & Winkelmann, T. (2017). Nutritional compound analysis and morphological characterization of spider plant (Cleome gynandra)-an African indigenous leafy vegetable. Food Research International, 100, 284-295.
182. Padilla, F. M., Gallardo, M., & Manzano-Agugliaro, F. (2018). Global trends in nitrate leaching research in the 1960–2017 period. *Science of the Total Environment*, *643*, 400-413.
183. Palmer, T., & Bonner, P. L. (2007). Enzymes: biochemistry, biotechnology, clinical chemistry. Elsevier.
184. Pandey, A., & Tripathi, S. (2014). Concept of standardization, extraction and pre phytochemical screening strategies for herbal drug. Journal of Pharmacognosy and phytochemistry, 2(5).
185. Paulo, L., Oleastro, M., Gallardo, E., Queiroz, J. A., & Domingues, F. (2011). Anti-Helicobacter pylori and urease inhibitory activities of resveratrol and red wine. Food Research International, 44(4), 964-969.
186. Perveen, S., El-Shafae, A. M., Al-Taweel, A., Fawzy, G. A., Malik, A., Afza, N., ... & Iqbal, L. (2011). Antioxidant and urease inhibitory C-glycosylflavonoids from Celtis africana. Journal of Asian Natural Products Research, 13(9), 799-804.

187. Peters, N., & Thiele-Bruhn, S. (2022). Major metabolites of NBPT degradation pathways contribute to urease inhibition in soil. Chemosphere, 303, 135163.
188. Pettersen, E. F., Goddard, T. D., Huang, C. C., Couch, G. S., Greenblatt, D. M., Meng, E. C., & Ferrin, T. E. (2004). UCSF Chimera: Un sistema de visualización para la investigación y el análisis exploratorios. J. Comput. Chem, 25, 1605-1612.
189. Philippot, L., Raaijmakers, J. M., Lemanceau, P., & Van Der Putten, W. H. (2013). Going back to the roots: the microbial ecology of the rhizosphere. *Nature reviews microbiology*, *11*(11), 789-799.
190. Piret, J., Désormeaux, A., & Bergeron, M. G. (2002). Sodium lauryl sulfate, a microbicide effective against enveloped and nonenveloped viruses. Current Drug Targets, 3(1), 17-30.
191. Prakash, O., & Bachan Upadhyay, L. S. (2004). Acetohydroxamate inhibition of the activity of urease from dehusked seeds of water melon (Citrullus vulgaris). Journal of Enzyme Inhibition and Medicinal Chemistry, 19(4), 381-387.
192. Qin, Y., & Cabral, J. M. (1994). Kinetic studies of the urease-catalyzed hydrolysis of urea in a buffer-free system. *Applied biochemistry and biotechnology*, *49*, 217-240.
193. Rai, M., Singh, A. V., Paudel, N., Kanase, A., Falletta, E., Kerkar, P., ... & Soos, M. (2023). Herbal concoction unveiled: a computational analysis of phytochemicals' pharmacokinetic and toxicological profiles using novel approach methodologies (NAMs). Current Research in Toxicology, 5, 100118.
194. Ramsay, K. S. T., Wafo, P., Ali, Z., Khan, A., Oluyemisi, O. O., Marasini, B. P., ... & Choudhary, M. I. (2012). Chemical constituents of Stereospermum acuminatissimum and their urease and α-chymotrypsin inhibitions. Fitoterapia, 83(1), 204-208.

195. Randive, K., Raut, T., & Jawadand, S. (2021). An overview of the global fertilizer trends and India's position in 2020. *Mineral Economics*, 1-14.
196. Raza, A., Hafeez, M. B., Zahra, N., Shaukat, K., Umbreen, S., Tabassum, J., & Hasanuzzaman, M. (2020). The plant family Brassicaceae: Introduction, biology, and importance. The Plant Family Brassicaceae: Biology and Physiological Responses to Environmental Stresses, 1-43.
197. Remde, A., & Conrad, R. (1990). Production of nitric oxide in Nitrosomonas europaea by reduction of nitrite. *Archives of Microbiology*, *154*(2), 187-191.
198. Rodríguez, S. B., Alonso-Gaite, A., & Álvarez-Benedí, J. (2005). Characterization of nitrogen transformations, sorption and volatilization processes in urea fertilized soils. *Vadose zone journal*, *4*(2), 329-336.
199. Rotz, C. A. (2004). Management to reduce nitrogen losses in animal production. *Journal of animal science*, *82*(suppl_13), E119-E137.
200. Ruiz-Herrera, J., & Gonzalez, J. (1969). A continuous method for the measurement of urease activity. Analytical biochemistry, 31, 366-374.
201. Runnie, I., Salleh, M. N., Mohamed, S., Head, R. J., & Abeywardena, M. Y. (2004). Vasorelaxation induced by common edible tropical plant extracts in isolated rat aorta and mesenteric vascular bed. Journal of Ethnopharmacology, 92(2-3), 311-316.
202. Salentin, S., Schreiber, S., Haupt, V. J., Adasme, M. F., & Schroeder, M. (2015). PLIP: fully automated protein–ligand interaction profiler. Nucleic acids research, 43(W1), W443-W447.
203. Sasidharan, S., Chen, Y., Saravanan, D., Sundram, K. M., & Latha, L. Y. (2011). Extraction, isolation and characterization of bioactive compounds from plants' extracts. African journal of traditional, complementary and alternative medicines, 8(1).

204. **Schlick**, P. A., Pearson, M. A., & Hausinger, R. P. (1997). 70 years of crystalline urease: what have we learned?. *Accounts of Chemical Research*, *30*(8), 330-337.
205. Schlick, T. (1996). Pursuing Laplace's vision on modern computers. In Mathematical approaches to biomolecular structure and dynamics (pp. 219-247). New York, NY: Springer New York.
206. Schönberg, A., & Latif, N. (1954). Furochromones and coumarins. XI. The molluscicidal activity of bergapten, isopimpinillin and xanthotoxin. Journal of the American Chemical Society, 76(23), 6208-6208.
207. Schrödinger, E. (2017). L'immagine del mondo. Bollati Boringhieri.
208. Shabana, S., Kawai, A., Kai, K., Akiyama, K., & Hayashi, H. (2010). Inhibitory activity against urease of quercetin glycosides isolated from Allium cepa and Psidium guajava. Bioscience, biotechnology, and biochemistry, 74(4), 878-880.
209. Shankar, S., Segaran, G., Sundar, R. D. V., Settu, S., & Sathiavelu, M. (2019). Brassicaceae-A classical review on its pharmacological activities. Int. J. Pharm. Sci. Rev. Res, 55(1), 107-113.
210. Sharma, S. K., Vij, A. S., & Sharma, M. (2013). Mechanisms and clinical uses of capsaicin. European journal of pharmacology, 720(1-3), 55-62.
211. Sharma, S., Rani, H., Kaur, G., Kumar, S., Sheikh, S., & Samota, M. K. (2024). Comprehensive overview of glucosinolates in crucifers: Occurrence, roles, metabolism, and transport mechanisms—A review. Phytochemistry Reviews, 1-28.
212. Shen, J. P., Zhang, L. M., Zhu, Y. G., Zhang, J. B., & He, J. Z. (2008). Abundance and composition of ammonia-oxidizing bacteria and ammonia-oxidizing archaea communities of an alkaline sandy loam. *Environmental microbiology*, *10*(6), 1601-1611.

213. Shilla, O., Dinssa, F. F., Omondi, E. O., Winkelmann, T., & Abukutsa-Onyango, M. O. (2019). Cleome gynandra L. origin, taxonomy and morphology: A review. African Journal of Agricultural Research, 14(32), 1568-1583.
214. Shrestha, R. S., Adhikari, A., Marasini, B. P., Jha, R. N., & Choudhary, M. I. (2013). Novel inhibitors of urease from Corydalis govaniana Wall. Phytochemistry Letters, 6(2), 228-231.
215. Shuman, L. M. (2017). Micronutrient fertilizers. In *Nutrient use in crop production* (pp. 165-195). CRC Press.
216. Singh, A. K., Singh, M., & Verma, N. (2017). Extraction, purification, kinetic characterization and immobilization of urease from Bacillus sphaericus MTCC 5100. *Biocatalysis and Agricultural Biotechnology*, *12*, 341-347.
217. Singh, H., Mishra, A., & Mishra, A. K. (2018). The chemistry and pharmacology of Cleome genus: a review. Biomedicine & Pharmacotherapy, 101, 37-48.
218. Smith, P. T., King Jr, A. D., & Goodman, N. (1993). Isolation and characterization of urease from Aspergillus niger. *Microbiology*, *139*(5), 957-962.
219. Smith, V. H., & Schindler, D. W. (2009). Eutrophication science: where do we go from here? *Trends in ecology & evolution*, *24*(4), 201-207.
220. Stein, L. Y., & Arp, D. J. (1998). Loss of ammonia monooxygenase activity in Nitrosomonas europaea upon exposure to nitrite. *Applied and Environmental Microbiology*, *64*(10), 4098-4102.
221. Steinfeld, H., Gerber, P., Wassenaar, T. D., Castel, V., & De Haan, C. (2006). *Livestock's long shadow: environmental issues and options*. Food & Agriculture Org..
222. Strock, J. S. (2008). Ammonification. In *Encyclopedia of ecology, five-volume set* (pp. 162-165). Elsevier.

223. Takshak, S., & Agrawal, S. Á. (2014). Secondary metabolites and phenylpropanoid pathway enzymes as influenced under supplemental ultraviolet-B radiation in Withania somnifera Dunal, an indigenous medicinal plant. Journal of Photochemistry and Photobiology B: Biology, 140, 332-343.
224. Tan, L., Su, J., Wu, D., Yu, X., Su, Z., He, J., ... & Su, Z. (2013). Kinetics and Mechanism Study of Competitive Inhibition of Jack-Bean Urease by Baicalin. The Scientific World Journal, 2013(1), 879501.
225. Tanaka, T., Kawase, M., & Tani, S. (2004). α-Hydroxyketones as inhibitors of urease. Bioorganic & medicinal chemistry, 12(2), 501-505.
226. Tariq, S. A., Ahmad, M. N., Obaidullah, Khan, A., Choudhary, M. I., Ahmad, W., & Ahmad, M. (2011). Urease inhibitors from Indigofera gerardiana Wall. Journal of Enzyme Inhibition and Medicinal Chemistry, 26(4), 480-484.
227. Tarun, E. I., Rubinov, D. B., & Metelitza, D. I. (2004). Inhibition of soybean urease by triketone oximes. Biochemistry (Moscow), 69, 1344-1352.
228. Telkar, S. G., & Pote, N. S. (2015). Soil erosion: Types and their mechanism. *Int. J. Econ. Plants*, *2*, 178-180.
229. Tian, T., Reverdy, A., She, Q., Sun, B., & Chai, Y. (2020). The role of rhizodeposits in shaping rhizomicrobiome. *Environmental Microbiology Reports*, *12*(2), 160-172.
230. Todd, M. J., & Hausinger, R. P. (1989). Competitive inhibitors of Klebsiella aerogenes urease: mechanisms of interaction with the nickel active site. Journal of Biological Chemistry, 264(27), 15835-15842.
231. Todd, M. J., & Hausinger, R. P. (2000). Fluoride inhibition of Klebsiella aerogenes urease: mechanistic implications of a pseudo-uncompetitive, slow-binding inhibitor. Biochemistry, 39(18), 5389-5396.

232. Tuley, A., & Fast, W. (2018). The taxonomy of covalent inhibitors. Biochemistry, 57(24), 3326-3337.
233. Uddin, G., Ismail, Rauf, A., Raza, M., Khan, H., Nasruddin, ... & Arifullah. (2016). Urease inhibitory profile of extracts and chemical constituents of Pistacia atlantica ssp. cabulica Stocks. Natural Product Research, 30(12), 1411-1416.
234. Uddin, N., Siddiqui, B. S., Begum, S., Ali, M. I., Marasini, B. P., Khan, A., & Choudhary, M. I. (2013). Bioassay-guided isolation of urease and α-chymotrypsin inhibitory constituents from the stems of Lawsonia alba Lam.(Henna). Fitoterapia, 84, 202-207.
235. Upadhyay, L. S. B. (2012). Urease inhibitors: A review.
236. Van den Heever, E. A. N. D., & Venter, S. L. (2006, December). Nutritional and medicinal properties of Cleome gynandra. In I International Conference on Indigenous Vegetables and Legumes. Prospectus for Fighting Poverty, Hunger and Malnutrition 752 (pp. 127-130).
237. Van Kessel, M. A., Speth, D. R., Albertsen, M., Nielsen, P. H., Op den Camp, H. J., Kartal, B., ... & Lücker, S. (2015). Complete nitrification by a single microorganism. *Nature*, *528*(7583), 555-559.
238. Vitolo, M. (2022). Notes on urea hydrolysis by urease. *J. Pharm. Pharm. Sci*, *11*(3), 96-135.
239. Vitousek, P. M., Hättenschwiler, S., Olander, L., & Allison, S. (2002). Nitrogen and nature. *AMBIO: A Journal of the Human Environment*, *31*(2), 97-101.
240. Wallace, W., & Nicholas, D. J. D. (1969). The biochemistry of nitrifying microorganisms. *Biological Reviews*, *44*(3), 359-389.
241. Wang, H. M., Cheng, K. C., Lin, C. J., Hsu, S. W., Fang, W. C., Hsu, T. F., ... & Lee, A. Y. L. (2010). Obtusilactone A and (−)-sesamin induce apoptosis in human lung cancer cells by inhibiting mitochondrial Lon

protease and activating DNA damage checkpoints. Cancer science, 101(12), 2612-2620.

242. Wang, H., Köbke, S., & Dittert, K. (2020). Use of urease and nitrification inhibitors to reduce gaseous nitrogen emissions from fertilizers containing ammonium nitrate and urea. Global Ecology and Conservation, 22, e00933.
243. Ward, B. B., Arp, D. J., & Klotz, M. G. (Eds.). (2011). *Nitrification*. American Society for Microbiology Press.
244. Ward, B. B., Devol, A. H., Rich, J. J., Chang, B. X., Bulow, S. E., Naik, H., ... & Jayakumar, A. (2009). Denitrification as the dominant nitrogen loss process in the Arabian Sea. *Nature*, *461*(7260), 78-81.
245. Weatherburn, M. (1967). Phenol-hypochlorite reaction for determination of ammonia. Analytical chemistry, 39(8), 971-974.
246. Wei, Q., Xu, J., Liu, Y., Wang, D., Chen, S., Qian, W., ... & Qi, Z. (2024). Nitrogen losses from soil as affected by water and fertilizer management under drip irrigation: Development, hotspots and future perspectives. Agricultural Water Management, 296, 108791.
247. Wu, D. W., Yu, X. D., Xie, J. H., Su, Z. Q., Su, J. Y., Tan, L. R., ... & Su, Z. R. (2013). Inactivation of jack bean urease by scutellarin: elucidation of inhibitory efficacy, kinetics and mechanism. Fitoterapia, 91, 60-67.
248. Xiao, Z. P., Wang, X. D., Peng, Z. Y., Huang, S., Yang, P., Li, Q. S., ... & Zhu, H. L. (2012). Molecular docking, kinetics study, and structure–activity relationship analysis of quercetin and its analogous as Helicobacter pylori urease inhibitors. Journal of agricultural and food chemistry, 60(42), 10572-10577.
249. Xu, G., Fan, X., & Miller, A. J. (2012). Plant nitrogen assimilation and use efficiency. *Annual review of plant biology*, *63*(1), 153-182.
250. Young, R. D., & Davis, C. H. (1980). Phosphate fertilizers and process technology. *The role of phosphorus in agriculture*, 195-226.

251. Zaborska, W., Krajewska, B., & Olech, Z. (2004). Heavy metal ions inhibition of jack bean urease: potential for rapid contaminant probing. Journal of Enzyme Inhibition and Medicinal Chemistry, 19(1), 65-69.
252. Zerner, B. (1991). Recent advances in the chemistry of an old enzyme, urease. *Bioorganic Chemistry*, *19*(1), 116-131.
253. Zhang, L. M., Hu, H. W., Shen, J. P., & He, J. Z. (2012). Ammonia-oxidizing archaea have more important role than ammonia-oxidizing bacteria in ammonia oxidation of strongly acidic soils. *The ISME journal*, *6*(5), 1032-1045.
254. Zhou, J. T., Li, C. L., Tan, L. H., Xu, Y. F., Liu, Y. H., Mo, Z. Z., ... & Xie, J. H. (2017). Inhibition of Helicobacter pylori and its associated urease by palmatine: investigation on the potential mechanism. PLoS one, 12(1), e0168944.
255. Zolghadr, L., Behbehani, G. R., PakBin, B., Hosseini, S. A., Divsalar, A., & Gheibi, N. (2022). Molecular dynamics simulations, molecular docking, and kinetics study of kaempferol interaction on Jack bean urease: Comparison of extended solvation model. Food Science & Nutrition, 10(11), 3585-3597.
256. Zuazo, V. H. D., & Pleguezuelo, C. R. R. (2009). Soil-erosion and runoff prevention by plant covers: a review. *Sustainable agriculture*, 785-811.
257. Zumft, W. G. (1997). Cell biology and molecular basis of denitrification. *Microbiology and molecular biology reviews*, *61*(4), 533-616.

Chapter 11

Publications

1. **Dutta, R**., Dutta, M., Hazra, A., Bhattacharya, E., Bose, R., & Biswas, S. M. (2024). Jack bean urease inhibition by different root fractions of Cleome gynandra L–Kinetic mechanism and computational molecular modelling. Industrial Crops and Products, 222, 119514.

2. **Dutta, R**., Bhattacharya, E., Pramanik, A., Hughes, T. A., & Biswas, S. M. (2022). Potent nutraceuticals having antioxidant, DNA damage protecting potential and anti-cancer properties from the leaves of four Ficus species. Biocatalysis and Agricultural Biotechnology, 44, 102461.

3. Bhattacharya, E., **Dutta, R**., Chakraborty, S., & Biswas, S. M. (2019). Phytochemical profiling of Artocarpus lakoocha Roxb. Leaf methanol extract and its antioxidant, antimicrobial and antioxidative activities. Asian Pacific Journal of Tropical Biomedicine, 9(11), 484-492.

4. Bhattacharya, E., Pal, U., **Dutta, R**., Bhowmik, P. C., & Mandal Biswas, S. (2022). Antioxidant, antimicrobial and DNA damage protecting potential of hot taste spices: A comparative approach to validate their utilization as functional foods. Journal of Food Science and Technology, 59(3), 1173-1184.

5. Bhattacharya, E., Saha, S., **Dutta, R**., Dutta, M., & Biswas, S. M. (2022). Fractionation based evaluation of phytochemical constituents, antimicrobial and allelopathic potential of Piper chaba, Hunter. stem and identification of “Pipercyclobutanamide-A” as a strong allelopathic agent. Biocatalysis and Agricultural Biotechnology, 42, 102356.

6. Hazra, A., Dutta, M., **Dutta, R**., Bhattacharya, E., Bose, R., & Biswas, S. M. (2023). Squalene synthase in plants–Functional intricacy and evolutionary divergence while retaining a core catalytic structure. Plant Gene, 33, 100403.

7. Bose, R., Paul, A., **Dutta, R**., Hazra, A., Pramanik, A., & Mandal Biswas, S. (2025). Synthesis, antimicrobial, anticancer evaluation and molecular docking with Bax and MDM2 of dibromosterculic acid. Natural Product Research, 39(5), 1065-1072.

Industrial Crops & Products 222 (2024) 119514

Contents lists available at ScienceDirect

Industrial Crops & Products

journal homepage: www.elsevier.com/locate/indcrop

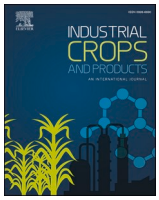

Jack bean urease inhibition by different root fractions of *Cleome gynandra* L – Kinetic mechanism and computational molecular modelling

Rajashree Dutta [a], Madhurima Dutta [a], Anjan Hazra [b], Ekta Bhattacharya [a], Rahul Bose [a], Suparna Mandal Biswas [a,*]

[a] *Agricultural and Ecological Research Unit, Indian Statistical Institute, 203, B.T. Road, Kolkata 700108, India*
[b] *Department of Botany, Victoria Institution (College), 78-B, A.P.C. Road, Kolkata 700009, India*

ARTICLE INFO

Keywords:
Cleome gynandra L.
Enzyme kinetics
Molecular docking
Molecular dynamics simulations
Natural urease inhibitors

ABSTRACT

Natural products with urease inhibiting potentialities would be valuable for enhancing nitrogen fertilizer formulations and developing new therapeutics against infectious diseases. Main focus of this research was to assess the inhibitory impact of various parts of *Cleome gynandra* (Cleomaceae) on jack bean urease activity, identify the responsible compounds, and ascertain their mode of enzyme inhibition and interactions with urease enzyme. Urease inhibitory potentiality of different plant parts of *C. gynandra* was determined using the phenol-hypochlorite method and mode of enzyme inhibition by Lineweaver-Burk kinetic analysis. LC-HRMS was carried out to identify the compounds of the active fractions. Molecular docking and simulations were executed to find out the binding affinity and interaction pattern of the isolated compounds at the active site of urease enzyme and to verify stability of protein-inhibitor complexes. The root of *C. gynandra* exhibited highest urease inhibitory potentiality with IC_{50} value of 1.529 mg/ml compared with leaf and stem. Among the different root fractions, water fraction revealed maximum anti-urease activity with IC_{50} values of 1.477 mg/ml followed by methanol (1.655 mg/ml) and acetone fractions (1.955 mg/ml). Inhibition kinetics indicated that these fractions were strong inhibitors of urease and exhibited a non-competitive mode of inhibition with K_i values of 184.911 μg/ml, 147.34 μg/ml, and 233.75 μg/ml respectively at 1000 mg/L concentration. LC-HRMS analysis confirmed the occurrence of glucocapparin, fluticasone propionate and lauryl hydrogen sulfate etc. in water fraction. Molecular modelling and simulation study suggested strong and stable interactions between the specified compounds of water fraction and active site of urease. Hence, the water fraction of *C. gynandra* roots represent a valuable source of natural urease inhibitors, for possible therapeutic applications and sustainable agricultural practices.

1. Introduction

Urease was the first enzyme to be crystallized and confirmed as a protein. Also, it was identified as the inaugural model of nickel metalloenzymes (Zerner, 1991). While urea breaks down through an elimination process in a liquid solution, the urease enzyme accelerates the conversion of the substrate into carbamate and ammonia as the initial byproducts. This shift in process clearly indicates the participation of a nickel ion in the enzyme's chemical reactions, and the fact has been independently verified. This chemical process has attracted significant interest for its impact on the health of living organisms, overall life quality, and agricultural productivity (Kappaun et al., 2018).

The activity of urease persists within human and animal cells, which may contribute to the development of certain diseases and heightened susceptibility to pathogenic infections (Aliyeva-Schnorr et al., 2023). Some specific pathogenic cells have the ability to release of cytosolic ureases, which can bind to intact bacterial cells and initiate the breakdown of urea in the human gastrointestinal tract (Burne and Chen, 2000).

The hydrolysis of urea results in the formation of ammonia, which raises the pH levels in the digestive system. This elevated pH creates an ideal environment for the growth of *Helicobacter pylori*, a harmful gram-negative bacteria associated with various gastrointestinal ulcers such as peptic and duodenal ulcers, also gastric cancer. Unfortunately, this bacterium has developed resistance to a wide range of antibiotics (Aguemon et al., 2005). Therefore, a significant focus is warranted on exploring substances that are not only highly effective in combatting *H. pylori* but also safe for the gastrointestinal tract.

* Corresponding author.
E-mail address: mondalsupa@gmail.com (S. Mandal Biswas).

https://doi.org/10.1016/j.indcrop.2024.119514
Received 16 March 2024; Received in revised form 15 July 2024; Accepted 24 August 2024
Available online 31 August 2024

Biocatalysis and Agricultural Biotechnology 44 (2022) 102461

Contents lists available at ScienceDirect

Biocatalysis and Agricultural Biotechnology

journal homepage: www.elsevier.com/locate/bab

Potent nutraceuticals having antioxidant, DNA damage protecting potential and anti-cancer properties from the leaves of four *Ficus* species

Rajashree Dutta [a,**], Ekta Bhattacharya [a], Arindam Pramanik [b], Thomas A. Hughes [b], Suparna Mandal Biswas [a,*]

[a] Agricultural and Ecological Research Unit, Indian Statistical Institute, 203, B.T. Road, Kolkata, 700108, India
[b] School of Medicine, Wellcome Trust Brenner Building, St James's University Hospital, University of Leeds, LS9 7TF, UK

ARTICLE INFO

Keywords:
Ficus species
Antioxidant activity
DNA Protection potential
Cytotoxic activity
Phytochemicals

ABSTRACT

In the present study, we have evaluated fractionation based phytochemical constituents, antioxidant activity, DNA damage protecting potential and anticancerous properties of leaves of common *Ficus* species (namely *Ficus virens, Ficus benghalensis, Ficus religiosa, Ficus elastica*) along with GCMS analysis for identification of major bioactive constituents. Methanol fraction of *F. virens* contained maximum amount of phenolics (1267.35 mg GAE/g dry extract) and flavonoids (1080.61 mg QE/g dry extract) whereas hexane fraction of *F. religiosa* possessed highest amount of tannins (123.76 mg TAE/g dry extract). Least amount of phytochemicals was recovered from *F. elastica*. Highest DPPH radical scavenging activity (IC_{50} = 108.28 μg/ml) was detected by methanol fraction of *F. benghalensis* whereas highest ABTS activity (IC_{50} = 105.56 μg/ml) by *F. benghalensis* and highest ferric reducing power by *F. virens* (359.44 mg QE/g dry extract). Leaf methanol fraction of *F. virens, F. religiosa* and *F. elastica* were able to prevent oxidative DNA damage at 0.1 mg/ml,0.2 mg/ml and 0.3 mg/ml respectively. Viability of normal breast cells was unaffected by methanol fraction of tested *Ficus* species at doses less than 160 μg/ml, whereas survival of breast cancer cells was decreased by *F. benghalensis* at 5 μg/ml. GCMS analysis of the purified methanol fraction of tested species revealed the presence of potent bioactive compounds such as carvacrol, phytol, tocopherol, benzophenone, dibutyl phthalate, lycopersen etc. All our experimental results along with the identification of the bioactive compounds supported the fact that leaves of tested *Ficus* species as rich source of phytochemicals with nutraceutical potentialities.

1. Introduction

Phytochemicals are secondary metabolites which not only have physiological functions in plants but also exert significant pharmacological effects especially for preventing oxidative damage to cells. Extensive research is going on in plant derived natural

Abbreviations: Ficus virens, FV; *Ficus benghalensis*, FB; *Ficus religiosa*, FR; *Ficus elastica*, FE; Hexane Fraction, HF; Ethyl acetate Fraction, EF; Acetone Fraction, AF; Methanol Fraction, MF.

* Corresponding author.
** Corresponding author.
E-mail addresses: rajashree1026@gmail.com (R. Dutta), ektabhattacharya1990@gmail.com (E. Bhattacharya), A.Pramanik@leeds.ac.uk (A. Pramanik), T.Hughes@leeds.ac.uk (T.A. Hughes), mondalsupa@gmail.com (S. Mandal Biswas).

https://doi.org/10.1016/j.bcab.2022.102461
Received 4 April 2022; Received in revised form 8 August 2022; Accepted 9 August 2022
Available online 14 August 2022

Original Article

Asian Pacific Journal of Tropical Biomedicine

journal homepage: www.apjtb.org

doi: 10.4103/2221-1691.270984

Impact factor: 1.59

Phytochemical profiling of *Artocarpus lakoocha* Roxb. leaf methanol extract and its antioxidant, antimicrobial and antioxidative activities

Ekta Bhattacharya[1], Rajashree Dutta[1], Swati Chakraborty[2], Suparna Mandal Biswas[1]✉

[1]*Agricultural and Ecological Research Unit, Indian Statistical Institute, 203, B.T. Road, Kolkata 700108, India*

[2]*Guru Nanak Institute of Pharmaceutical Science & Technology Panihati, Kolkata 700114, India*

ARTICLE INFO

Article history:
Received 11 June 2019
Revision 23 July 2019
Accepted 17 October 2019
Available online 20 November 2019

Keywords:
Moraceae
Bioactive compounds
Natural pharmaceuticals
Diethyl phthalate

ABSTRACT

Objective: To explore the phytochemical profile of *Artocarpus lakoocha* Roxb. leaves both qualitatively and quantitatively, and validate its role as a potent antioxidant and antimicrobial agent.

Methods: Extraction and isolation of different compounds were done from the leaves of *Artocarpus lakoocha* based on solvent fractionation method. Subsequently, quantitative and qualitative phytochemical profiling along with antioxidant, antimicrobial and antioxidative activities were tested following standard protocols.

Results: Among the five fractions, methanol fraction of *Artocarpus lakoocha* exhibited higher content of phytochemical compounds [phenols = (3 175.21±290.43) mg GAE/g dry extract, flavonoids = (1 173.15±47.52) mg QE/g dry extract and tannins = (923.53±95.21) mg TAE/g dry extract] as compared to other fractions. The methanol fraction showed the highest antioxidant activity in DPPH and ABTS radical scavenging assays with IC_{50} of (111.98±34.20) μg/mL and (138.26±0.66) μg/mL, respectively, and the best reduction potential with a value of (316.81±2.96) mg QE/g dry extract in reducing power assay. There was significant correlation between the amount of phytochemicals and antioxidant activities. Moreover, the extract successfully protected Lambda phage DNA from damage at 5 and 6 mg/mL concentration and exhibited substantial bactericidal as well as fungicidal activity. The GC-MS analysis of methanol fraction of *Artocarpus lakoocha* revealed diethyl phthalate as the main phytochemical compound, along with 3,4-dihydroxymandelic acid, 9-octyl eicosane and 7,8-didehydro-3-methoxy-17-methyl-6-methylene morphinan.

Conclusions: The methanol fraction of *Artocarpus lakoocha* could be used as a potent antioxidant and antimicrobial agent for sustainable agriculture and pharmaceutical purposes.

1. Introduction

Plants are rich sources of secondary metabolites, such as phenols, tannins, and flavonoids, which have been found to have *in vitro* antimicrobial and antioxidant properties. Control of plant pathogens and combating plant's stress by biological means is of great significance for sustainable agriculture and restoring healthy ecosystems. At present, major research emphasis has been given to discover biologically active natural products from various plants that

✉Corresponding author: Suparna Mandal Biswas, Agricultural and Ecological Research Unit, Indian Statistical Institute, 203, B. T. Road, Calcutta 700108, India.
Tel: (+91) (033) 25753225
Fax: (+91) (033) 25753049
E-mail: suparna@isical.ac.in

How to cite this article: Bhattacharya E, Dutta R, Chakraborty S, Mandal Biswas S. Phytochemical profiling of *Artocarpus lakoocha* Roxb. leaf methanol extract and its antioxidant, antimicrobial and antioxidative activities. Asian Pac J Trop Biomed 2019; 9(11): 484-492.

J Food Sci Technol
https://doi.org/10.1007/s13197-021-05122-4

ORIGINAL ARTICLE

Antioxidant, antimicrobial and DNA damage protecting potential of hot taste spices: a comparative approach to validate their utilization as functional foods

Ekta Bhattacharya[1] · Ujjaini Pal[1] · Rajashree Dutta[1] · Prasanta C Bhowmik[2] · Suparna Mandal Biswas[1]

Revised: 13 April 2021 / Accepted: 26 April 2021

Abstract Hot taste spices have enormous health benefits starting from kitchen to pharmaceutical laboratories. Our present study is focused on phytochemical and pharmacological screening of six hot taste spices namely *Zingiber officinale* (ginger), *Capsicum annuum* (chilli), *Piper chaba* (java long pepper), *Piper nigrum* (black pepper), *Syzygium aromaticum* (clove), *Trachyspermum ammi* (carom). Among all six spices, clove and ginger exhibited strong antioxidant activity owing to higher phytochemical contents. Significant antifungal activity (IZD $\geq$ 11 mm) was revealed by all six spices except hexane fraction of carom whereas strong antibacterial activity with lowest MIC was displayed by clove, ginger and chilli. DNA was successfully protected from oxidative damage by clove, ginger followed by chilli, java long pepper and carom but black pepper could only partially protect DNA damage even at 4 mg/ml concentration. Based on the DNA damage protecting potentials and antioxidant activities clove, ginger, java long pepper and carom may be utilized for neutraceuticals development. Antimicrobial activities suggested that clove, ginger, java long pepper and chilli may be useful as food preservatives. Fractionated bioactivity of the all the six HTS would help for targeted extraction and development of nutraceuticals from these commonly used medicinal spices.

Keywords Spices · Antiradical potential · Oxidative DNA damage · Bioactive · Nutraceuticals

Abbreviations

HTS	Hot taste spices
ZO	*Zingiber officinale*
CA	*Capsicum annuum*
PC	*Piper chaba*
PN	*Piper nigrum*
SA	*Syzygium aromaticum*
TA	*Trachyspermum ammi*
DPPH	2,2-Diphenyl-1-picrylhydrazyl
ABTS	2,2′-Azino-bis (3-ethylbenzothiazoline-6-sulfonic acid)
TBA	Thiobarbituric acid
TCA	Trichloroacetic acid
RPA	Reducing power assay
LPA	Lipid peroxidation assay
MDA	Malondialdehyde
IZD	Inhibition zone diameter
MIC	Minimum inhibitory concentration

✉ Ekta Bhattacharya
ektabhattacharya1990@gmail.com

✉ Suparna Mandal Biswas
suparna@isical.ac.in

Ujjaini Pal
ujjaini.pal01@gmail.com

Rajashree Dutta
rajashree1026@gmail.com

Prasanta C Bhowmik
pbhowmik@umass.edu

[1] Agricultural and Ecological Research Unit, Indian Statistical Institute, 203, B.T. Road, Kolkata 700108, India

[2] Stockbridge School of Agriculture, University of Massachusetts, 18 Stockbridge Hall, Campus Centre Way, Box 3724580, Amherst, MA 01003-7245, USA

Published online: 04 June 2021

Biocatalysis and Agricultural Biotechnology 42 (2022) 102356

Contents lists available at ScienceDirect

Biocatalysis and Agricultural Biotechnology

journal homepage: www.elsevier.com/locate/bab

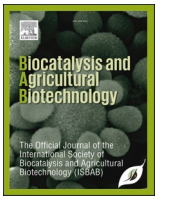

Research Paper

Fractionation based evaluation of phytochemical constituents, antimicrobial and allelopathic potential of *Piper chaba*, Hunter. stem and identification of "Pipercyclobutanamide-A" as a strong allelopathic agent

Ekta Bhattacharya *, Sayani Saha, Rajashree Dutta, Madhurima Dutta, Suparna Mandal Biswas *

Agricultural and Ecological Research Unit, Indian Statistical Institute, 203, B.T. Road, Kolkata, 700108, India

ARTICLE INFO

Keywords:
Piper chaba
Hunter.
Pipercyclobutanamide-A
Allelopathic potential
Antimicrobial activity
Spices
Phytochemicals

ABSTRACT

Piper chaba, Hunter. is a less known medicinal spice. Its medicinal properties have been studied thoroughly but its role as a source of agrochemicals has not been studied yet. So, in the present work, we are interested to explore its other biological activities. Fractionated quantitative biochemical analysis revealed that all fractions contained substantial amounts of phenolics (ranging from 863.75 mg to 1073.11 mg GAE/g of dry extract), flavonoids (164.01 mg to 244.57 mg QE/g of dry weight) and tannins (42.86 mg to 64.88 mg TAE/g dry extract) except acetone fraction. All fractions of *P. chaba* revealed strong fungicidal activity with Inhibition Zone Diameter [IZD] ranging from 32.49 to 36.66 mm except acetone fraction. In case of bactericidal activity, all the fractions except hexane fraction exhibited strong effect with IZD ranges from 14.96 to 30.39 mm against all the tested species. Dose dependent bioassay experiment on rice showed that methanol fraction of *P. chaba* possesses strong allelopathic activity with IC_{50} value 202.77 μg/mL for root length and 509.1 μg/mL for shoot length. As methanol fraction of *P. chaba* exhibited strong allelopathic activity, we were interested to identify the actual compound responsible for that activity. LCMS analysis of purified methanol fraction of *P. chaba* revealed the presence of "Pipercyclobutanamide-A" as a major compound– and this is the first report of this compound from stem of *P. chaba*. Therefore, methanol fraction of *Piper chaba* could be used as natural source of compounds with agrochemical and antimicrobial potential for sustainable agriculture and pharmaceutical purposes.

1. Introduction

Plant bioactive compounds (BACs) provide infinite opportunities for development of natural agrochemicals such as biopesticides, bioherbicides or biofertilizers due to vast diversity of secondary metabolites (Guerriero et al., 2018; Isah, 2019). Secondary metabolites of plants are metabolic intermediates or products which are not essential for growth and development but play various important functions in the living plants such as resistance against pathogens, pests, and repulsion against herbivores; reaction to environmental stresses, and mediating ecological interactions (Yang et al., 2018; Jain et al., 2019; Aguirre-Becerra et al., 2021). These compounds are

* Corresponding authors.
E-mail addresses: ektabhattacharya1990@gmail.com (E. Bhattacharya), suparna@isical.ac.in (S. Mandal Biswas).

https://doi.org/10.1016/j.bcab.2022.102356
Received 17 September 2021; Received in revised form 8 April 2022; Accepted 21 April 2022
Available online 29 April 2022

NATURAL PRODUCT RESEARCH
2025, VOL. 39, NO. 5, 1065–1072
https://doi.org/10.1080/14786419.2023.2294107

Taylor & Francis
Taylor & Francis Group

Synthesis, antimicrobial, anticancer evaluation and molecular docking with Bax and MDM2 of dibromosterculic acid

Rahul Bose[a], Ayan Paul[a], Rajashree Dutta[a], Anjan Hazra[a], Arindam Pramanik[b,c] and Suparna Mandal Biswas[a]

[a]Agricultural and Ecological Research Unit, Indian Statistical Institute, Kolkata, India; [b]School of Medicine, University of Leeds, United Kingdom; [c]Amity Institute of Biotechnology, Amity University, Uttar Pradesh, India

ABSTRACT

Dibromosterculic acid [8-(1,2-dibromo-2-octylcyclopropyl)-octanoic acid], a new synthetic derivative was prepared by bromination of sterculic acid. This synthetic derivative showed strong fungicidal activity against two pathogenic fungal species namely *Penicillium chrysogenum* and *Aspergillus niger* with minimum inhibitory concentration (MIC) value of 0.007 mg/ml and good bactericidal activity against *Bacillus subtilis* and *Xanthomonas sp.* with MIC value of 0.015 mg/ml. Cytotoxic activity on both normal (MCF-10A) and cancerous (MDA-MB-468) cell lines revealed that the survivability percentage of normal cells was unaffected, whereas cancerous cells were decreased greatly by dibromosterculic acid with 50% survivability at 9 µg/ml concentration. Molecular-docking using AutoDock 4.2 with Bax exhibited strong pi-sigma interaction with PHE-93, pi-alkyl and alkyl interaction with TRP-139, ARG-89 and PHE-92 whereas MDM2 revealed strong hydrogen bond interaction with GLN-59 and pi-alkyl interaction with PHE-55. All experimental parameters suggested that this synthetic derivative would be valuable for target-specific drug development with nominal side effects.

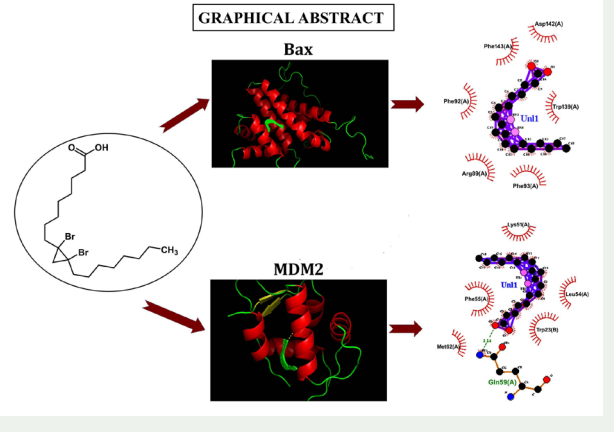

ARTICLE HISTORY

Received 26 December 2022
Accepted 4 December 2023

KEYWORDS

Sterculia foetida; L.; dibromosterculic acid; cytotoxicity; molecular-docking; Bax; MDM2 (p53 inhibitor)

CONTACT Rahul Bose rahulbosebiotech@gmail.com; Suparna Mandal Biswas mondalsupa@gmail.com
Supplemental data for this article can be accessed online at https://doi.org/10.1080/14786419.2023.2294107.
This article has been corrected with minor changes. These changes do not impact the academic content of the article.

Plant Gene 33 (2023) 100403

Contents lists available at ScienceDirect

Plant Gene

journal homepage: www.elsevier.com/locate/plantgene

Squalene synthase in plants – Functional intricacy and evolutionary divergence while retaining a core catalytic structure

Anjan Hazra *, Madhurima Dutta, Rajashree Dutta, Ekta Bhattacharya, Rahul Bose, Suparna Mandal Biswas *

Agricultural and Ecological Research Unit, Indian Statistical Institute, 203, B.T. Road, Kolkata 700108, India

ARTICLE INFO

Keywords:
Differential expression
Gene copy number
Molecular evolution
Protein 3d structure
Squalene
Squalene synthase (SQS)

ABSTRACT

Squalene is the crucial intermediate for the biosynthesis of many bioactive triterpenoids, such as phytosterol in plants or cholesterol in animals. Squalene synthase (SQS) is the essential gene of the squalene biosynthetic pathway, which catalyzes the head-to-head condensation of two farnesyl pyrophosphate or farnesyl diphosphate (FPP) molecules in a two-step reaction and formation of linear C_{30} squalene. SQS ubiquitously occurs in all eukaryotic organisms. However, the activity of this gene varies significantly, leading to diverse squalene content in plants. The present study focused on the variation in the expression landscape of SQS gene copies with varying evolutionary backgrounds. Afterward, a reflection of the sequence divergence on the catalytic structure of the protein was examined. The genome-scale mining of the SQS homologs revealed varying degrees of duplication events, sequence evolution of the gene sequence itself, and the adjoining regulatory architecture. Contrasting expressional patterns and the regulatory modules pinpoint the importance of transcriptional regulation of this essential gene. Three-dimensional organizations of SQS from diverse evolutionary taxa and their consensus structures enlightened the conservation of critical catalytic domains, nonetheless divergence in the majority of the protein. As a whole, the outputs of this study provide some valuable insights for understanding the functional regulation of SQS under different tissues and environments.

1. Introduction

Squalene, a natural triterpene hydrocarbon, is known for its crucial role as a precursor in phytosterol or cholesterol synthesis in plants, animals, and humans (Reddy and Couvreur, 2009). As an essential intermediate for synthesizing diverse bioactive secondary metabolites, squalene plays vital cellular functions in organisms (Ghimire et al., 2016). Squalene has various beneficial roles in human health, such as antioxidant and anticancer effects, decreasing cardiovascular diseases, enhancing the immune system, and application as a drug adjuvant (Gopakumar, 2012; Gohil et al., 2019) hence received much attention. It is also used as an additive, supplement, or nutraceutical in the food and cosmetic industry (Narayan Bhilwade et al., 2010; Popa et al., 2015). The primary commercial source of squalene was the liver of marine animals such as deep-sea sharks, whose squalene content was reported as high as 79% of the total oil (Lozano-Grande et al., 2018). Squalene is considered an essential constituent of deep-water animals for surviving in the oxygen-deficient, high-pressure saline environment of the sea (Lozano-Grande et al., 2018). However, use of these marine animals is restricted for the use of SQ as per animal protection regulations. At the same time, the presence of organic pollutants may cause deadly disease, cancer. Therefore it is imminent to explore new natural sources of plant origin (Turchini et al., 2010). The expression of squalene in plants is lineage-specific mainly, which also varies across tissues and growth conditions (Lozano-Grande et al., 2018). A literature overview shows that some plant sources of squalene are soybean oil (9.9 mg/100 g), grape oil (19.1 mg/100 g), olive oil (564 mg/100 g), and *Amaranthus* seeds (5942 mg/100 g) (Toderich et al., 2020). Understanding its genetic control is essential to apprehend the factors responsible for squalene content diversity in plants.

Squalene synthase (SQS) is the essential branch point enzyme, which shifts the assimilated carbon flux into triterpenes and sterol biosynthetic processes in plants (Aminfar and Tohidfar, 2018). Squalene synthase participates in a two-step reaction in which two identical farnesyl diphosphate (FPP, C_{15}) molecules condensed into presqualene diphosphate (PSPP), which is further reduced to squalene with the

* Corresponding authors.
E-mail addresses: anjanhazraresearch@gmail.com (A. Hazra), mondalsupa@gmail.com (S.M. Biswas).

https://doi.org/10.1016/j.plgene.2023.100403
Received 11 October 2022; Received in revised form 19 November 2022; Accepted 3 January 2023
Available online 5 January 2023